University of Massachusetts Medical School

eScholarship@UMMS

2018-01-19

Role of JIP1-JNK Signaling in Beta-Cell Function and Autophagy

Seda Barutcu
University of Massachusetts Medical School

Let us know how access to this document benefits you.

Follow this and additional works at: https://escholarship.umassmed.edu/gsbs_diss

 Part of the Biology Commons, Cell Biology Commons, and the Cellular and Molecular Physiology Commons

ROLE OF JIP1-JNK SIGNALING IN BETA-CELL FUNCTION
AND AUTOPHAGY

A Dissertation Presented

By

SEDA BARUTCU

Submitted to the Faculty of the

University of Massachusetts Graduate School of Biomedical Sciences, Worcester

in partial fulfillment of the requirements for the degree of

DOCTOR OF PHILOSOPHY

January 19th, 2018

Program in Molecular Medicine

ROLE OF JIP1-JNK SIGNALING IN BETA-CELL FUNCTION
AND AUTOPHAGY

A Dissertation Presented

By

Seda Barutcu

This work was undertaken in the Graduate School of Biomedical Sciences

Program in Molecular Medicine

Under the mentorship of

Roger J. Davis, Ph.D., Thesis Advisor

Amy K. Walker, Ph.D., Member of Committee

David A. Guertin, Ph.D., Member of Committee

Dale L. Greiner, Ph.D., Member of Committee

Gokhan S. Hotamisligil, Ph.D., External Member of Committee

Michael P. Czech, Ph.D., Chair of Committee

Anthony Carruthers, Ph.D.,
Dean of the Graduate School of Biomedical Sciences

Program in Molecular Medicine

January 19th, 2018

DEDICATION

This thesis is dedicated to my beloved soulmate and husband, Rasim Barutcu for his irreplaceable support as a colleague; and my beloved older sisters Sevim Ozturk, Neslihan Roche, Sevilay Uzunoglu for being my lifelong mentors.

ACKNOWLEDGMENTS

I would like to thank my thesis advisor Dr. Roger Davis for giving me the opportunity to work in his lab, and learn from his expertise. I also thank all the past and present members of the Davis Lab that I had a chance to work with, for their contribution to my scientific development, and for their friendship.

I would like to thank my thesis research and defense committee members Dr. Michael Czech, Dr. Amy Walker, Dr. David Guertin, Dr. Peter Pryciak, Dr. Dale Greiner and Dr. Gokhan Hotamisligil for their time, guidance and support throughout my thesis research and dissertation.

I would like to thank my collaborators Dr. Agata Jurczyk, Dr. Rita Bortell, and Dr. Laura Alonso for their valuable scientific discussion and guidance. I would also like to thank Dr. Lara Strittmatter for her generous help with electron microscopy; Dr. Alper Kucukural for his generous help with bioinformatics analysis and enjoyable scientific discussions; and Dr. Gregory Pazour for his valuable scientific advice and guidance.

I would finally like to thank all my family and friends for their love, and support.

ABSTRACT

Proper functioning of endocrine cells is crucial for organismal homeostasis. The underlying mechanisms that fine-tune the amount, and the timing of hormone secretion are not clear. JIP1 / MAPK8IP1 (JNK interacting protein 1) is a scaffold protein that mediates cellular stress response, and is highly expressed in endocrine cells, including insulin secreting β-cells in pancreas islets. However, the role of JIP1 in β-cells is unclear. This study demonstrates that β-cell specific *Jip1* ablation results in decreased glucose-induced insulin secretion, without a change in *Insulin1* and *Insulin2* gene expression. Inhibition of both JIP1-kinesin interaction, and JIP1-JNK interaction by genetic mutations also resulted in decreased insulin secretion, suggesting that JIP1 may mediate insulin vesicle trafficking through interacting with kinesin and JNK. Autophagy is a cellular recycling mechanism and implicated in the β-cell function. Both JIP1 and JNK are proposed to regulate autophagy pathway. However, it is unclear whether JNK plays a role in the promotion or suppression of autophagy. The findings of this study show that JNK is not essential for autophagy induction, but can regulate autophagy in a cell and context specific manner. The results in this thesis implies a mechanism that link cellular trafficking and stress signaling pathways in the regulated hormone secretion. In addition to the known role of JIP1 in metabolism and insulin resistance, this finding may also be relevant to endocrine pathologies.

AUTHOR CONTRIBUTIONS

In Chapter 2, Agata Jurczyk and Sambra Reddick performed the islet perifusion experiments. Caroline Morel and Claire Standen generated and characterized the JIP1^{YA} mice, Myoung Sook Han assisted with the blood analysis, and Norman Kennedy generated the JIP2^{LoxP} mice.

In Chapter 3, Santiago Vernia provided the primary hepatocytes, and Nomeda Girnius performed the kidney epithelial cell experiments.

TABLE OF CONTENTS

LIST OF FIGURES AND TABLES

CHAPTER 1: INTRODUCTION

1.1 The endocrine system and autophagy in metabolism

1.1.1 Regulation of energy homeostasis by the endocrine system

Regulation of energy storage, mobilization, and consumption is crucial for complex organisms to ensure proper functioning of vital organs. The brain is dependent on glucose for its energy use, although during prolonged fasting it can utilize ketone bodies in addition to glucose [1]. On the other hand, very high glucose levels can cause hyperosmolar crisis, which is a life-threatening condition [2]. Moreover, a prolonged increase in glucose levels can cause organ and tissue dysfunction, such as the endothelial pathologies observed in diabetic patients [3]. Thus, it is crucial for an organism to maintain its blood glucose level at the physiological range, which is ~80-120 mg/dl.

Multiple organs co-operate to regulate the utilization of fuels (glucose, fatty acids, and amino acids) during fasting and feast [4]. Fasting and feast represent two extreme metabolic states where an organism needs distinct responses. The neuroendocrine system regulates the switch from the anabolic state during feast to a katabolic state during fasting; and vice-versa [5-8]. Increased insulin after a meal consumption directs the fuel, in the form of glucose, amino acids, and lipids to the tissues such as fat, liver, and muscle; where they are used, or stored. In fed state, protein synthesis is also increased in parallel with growth [9].

In the fasting state, mostly the liver can provide its stored glucose to the circulation for utilization by other tissues. Elevated circulating glucagon levels in fasting state increases hepatic glucose production [10]. Mobilization of the liver

glycogen depots provides the majority of the blood glucose during the first hours of fasting. Gluconeogenesis is gradually increased and becomes the only source of glucose after ~24 hours of fasting, when liver glycogen depots are depleted [11]. Although other tissues, such as the muscle, can store glycogen, they cannot mobilize it to the circulation since they lack glucose 6-phosphatase, which catalyzes the final dephosphorylation step of glucose that is required for the export of glucose [12]. However, muscle and fat contribute to gluconeogenesis by providing amino acids, fatty acids, and glycerol to the liver [13]. Glucogenic amino acids can be catabolized to pyruvate, which is the main substrate of gluconeogenesis, while fatty acid oxidation mainly provides the energy for gluconeogenesis. Fatty acids can be utilized as fuel by many tissues, especially during prolonged starvation.

One exception that can overcome the effects of high insulin during feast is the adrenergic "fight or flight" response [14]. Increased adrenergic signaling suppresses insulin secretion and action, and induces glycogenolysis and gluconeogenesis in the liver in addition to the fatty acid mobilization from fat. Thus, the availability of fuel becomes the highest for vital tissues for maximum performance capacity in a life-threatening situation [15, 16]. On the other hand, prolonged stress and adrenergic stimulus can adversely affect the blood glucose levels, especially in diabetic patients [17].

The neuroendocrine system facilitates the communication between fat, muscle, and liver to fine-tune energy balance during feast, fast, and stress conditions (Figure 1.1.).

Neuroendocrine Regulation of Energy Homeostasis

Effected Tissues	Decreased by:	Metabolic Response	Increased by:
	Insulin	Gluconeogenesis	Glucagon, Cortisol, Sympathetic Nerv
	Insulin	Glycogenolysis	Glucagon, Epinephrine
	Insulin	Lipolysis	Epinephrine
	Insulin	Ketogenesis	Glucagon, Epinephrine
	Glucagon	Protein Synthesis	Insulin, GH, TH, Steroids
	Glucagon	Glycogen synthesis	Insulin
	Epinephrine	Lipogenesis	Insulin
		Thermogenesis	TH

Figure 1.1. A summarized presentation of energy regulation by neuroendocrine system.

1.1.2. Endocrine dysfunction and obesity

In obesity, energy balance is biased towards the increased lipid storage and decreased energy expenditure. Although the main etiology of the worldwide obesity pandemic is increased food consumption and sedentary lifestyle, there are various diseases that can cause obesity, including endocrine tissue dysfunction.

For instance, Cushing syndrome, where there is elevated circulating cortisol, is presented by an increase in the abdominal obesity, in addition to the other effects of high cortisol [18, 19]. Cushing syndrome is mostly caused by a pituitary adenoma, secreting adrenocorticotrophic hormone (ACTH). Although, less frequently, a cortisol secreting adrenal tumor can also cause Cushing syndrome.

Insulinoma, where there is an uncontrolled increase in the circulating insulin levels, can also cause obesity [20]. In this case, increased food consumption to compensate the hypoglycemic effect of the increased insulin levels is the main cause of the obesity.

Although adipose tissue is best known for its fat storage capacity, adipocytes also have endocrine functions and can signal to the other tissues to regulate the energy metabolism. Leptin, a hormone secreted from adipose tissue after a meal targets the hypothalamus to inhibit further food intake [21]. Genetic deletion of leptin, or the leptin receptor, results in hyperphagia and obesity in humans and rodents [21-25].

5

In conclusion, hormonal balance is crucial for a healthy energy distribution. Thus, over-functioning or under-functioning of endocrine cells can contribute to the metabolic dysregulation and related diseases.

1.1.3. Obesity-induced insulin resistance, and beta-cell dysfunction

One of the important complications of obesity is the increased insulin resistance that is associated with hyperinsulinemia and may progress to type-II diabetes. However, the mechanism of the insulin resistance in obesity is incompletely understood [26].

In the abdominal obesity, fat deposition in the visceral space and ectopic organs, such as the liver is increased. This specific localization of fat deposition is implicated in the metabolic dysfunction of obesity [27]. Overexpansion of the fat depots may cause an uncontrolled release of free fatty acids, accompanied by chronic inflammation, which can contribute to the increased insulin resistance in obesity [28, 29].

Progressive obesity-induced hyperinsulinemia, and insulin resistance can result in islet expansion of islets and eventually β-cell dysfunction. Moreover, increased circulating lipids and inflammatory cytokines in obesity can also have adverse effects on beta-cell function [30-33].

1.1.4. Autophagy and energy homeostasis

Similar to organismal fuel management, a cell can react to the environmental nutrient status and redirect its fuel and resources to necessary cellular pathways. Autophagy is a cellular self-recycling mechanism where a portion of the cytoplasmic content is targeted to the lysosomal pathway for degradation [34]. This process can be selective, such as mitophagy, where mitochondria is selectively targeted for the autophagosomal degradation. Or it can be non-selective, termed macro-autophagy. For the rest of the text by "autophagy" I will refer to macro-autophagy.

Starvation-induced autophagy is important for the survival of the cell in a nutrient deprived environment, and is regulated by the energy sensors of the cell, such as the mTOR/AMPK (mammalian target of rapamycin/AMP Kinase) pathway[35] (Figure 1.2.). Many ATG (autophagy related gene) proteins cooperate to regulate the initial double membrane formation which captures the cytoplasmic content for targeting to lysosome [36, 37].

Autophagy contributes to overall organismal development by regulating cellular catabolic processes [38, 39]. It is implicated in many diseases, such as cancer and neurodegeneration [40, 41]. Moreover, autophagy contributes to the organismal energy balance and is implicated in obesity and endocrine cell function [42, 43]. For instance, lipophagy, a specific form of autophagy that recycles lipids, can regulate cellular lipid metabolism [44]. Systemic decrease in autophagy in mice with heterozygous deletion of *Atg7* (autophagy related gene)

resulted in aggregated progression of obesity-induced diabetes, suggesting that

autophagy is required for the organismal response to the metabolic stress [45].
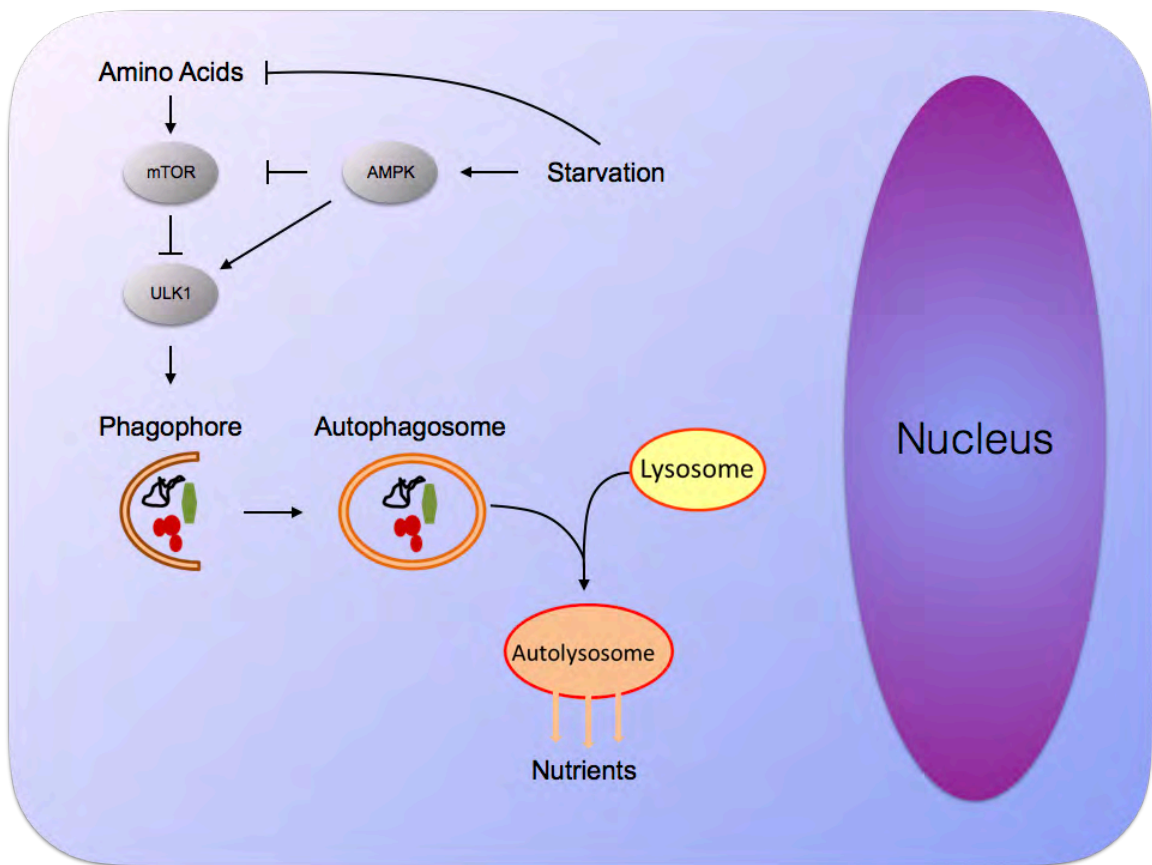
Figure 1.2. Regulation of autophagy by energy sensing mTOR/AMPK
pathway.

However, it is possible that in a tissue specific context, decreased

autophagy can both promote or inhibit obesity. For instance, the deficiency of

ATG7, an autophagy related gene, in the muscle and liver of mice results in decreased obesity and increased insulin sensitivity after a high fat diet challenge [46]. This effect was attributed to the mitochondrial dysfunction-induced FGF-21 expression in the autophagy deficient tissues. FGF-21 (fibroblast growth factor-21) is known for its beneficial effects in obesity [47, 48]. On the other hand, ATG7 deficiency in POMC (Proopiomelanocortin) neurons in hypothalamus results in decreased α-MSH (α-melanocyte stimulating hormone) levels, and consequently decreased lipolysis in adipose tissue and increased obesity [49]. Autophagy is also implicated in endocrine cell function [43]. Beta-cell specific deletion of ATG-7 resulted in decreased insulin secretion, and impaired glucose tolerance in mice [50]. Autophagy deficient beta-cells were more prone to cell death, and ATG-7 deficiency resulted in decreased beta-cell mass in obesity [51, 52]. Moreover, more recently, autophagy was implicated in the removal of old insulin vesicles and promotion of young insulin vesicle secretion [53]. These studies suggest that autophagy in β-cells may play a role in both insulin secretion, and the expansion of β-cell mass in response to metabolic stress.

More recently, an interesting idea was proposed, where autophagosomes could target its content to the secretory pathway, rather than lysosomal degradation [54]. Although more research is needed to support of this concept, this mechanism may provide a previously unexplored area of cellular autophagy-endocrine regulation bridge.

1.2 Stress signaling pathways in energy homeostasis

1.2.1 MAPK pathways and cellular stress response

Similar to complex organisms, cells constantly reshape their biological behavior in response to the changes in their dynamic environment. These changes include molecular signals, as well as mechanical stress conditions such as pressure, stretch, or contact loss. Among the molecular signals, circulating or paracrine-acting factors such as hormones, cytokines, growth factors, and cellular nutrients are among the most studied factors that result in a biological response in cells. Mitogen activated protein kinase (MAPK) group represents JNK, p38 and ERK protein families which regulate cellular responses to these various extracellular signals (Figure 1.3.).

MAPKs are evolutionarily conserved serine/threonine kinases, and are activated by a kinase cascade mechanism [55]. Thus, an extracellular stimulus results in phosphorylation and activation of a MAPK Kinase Kinase (MAP3K), which then phosphorylates and activates a downstream MAPK Kinases (MAP2K); lastly phosphorylation and activation of MAPK by MAP2K results in transcriptional or non-transcriptional changes that shape cellular response [56]. With multiple upstream activators and downstream targets, as well as cross-signaling, MAPK pathways are highly complex, thus require regulatory mechanisms, such as scaffold proteins, for selectivity and specificity.
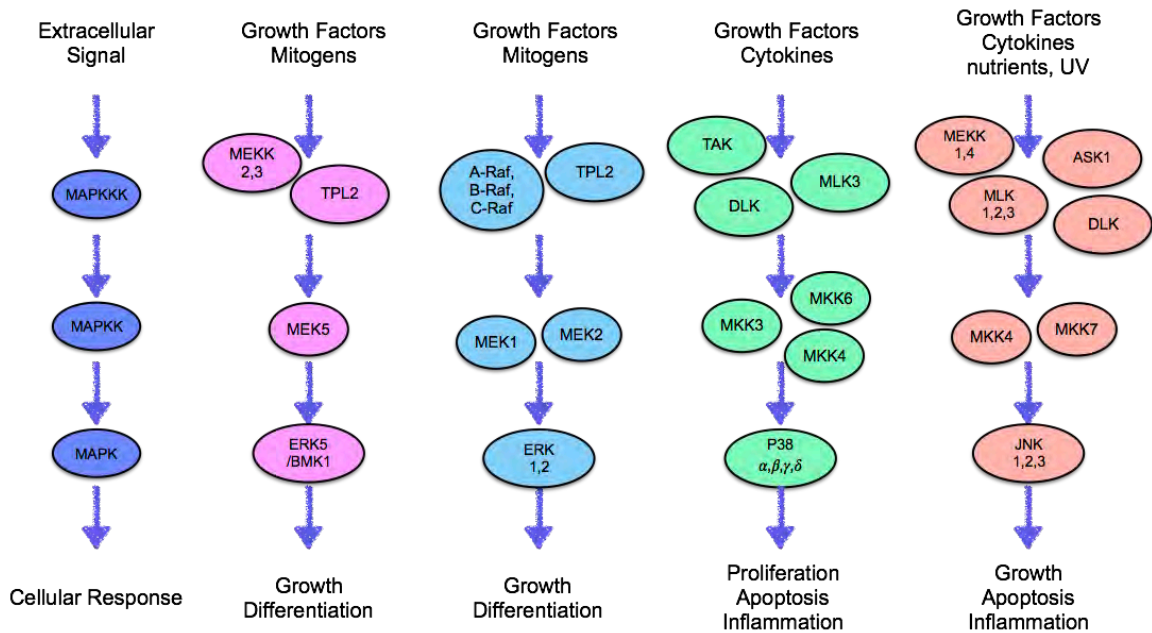
Figure 1.3. A summarized presentation of MAPK signaling components, and relevant pathways.

1.2.2 Role of MAPK pathways in metabolic regulation

MAPK signaling modules can respond to environmental changes. Dysregulation of energy homeostasis results in the alteration of the extracellular signals such as circulating hormones and nutrients. These changes can activate MAPK pathways, which also mediates cellular response to the metabolic dysregulation. For instance, insulin stimulation can activate ERK, p38 and JNK in the of muscle of lean animals, while this activation was suppressed in obese animals [57]. Another example is that TNF-α, a cytokine that is increased in the circulation of obese organisms, can also induce the activation of all MAPK families [58].

Accordingly, activation of the MAPK pathways in obesity is implicated in the alterations of the metabolic regulation. The ERK pathway is implicated in the regulation of adipogenesis, and activation of ERK pathway can contribute to the progression of obesity and insulin resistance [59-61]. Additionally, p38 activation by MKK6 can mediate the metabolic regulation. MKK6 deficient mice are reported to gain less weight after a high fat diet challenge, which was associated with increased brown adipose tissue thermogenesis [62].

In the context of metabolic regulation, JNK is the most extensively studied MAPK and is discussed in more detail in the following section.

1.2.3 Role of JNK in metabolism and energy homeostasis

1.2.3.1 Increased JNK activation during metabolic dysfunction

In obese mouse models, JNK activation is increased in a variety of tissues such as fat, liver, and muscle; and obesity-induced JNK activation is implicated in the diet induced obesity progression and insulin resistance [63]. However, which changes in an obese organism result in the activation of JNK is still unclear. There are multiple mechanisms proposed for the widespread JNK activation observed in obesity, and it is possible that a collective effect of these mechanisms can contribute to the JNK activation.

The increase in the circulating free fatty acids in obese individuals is implicated in obesity induced insulin resistance and beta-cell dysfunction [64-66].

Increased circulating free fatty acids in obesity is also proposed to be a mechanism for JNK activation. In support of this idea, 3T3-L1 adipocytes, primary hepatocytes, and pancreas beta-cells showed increased JNK activation upon treatment with free fatty acids [67, 68]. Furthermore, treatment of MEF (mouse embryonic fibroblasts) with saturated fatty acids but not unsaturated fatty acids induced PKC (Protein kinase C) activity, which resulted in an increased MLK3 mediated JNK activation via SRC-VAV signaling [69-73]. Both MKK4 and MKK7 play role in this pathway [69, 71]. Concordantly, both MLK3 deficient [72], and MLK2,3 deficient mice showed decreased JNK activation after a high fat diet challenge, in addition to a decreased obesity and insulin resistance [70].

Increased inflammation and circulating cytokines in obesity is another factor that contributes to increased insulin resistance [74, 75]. These secreted cytokines can be another player to activate MLK-JNK pathway in obesity [76, 77].

Increased circulating basal insulin levels in an obese organism can be another mechanism that may mediate sustained JNK activation [78].

1.2.3.2 Contribution of JNK to diet-induced obesity and insulin resistance.
JNK1 deficient mice are protected against obesity and insulin resistance when fed a high fat diet, suggesting a role for high fat diet-induced JNK1 activation in the progression of obesity [63]. The role of JNK1 activation in obesity and related metabolic dysregulation is a combined effect of JNK1 in adipose tissue, muscle, myeloid cells and central nervous system [79-81]. On the other hand,

13

JNK1 deficiency in liver increased obesity-induced liver steatosis (liver fat deposition), while JNK1 and JNK2 double deficiency in liver resulted in improved glucose homeostasis; suggesting that differential regulation of JNK1 and JNK2 may have distinct roles in the liver [82, 83].

Previous studies using mouse models to study the role of the JNK pathway in metabolism are summarized in Table 1.

Table 1.1. Gene deletion studies in mouse models that examine the role of JNK pathway in metabolism.

Deleted Gene [ref]	Targeted Tissue	Metabolic Phenotype
JNK1 (MAPK8) [63]	Whole body	Decreased obesity, increased insulin sensitivity.
JNK2 (MAPK9) [63]	Whole body	No change in body weight or insulin sensitivity.
JNK3 (MAPK10) [84]	Whole body	Increased obesity and increased food intake
JNK1 [81, 85]	Nervous System (*Nestin-Cre*)	Decreased obesity. Increased energy expenditure via increased thyroid axis activity.
JNK3 [84]	Neurons (*Pomc-Cre*)	No change in obesity or food intake.
JNK3 [84]	Neurons (*Agrp-Cre*)	Increased obesity and increased food intake

Deleted Gene	Targeted Tissue	Metabolic Phenotype
JNK3[84]	Neurons (*Leprb-Cre*)	Increased obesity and increased food intake
JNK1, JNK2 [86]	Pituitary Gland (*Cga-Cre*)	Decreased obesity. Increased TSH expression caused by decreased Dio2 expression and negative feedback inhibition.
JNK1 [82]	Liver (*Albumin-Cre*)	Increased hepatic steatosis. Decreased glucose tolerance and increased insulin resistance.
JNK1 [80]	Adipose Tissue (*Fabp4-Cre*)	Decreased fat mass, increased hepatic insulin action
JNK1 [79]	Muscle (*Mck-Cre*)	No change in obesity, increased insulin sensitivity in muscle
JNK1, JNK2 [83]	Liver (*Albumin-Cre*)	Improved glucose tolerance
JNK1 [80]	Myeloid Cells (*LysM-Cre*)	No effect on diet-induced obesity and insulin resistance
JNK1, JNK2 [87]	Myeloid Cells (*LysM-Cre*)	No change in obesity. Decreased obesity-induced inflammation and increased insulin sensitivity

Table 1.1. (Continued) Gene deletion studies in mouse models that examine the role of JNK pathway in metabolism. Promoters of the *Cre-Recombinase* for the tissue specific gene targeting is indicated in the parenthesis.

The studies summarized above show that JNK has a broad effect on the regulation of energy metabolism. Considering that JNK can target almost hundred proteins [88], it is of importance to evaluate the signal-specific interactors of JNK to understand the underlying mechanisms of its cell and context specific functions. Scaffold proteins is discussed in the following sections, as a regulatory factor for the specificity of MAPK signaling pathways.

1.3 JIP1, a scaffold protein in stress signaling, and its relevance to metabolism

1.3.1 Signaling complex assembly by scaffold proteins

The cell, as a multi-task unit, can regulate various internal obligations and processes, as well as extra-cellular stimulus-mediated responses, simultaneously, but at the same time, separately and remotely. To achieve this regulation, compartmentalization of signaling molecules within their functionally relevant environment is essential [89-92].

Scaffold proteins provide such a regulatory mechanism by mediating signaling complex assembly. Scaffold proteins can interact with multiple components of a signaling module and, bring them in proximity [89, 93-95]. In 1994, the first example of this phenomenon was described in yeast, where Ste-5 scaffold protein formed complex with stress signaling proteins, MAP3 Kinase

16

(Ste11), MAP2 Kinase (Ste7) and MAP Kinase(Fus3), to enhance mating-related signal transduction [96, 97].

Additional studies on a variety of scaffold proteins provided evidence that, the function of scaffold proteins in regulating signal transduction is more complex and multi-dimensional than merely being a signal-specific platform for protein interactions [55, 95]. For instance, ERK scaffold protein KSR can associate with Raf1 at the plasma membrane, and this localization is regulated by Ras in response to growth factor stimulus [98]. Ste-5 scaffold protein can also recruit assembled signaling complex to the cellular membrane [99-101].

In addition to compartmentalization, post-translational modifications of proteins in a signaling module can also provide an additional fine tuning to ensure proper timing and localization of a specific signal [89-92]. For instance, scaffold proteins possess multiple phosphorylation sites and, phosphorylation status of these sites can induce or inhibit scaffold mediated signal transduction in a context-dependent manner [102-104]. Thus, scaffold proteins can regulate not only complex assembly, but also localization and timing of the signal activation.

Taken together, current knowledge about scaffold proteins advocates that, better understanding of their function can significantly improve our understanding of how the complex cellular signaling machinery works. Importantly, with recent technological advancement, synthetic scaffold designs in the future may enable us to simulate or inhibit specific signals in a cell without deteriorating other cellular functions [105-108].

1.3.2 JIP family of scaffold proteins

The JIP family of scaffold proteins consist of 4 members, JIP1, JIP2, JIP3, and JIP4, which were all identified by their interaction with JNK [109-114]. JIP1 and JIP2 are structurally similar and have a JNK binding domain close to the N-terminus, in addition to SH3 and PTB domains near the C-terminus [109, 110]. While JIP3 and JIP4 share many common structures among each other, they are structurally distinct from JIP1 and JIP2. For instance, JIP3 and JIP4 have a putative transmembrane domain close to the C-terminus, which is absent in JIP1 and JIP2 proteins. In addition, there are multiple coiled-coil domains and a leucine zipper domain close to the N-terminus of the JIP3 and JIP4 proteins [112, 114] (Figure 1.4).
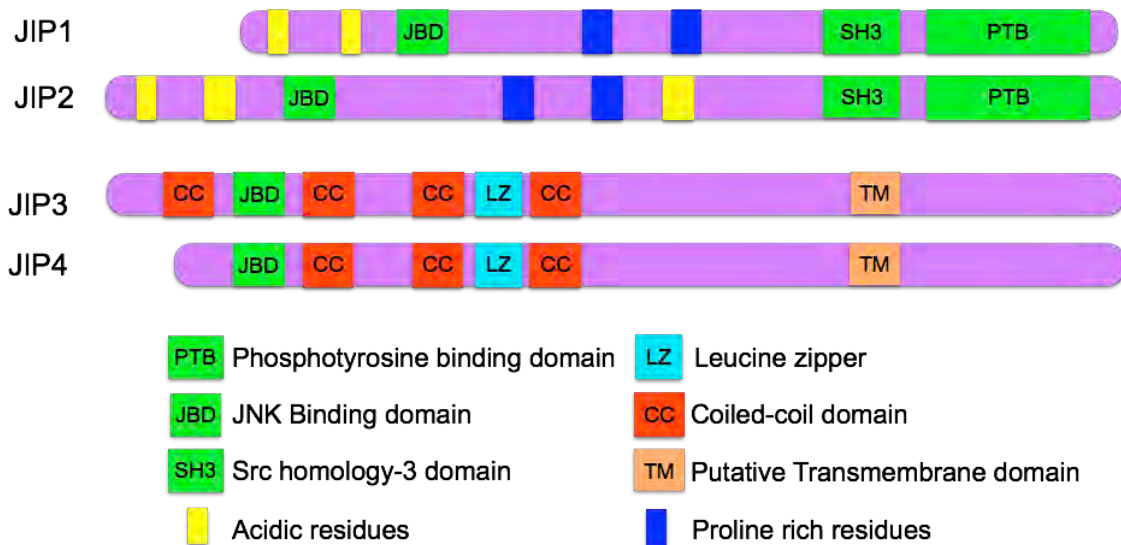
Figure 1.4. Structural and functional features of the JIP family of scaffold proteins.

JIP proteins can functionally differ by their upstream kinase interactors, downstream targets, and additional interacting proteins. For instance, while JIP1 specifically activates JNK signaling and does not interact with other mitogen activated protein kinases (p38 and ERK), JIP2 can interact with p38 and promote p38 activation downstream of Rac signaling via interacting Tiam1 and RasGEF1 [115, 116]. JIP3 can mediate LPS induced JNK activation via interacting with TLR4 and MEKK1 [117]. JIP4 can promote p38 MAPK activation through interacting with MKK3, and MKK6 [114]. Altogether, these represent examples of specific MAP kinase activation by distinct scaffold proteins. Some important interaction partners of JIP family proteins with stress signaling pathway components are summarized in Figure 1.5.
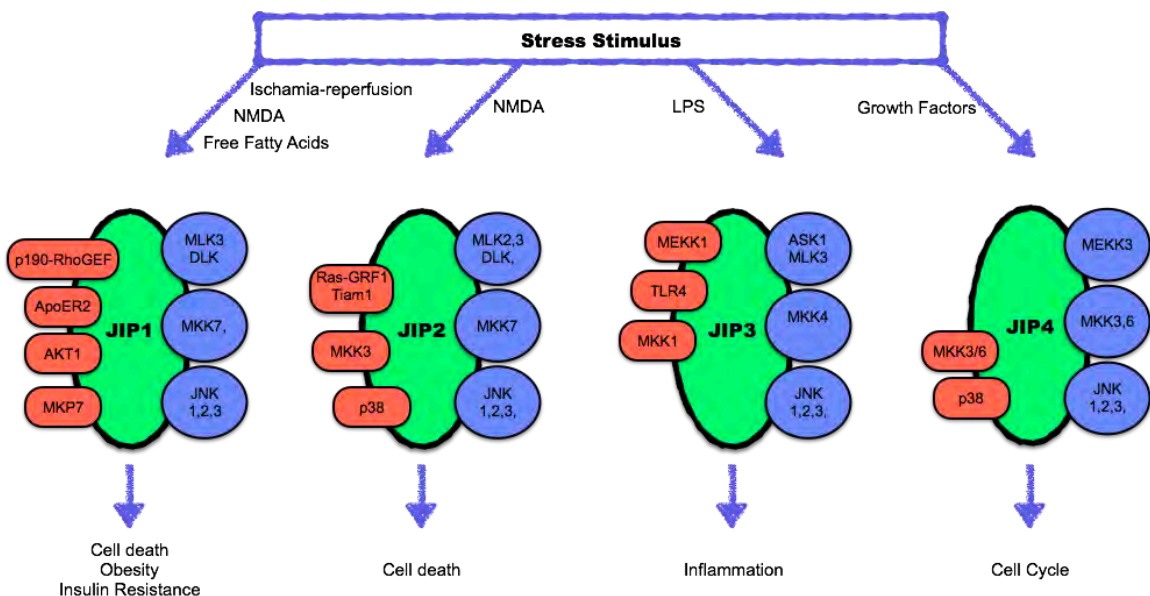
Figure 1.5. Cartoon representing a summary of selected interaction partners of JIP family scaffold proteins.

In addition to interacting with stress signaling pathway components, all JIP proteins can interact with Kinesin Light Chain, and are implicated in the regulation of intracellular trafficking [114, 118-122]. The following sections will focus on JIP1 and its physiologic function.

1.3.3 Genomic locus, and expression profile of MAPK8IP1/JIP1

1.3.3.1 *Mapk8ip1* genomic locus

JIP1 is encoded by the *Mapk8ip1* gene, located on chromosome 11 in human, and chromosome 2 in mouse (Figure 1.6. &1.7.) [123].
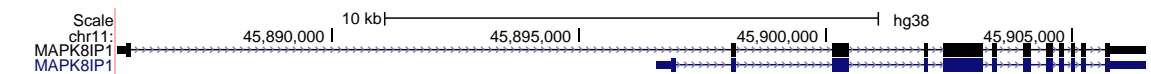
Figure 1.6. The scheme of the human Mapk8ip1 locus obtained from UCSC Genome Browser (hg38).
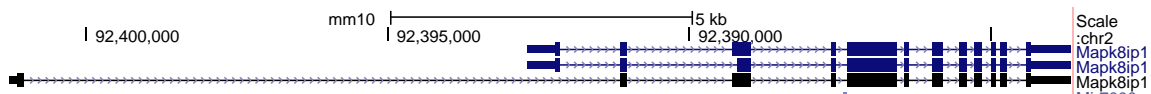
Figure 1.7. The scheme of the mouse Mapk8ip1 locus obtained from UCSC Genome Browser (GRCm38/mm10).

A specific JIP1 antibody detects two bands in the immunoblots of the mouse brain, which correspond to the ~90 and ~110 KD sizes. This non-

homogenous size of the JIP1 protein can be a consequence of the differential

regulation of gene expression at the transcriptional and translational levels, in

addition to the post-translational modifications. However, it is unclear which end

products correspond to the high and low molecular weight JIP1 proteins.

For instance, the genes coding the JIP1 protein in human and mouse

have two alternative exon-1 sequences with distinct start sites and 5'UTRs [124]

(Figure1.1 &1.2). The mouse *Mapk8ip1* locus, different from human *MAPK8IP1*,

has two alternative exon-3 splice junctions, long and short exon-3, which adds

another variability to the *Mapk8ip1* transcript (Figure 1.1. &1.2.). Moreover, an

in-frame ATG at the short exon-3 junction, with an ~10 nucleotide upstream

internal ribosome entry site (IRES) consensus sequence may provide a possible

translation start site for an alternative smaller protein [124]. This in-frame ATG is

conserved in both mouse and human.

It is yet to be discovered which coding sequences correspond to the

differently sized JIP1 proteins. Another remaining question is, what are the

functional differences of these proteins in the context of stability, subcellular

localization and specificity.

1.3.3.2 JIP1 expression profile

JIP1 protein is expressed in humans, rodents, *Drosophila* (APLIP1) and *C.

elegans*. During embryogenesis, JIP1 is localized to the growth cones of

developing neurons and can be detected in the brain protein lysates as early as

day E15 [125]. Initial studies detected JIP1 expression in the brain, and the

insulin-secreting beta-cells in adult mouse, rat, and human [109, 110, 123, 124,

126]. This expression pattern is thought to be at least partially regulated by

REST, a zinc finger transcription repressor expressed in many tissues except

brain and endocrine cells [127]. REST can bind to the 21-bp RE-1 silencer

element (NRSE) on the promoter region of the *Mapk8ip1* gene

(-229 to -209 base pair) and may contribute to the inhibition of the JIP1

expression in the non-neuronal and non-endocrine cells [128].

ENSG00000121653.7 Gene Expression
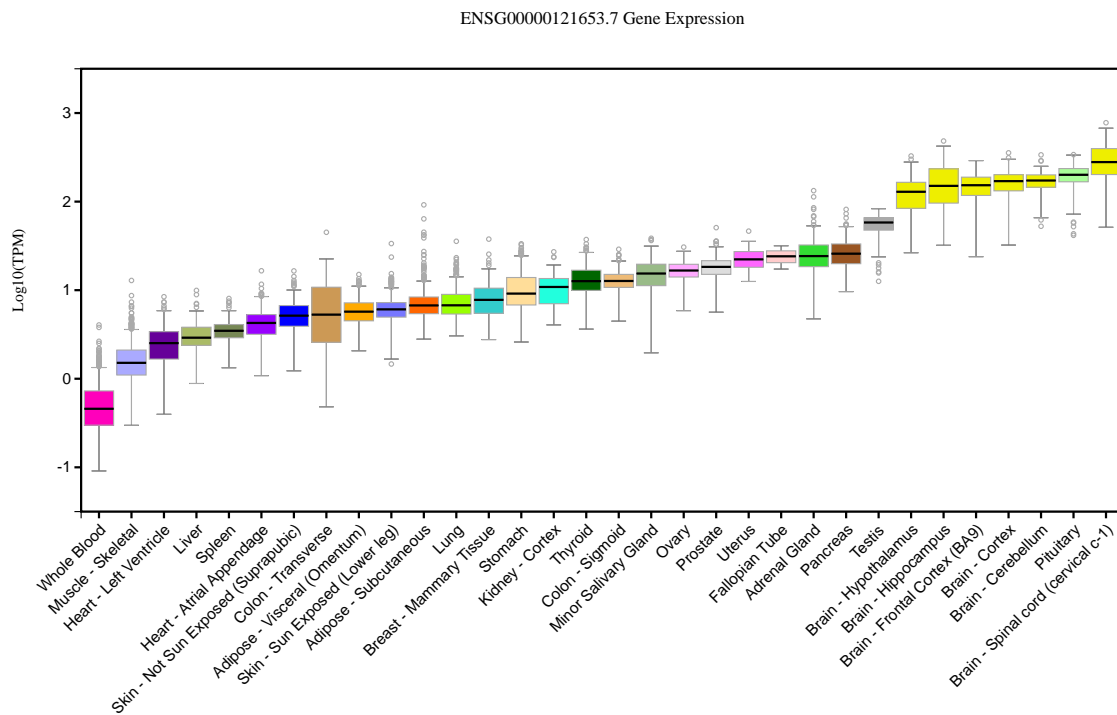
Figure 1.8. Mapk8ip1 expression data obtained from Genotype-Tissue
Expression Database (GTEx) [129]. The Y-axis shows gene expression level in
Transcripts Per Million (TPM). The X-axis represents various tissues ordered by
Mapk8ip1 expression level.

Additional studies showed JIP1 expression in other endocrine tissues, such as the pituitary gland [125, 130]. Moreover, current published deep sequencing data from various tissues show a low level or lack of JIP1 expression in many non-neuronal and non-endocrine tissues (Figure 1.8.) [129]. Examples of such tissues include but not limited to the muscle, liver, and whole blood. Besides, additional endocrine tissues such as adrenal gland and testis also show robust JIP1 expression (Figure 1.8.) [129]. On the other hand, JIP1 expression can be observed in some non-neuroendocrine tissues such as the adipose tissue [71], urothelial epithelium [131] and the kidney (Figure 1.8).

1.3.4 Interaction partners of JIP1

JNK-interacting protein-1 (JIP1) was first identified in a yeast 2-hybrid screen via its interaction with JNK [109]. The following studies described the scaffolding function of JIP1, and its interaction with upstream kinases in the JNK pathway, MKK7 and MLK group of MAPKKKs [93, 132].

The JNK binding domain of JIP1 is located close to the N-terminus region [109]. Especially the four residues of JIP1, Arg-156, Pro-157, Leu-160, and Leu-162, are important for the JIP1-JNK interaction [109]. The physical interaction between JIP1 and JNK is required for JIP1 mediated JNK activity enhancement [132, 133]. There are three JNK proteins, encoded by *Mapk8* (JNK1), *Mapk9* (JNK2) and *Mapk10* (JNK3) genes [134]. JIP1 can interact with all three JNK proteins with a higher affinity compared with JIP2 [110]. Additionally, alternative

splicing of the genes encoding the JNK proteins results in a total of ten JNK isoforms; four JNK1 (JNK1α1, JNK1α2, JNK1β1, JNK1β2), four JNK2 (JNK1α1, JNK1α2, JNK1β1, JNK1β2), and two JNK3 (JNK3α1, JNK3α2) [135]. The binding affinity of JIP1 is higher to all JNK1 and JNK3 isoforms, compared with the JNK2 isoforms; except for the JNK2α1 isoform, which shows a higher affinity to JIP1 compared with other JNK2 isoforms [110].

JIP1 can be phosphorylated on multiple sites and the phosphorylation status of JIP1 can contribute to the regulation of JNK signaling mediated by JIP1 [136]. For instance, phosphorylation of JIP1-Thr^{103} by JNK can promote JIP1-mediated JNK activation by regulating MLK3 dynamics [137, 138]. In addition, JIP1 can mediate free fatty acid-induced JNK activation through interacting MLK3 [70, 71], SRC [69] and VAV [73]; and upon lipid stimulation, phosphorylation of JIP1 on Tyr^{429} and Tyr^{427} mediates lipid shaft localization of JIP1 and its interaction with SRC [73]. On the other hand, interaction of JIP1 with MKP7, a phosphatase, can act as a negative regulator of JIP1-mediated JNK activation [139].

JIP1 can also interact with AKT (Protein kinase B), which is a serine/threonine protein kinase implicated in various cellular functions including metabolic regulation, cell survival and motility [140]. It is proposed that JIP1 can promote AKT activation by interacting with the PH domain on AKT, and increasing PI3K dependent AKT activation under submaximal growth factor concentrations [141, 142]. The interaction of JIP1 with AKT does not require the

24

JNK binding domain of JIP1 [141]. However, overexpression of AKT can suppress JIP1-JNK interaction, and consequently decrease JIP1-mediated JNK activation [141-143]. These data suggest that the role of JIP1 in AKT and JNK activation is either mutually exclusive or competitive, or both.

Notch can also inhibit JIP1-mediated JNK activation [144]. Notch is a cell surface receptor that is implicated in the regulation of cell faith and development [145]. Presenilin induces the cleavage of Notch1 by γ-secretase to release Notch1-IC (Active intracellular domain) [146]. The cleaved intracellular domain of Notch can interact with the JNK binding domain of JIP1 and inhibit JIP1-mediated JNK activation [144]. It is suggested that the JIP1-Notch interaction also has an inhibitory effect on the Notch signaling. In addition to the Notch, JIP1 can interact with RBP-Jk, which is a target of the active Notch-IC. JIP1 interaction with RBP-Jk results in the retention of RBP-Jk in the cytoplasmic compartment, thus inhibiting its transcriptional effects. Concordantly, $Jip1^{-/-}$ MEFs show increased Notch1 activity [147].

Another noteworthy interaction partner of JIP1 is the vaccinia virus protein B1K Kinase, and TAK1 (MAP3K). B1R kinase can interact with JIP1; and this interaction can facilitate the JIP1-TAK1 interaction, which may play a role for the virulence [148]. This represents an example of how an external pathogen can use the scaffold proteins to alter the cellular functions in its own advantage.

JIP1 can interact with a wide-array of proteins implicated in multiple cellular functions, suggesting a central role for JIP1 in the regulation of cellular signaling (Table 1.2.)

Table 1.2. Interaction partners of JIP1. (Please note that binging site information is mostly limited to co-expression and mutation analysis, thus may not reflect all specific residues that are important for interaction.

JIP1-interacting protein [ref]	Binding site on interacting protein	Binding site on JIP1	Functional Relevance	Interaction with other JIP proteins
JIP1 [109, 149]	SH3	SH3	Cellular stress response	JIP2,3,4 [150]
JNK [109]	C terminus[133] (aa Glu^{339}, Glu^{331})	JBD (aa 156-162)	Cellular stress response	JIP2, JIP3 [112], JIP4
MKK7β1 [132, 133]	N terminus[133] aa 146-246	aa 283-660 aa 200-211[133]	Cellular stress response	JIP2, JIP3 [112]
MLK2-3 [132]		aa 471-660	Cellular stress response	JIP2, JIP3 [112]
DLK [132]	N Terminus[133, 151] (aa Phe^{177}, Leu^{397}, Asp^{398})	aa 471-660	Cellular stress response	JIP2
HPK1 [132]	Possibly indirect	Possibly indirect	Cellular stress response	-
LZK [152]	Kinase Catalytic Domain	C Terminus	Cellular stress response	-
Src Family [153, 154] Lyn, Fyn, cSrc, Yes	SH2 Domain	unknown	Cellular Stress Response	-

JIP1-interacting protein [ref]	Binding site on interacting protein	Binding site on JIP1	Functional Relevance	Interaction with other JIP proteins
VAV [73]	SH2 Domain	unknown	Cellular stress response	-
SHIP2 [155]	unknown	unknown	Cellular stress response	-
MKP7 [139]	aa 394-443	C-Terminus	Cellular stress response	JIP2
c-Abl [156]	unknown	unknown	Axonal Growth Cytoskeleton Organization	-
RhoGEF [157]	C Terminus aa 1543-1615	PTB domain	Cytoskeletal dynamics Actin organization	-
Tau (MAP) [158]	unknown	unknown	Cytoskeletal dynamics Alzheimer's Disease	-
Kinesin Light Chain [118, 119]	TPR Coiled coil[159]	C Terminus	Anterograde Trafficking	JIP2, JIP3, JIP4 [114, 120]
Kinesin Heavy Chain [160] (KIF5)	Stalk and tail	Aa307-700	Anterograde Trafficking	
ARP1 [150]	unknown	unknown	Dynein mediated retrograde trafficking	-
P150^{glued} [160]	C-Terminus	aa 307-700	Dynein mediated retrograde trafficking	-
Rab10 [161]	unknown	aa 283-649	Vesicle transport Neuron polarization	-
AKT-1 [141]	PH Domain (aa 61-112)	aa 287–487 & aa 488–711	Cell survival, metabolism	-

JIP1-interacting protein [ref]	Binding site on interacting protein	Binding site on JIP1	Functional Relevance	Interaction with other JIP proteins
IRS1, IRS2 [150]	unknown	aa 282-470	Insulin Signaling	JIP2
RalGDS [162]	unknown	unknown	AKT signaling Cellular metabolism	-
LRP2 [163]	unknown	PTD domain	Low Density Lipoprotein receptor signaling	JIP2
Megalin [163]	unknown	PTD domain	Low Density Lipoprotein receptor signaling	JIP2
ApoER-2 [163, 164]	C-terminus (Isoform-specific proline rich domain)	PTD domain	Low Density Lipoprotein receptor signaling, Endocytosis	JIP2
Pax2 [165]	Unknown	Unknown	Development (Kidney, optic cup, etc.)	-
Notch1 [144]	IC domain	JBD	Cell growth and differentiation	-
RBP-Jk [147]	Proline Rich Domain	C-terminus (SH3)	Notch Signaling	-
APP [166, 167]	Cytoplasmic domain (AID)	PTB	Alzheimer's Disease	-
Viral B1R Kinase [148]	unknown	aa 282-660	Vaccinia Virus Virulence	-
TAK1 [148]	unknown	unknown	Vaccinia Virus Virulence	-
VRK2 [168]	unknown	aa 471-660	IL1β signaling	-
LC3B [169]	unknown	aa 312-331 (LIR Domain)	Autophagy	-
AnkyrinG [150]	unknown	unknown	Ion channel regulation	-

JIP1-interacting protein [ref]	Binding site on interacting protein	Binding site on JIP1	Functional Relevance	Interaction with other JIP proteins
Heat Shock Proteins HSP90, HSP70 [150]	unknown	unknown	Stress Response	-
GRP58 [150]	unknown	unknown	Stress Response Protein folding	-
Proteosomal Proteins Adrm1, Pad1 [150]	unknown	unknown	Proteosomal Degradation	-

Table 1.2. cont'd

1.3.5 Physiological function of JIP1 in vivo and in energy homeostasis

Thompson et al. suggested that homozygous JIP1 deletion results in early embryonic cell death. Thus, JIP1 deficient mice were not viable [170]. On the other hand, JIP1 deficient mouse lines established by two independent groups, Whitmarsh et al., and Im et al., were viable and fertile with expected Mendelian ratios [119, 171]. All three studies reported a complete ablation of both ~90 KD and ~110 KD JIP1 proteins. However, Whitmarsh et al. and Im et al. targeted a smaller region around the exon3, while Thompson et al. targeted the complete *Mapk8ip1* locus [119, 170, 171]. There is a predicted microRNA coding sequence (Mir7000) in intron4 of *Mapk8ip1* (Figure 1.9.).
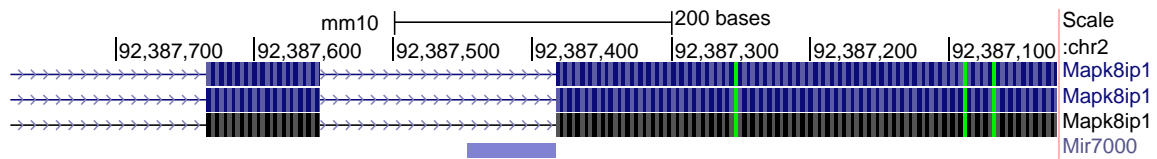
Figure 1.9. Mapk8ip1 exon4-exon5 region showing Mir7000 on intron 4. The scheme is obtained from UCSC Genome Browser (GRCm38/mm10).

Moreover, a previously uncharacterized gene (1700029I15Rik) is located at ~75bp downstream of the 3' end of the *Mapk8ip1* gene (Figure 1.10.) [172]. Thus, it is possible that the deletion of the complete *Mapk8ip1* locus would affect multiple gene functions, which may contribute to the lethal phenotype observed by Thompson et al [170].
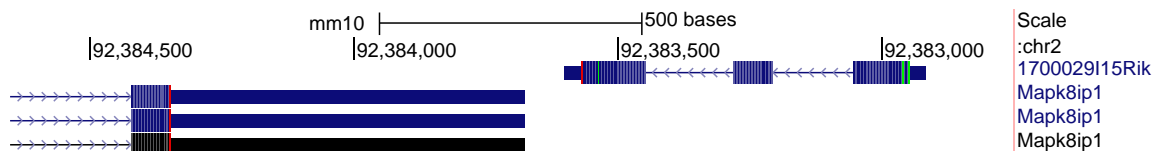
Figure 1.10. Mapk8ip1 exon12 and 3'UTR region showing the close localization of the annotated gene 1700029I15Rik. The scheme is obtained from UCSC Genome Browser (GRCm38/mm10).

JIP1 deficient mice established by Whitmarsh et al. and Im et al. did not show a growth abnormality but there was a protective effect of JIP1 deficiency under some stress conditions. For instance, kainic acid (excitotoxic stress) or oxygen and glucose deprivation-induced JNK activation was suppressed in JIP1

deficient neurons. Consequently, JIP1-deficient neurons were resistant to the

stress induced apoptosis [119]. Moreover, JIP1-deficient mouse brains showed

decreased infarct volume after ischemia-reperfusion, in addition to a decrease in

the P-JNK levels, compared with WT mouse brains [171].

Earlier studies proposed that JIP1 is localized to the nucleus in β-cells and

may promote GLUT-2 expression [126]. In addition, a S59N mutation in human

*Mapk8ip1/*JIP1 locus was associated with a late onset type-II diabetes.

However, JIP1 S59N mutation was accompanied with a *Pdx-1* mutation in these

patients, suggesting a complex genetic contribution [173]. On the other hand,

JIP1 deficient mice did not show a diabetic phenotype [150, 174]. Thus, the role

of JIP1 in pancreas β-cell is still unclear.

Obesity is another stress condition that can activate JNK in many tissues

[63]. JIP1 deficient mice were less obese compared with the WT controls after a

high fat diet challenge [71]. This leaner phenotype was accompanied by a

decrease in the obesity-induced JNK activation in adipose tissue, an increase in

insulin sensitivity [174]. Moreover, mice harboring a point mutation on a JNK

phosphorylation site of JIP1 (*Mapk8ip1/Jip1*^{Thr103Ala}) that disrupts JIP1-mediated

JNK activation also showed suppressed JNK activation in the adipose tissue

after a high fat diet challenge [138]. *Jip1*^{Thr103Ala} mutant mice were more insulin

sensitive compared with the wild type controls [138]. In a more recent study, a

JIP1 mutant mice with point mutations in the JNK binding domain of JIP1

(*Mapk8ip1/Jip1*$^{\Delta JBD}$) also showed a decreased JNK activation caused by

decreased JIP1-JNK interaction, and improved metabolic phenotype on high fat diet [73].

In consideration with the known role of JNK in metabolic regulation (please see section 1.2.2.), these data suggest that the improved metabolic phenotype observed in JIP1 deficient mice may be a consequence of a decrease in high fat diet-induced JNK activation. On the other hand, given the multiple protein interactors of JIP1, and the complexity of the metabolic regulation, it is thus crucial to evaluate the tissue specific roles of JIP1 to better understand its role in metabolism.

1.3.6 Subcellular localization of JIP1 and its role in intracellular trafficking

JIP1 primarily exhibits a cytoplasmic localization and it is mostly absent from the nucleus [109, 110, 157]. Moreover, overexpression of JIP1 caused sequestration of its binding partners, JNK and MKK7, in the cytoplasm together with JIP1 [109, 132]; this finding supports the idea that JIP1 can influence the intracellular localization of its binding partners.

While exogenously expressed JIP1 is detected throughout the cytoplasm, endogenous JIP1 in insulinoma cells was detected peripherally, adjacent to the cell membrane at the cell protrusions [110]. Furthermore, microscopic analysis of brain sections from mice and rats show that JIP1 is also localized peripherally in the neurons [125, 175]. However, the peripheral localization of JIP1 can dynamically be regulated. For instance, while undifferentiated N1E-115

neuroblastoma cells show diffuse cytoplasmic JIP1 localization, as these cells are differentiated to neurons, JIP1 becomes concentrated at the extending neurites [157]. Moreover, when neurons were stimulated with an anoxic stress to activate JNK, peripherally localized JIP1 accumulated at the perinuclear region, where it co-localized with phospho-JNK [119]. These data suggest that depending on the functional need, JIP1 can dynamically be mobilized from one compartment of the cell to another.

Kinesin and dynein motor proteins can mediate intracellular trafficking of their cargos [176]. Kinesin is composed of two kinesin heavy chains and two kinesin light chains. In the absence of cargo binding, kinesin light chains keep the complex in an inactive state. Upon activation, kinesin moves towards the plus end on microtubules, carrying its cargo to the cell periphery. Dynein motor activity is mediated by the dynactin, which is a 23-subunit complex [177]. When activated, dynein motor moves towards the minus end of the microtubules, to the perinuclear region.

The terminal residues at the C-terminus of JIP1 interacts with the TPR (Tetratricopeptide Repeat) domain of the kinesin light chain, and this interaction is required for the anterograde transport and peripheral localization of JIP1 in neurons [118-120]. A JIP1 construct that is missing JNK binding domain can still be localized to the axon tips when ectopically expressed in neuronal cell lines. This suggests that either JNK binding is not essential for kinesin mediated JIP1 trafficking, or JIP1 dimerization with endogenous JIP proteins, which can still bind

JNK, may compensate for the role of the direct JIP1-JNK interaction [118, 178]. Nevertheless, a more recent study using JIP1 knockout neurons demonstrated that the JNK binding of JIP1 is not essential for the role of JIP1 in kinesin-mediated fast-velocity axonal transport [159].

JIP1 can also interact with proteins in the dynactin complex, such as ARP1 (actin related protein centractin), and p150^{glued} [150, 160, 177, 179]. The interaction of JIP1 with kinesin and dynactin is implicated in the regulation of bidirectional trafficking of various cargos, such as Amyloid Precursor Protein [159, 180, 181] (APP), mitochondria [121], synaptic vesicles, and autophagosomes [169]. However, there is also evidence for a non-essential role for JIP1 in cargo trafficking. For instance, *Jip1$^{-/-}$Jip2$^{-/-}$* double mutant mice did not show a major defect in the localization of mitochondria, and Synapsin-1, a synaptic vesicle marker, in cerebellar granule neurons (CGN) [153]. Additionally, JIP1 knockdown in neurons did not affect the anterograde or retrograde trafficking of APP in axons [182]. These studies suggest that, the role of JIP1 in cargo trafficking, may be essential in a specific stress condition. Mitochondria and synaptic vesicle transport defect was observed in a *Drosophila* model [183]. Thus, the phenotypic differences caused by JIP1 dysfunction may reflect the differences between *Drosophila* versus mammalian JIP1, or a cell and context specific effect. Furthermore, JIP3-JIP1 heterodimer interaction with kinesin can co-operate for vesicle trafficking, and this role of JIP3 in the absence of JIP1 and JIP2 may compensate for the trafficking in the mammalian brain tissue [178,

184]. For instance, JIP1 ectopic expression can partially rescue the brain developmental defects in JIP3 deficient mice [185]. In conclusion, the role of JIP1 in the cargo transport may be highly specific to certain stress conditions in specific cells, thus, more research is needed to understand its regulation.

Although JIP1 can mediate the cargo trafficking, early studies proposed that JIP1 binding to kinesin is not sufficient to activate the motor protein, and the presence of some regulatory mechanism is needed to activate kinesin once JIP1 is loaded [186, 187]. Co-operative binding of JIP1 to kinesin light chain and Fez1 to kinesin heavy chain was proposed as a mechanism that may activate kinesin [187]. However, more recent studies showed that JIP1 can interact not only with kinesin light chain but also with kinesin heavy chain. The JIP1-Kinesin heavy chain interaction was sufficient to activate kinesin motor transport on microtubules [160]. It was proposed that the selectivity of JIP1 between kinesin and dynein complexes dependent on the phosphorylation status of JIP1. Concordantly, phosphorylation of JIP1 on Ser^{421} enhanced the anterograde transport of APP supporting a possible role for JNK activation on anterograde trafficking [160]. On the other hand, MAP Kinase Phosphatase-1 activity enhanced JIP1-mediated retrograde transport in neurons [169].

Despite this evidence for a role of JNK in anterograde trafficking by phosphorylating JIP1, there are studies suggesting an alternative or an additional role for JNK in the regulation of kinesin-mediated cargo trafficking. For instance, in *Drosophila*, activation of the JNK pathway resulted in a decrease JIP1-kinesin

interactions [183]. In addition, Morfini et al. proposed that JNK can inhibit fast axonal transport by phosphorylating kinesin and inhibiting kinesin-microtubule interactions [188, 189]. These studies suggest that activated JNK may enhance cargo dissociation from the kinesin and microtubules.

In cultured neurons, JIP1 is detected in a subset of neurites (cell protrusion) [190]. This result suggests that the peripheral localization of JIP1 in selected neurites require some regulatory mechanisms other than kinesin interaction. Reed et al. showed that JIP1 was preferentially trafficked to the neurites that have acetylated microtubules, concordantly a genetic mutation that causes acetylation of all cellular microtubules resulted in a non-preferential localization of JIP1 to the all neurites [190]. This data highlights the importance of a possible crosstalk between the scaffold proteins and the post-translational modifications of microtubules in selective cargo trafficking.

Taken together, although sufficient evidence implies a role for JIP1 in the intracellular cargo trafficking, the regulatory mechanisms, and the relevance to the cellular function, especially in the context of endocrine cells is unclear.

1.4 Rationale and Objectives

1.4.1 Examining the role of JIP1-JNK pathway in beta cell function

Although the role of JNK in the regulation of energy metabolism is extensively studied in many tissues with gene targeting strategies (Discussed in section 1.2.2.), the role of JIP1 and JNK in pancreatic β-cells is unknown.

Lanuza-Masdeu et al. showed that pancreas β-cell specific over-expression of MKK7 increased JNK activation in β-cells and resulted in decreased insulin secretion [191]. In addition, Kaneto et al. reported that activation of JNK in β-cells mediates oxidative-stress induced inhibition of insulin expression [192]. However, the conclusions in these studies regarding the role of JNK in β-cells were driven by indirect evidence and treatment of β-cells with non-specific JNK inhibitors.

Bonny et al. suggested that JIP1 can localize to the nucleus to promote Glut-2 (Glucose transporter-2) expression in beta cells [126]. But, these studies were performed mostly in *ex-vivo* system. Furthermore, the nuclear localization of JIP1 is questionable since many studies showed non-nuclear JIP1 localization in the b-cells, in addition to the neurons [109, 110, 125, 132, 157, 175].

Taken together, it is still a question whether JIP1-JNK pathway regulates insulin production and secretion in *in-vivo* system. To test if there is a role for JIP1 in β-cell function, I have ablated the *Jip1/Mapk8ip1* gene specifically in pancreas β-cells and evaluated the b-cell function with *in-vivo* and *ex-vivo* methods. Results of these studies are presented and discussed in Chapter-2.

1.4.2 Examining the role of JNK pathway in autophagy

Autophagy is implicated in the regulation of energy metabolism and endocrine cell function (Discussed in section 1.1.4.). Previous studies imply a role for both JIP1 and JNK in the regulation of autophagy flux. Fu et al.

suggested that JIP1-mediated autophagosome trafficking from neuronal axon tips to the cellular soma is important for autolysosome formation and neuronal autophagy flux [169]. On the other hand, there are contrary results regarding the effect of JNK on autophagy. Wei et al. proposed that starvation-induced phosphorylation of Bcl-2 by JNK is required for Beclin-1 release, and autophagy induction [193]. In contrary, Xu at al. reported that JNK deficient primary neurons show increased autophagy, and this effect was related to the differential FOXO-dependent expression of autophagy related genes in JNK deficient cells [194].

These data suggest that different mechanisms may account for the opposing effects of JNK on the regulation of autophagy in different cell types. Since Bcl-2 can also be phosphorylated by other kinases [195-197], I first re-evaluated the mechanism of the JNK-mediated autophagy in mouse embryonic fibroblasts (MEF). Furthermore, I have also tested the role of JNK in autophagy in primary hepatocytes and kidney epithelial cells to identify possible differences of the cell specific JNK effect on autophagy. Results of this study are presented and discussed in more detail in Chapter-3.

1.5 References for Chapter 1

1.   LaManna JC, Salem N, Puchowicz M, Erokwu B, Koppaka S, Flask C, Lee Z: **Ketones suppress brain glucose consumption.** *Adv Exp Med Biol* 2009, **645:**301-306.
2.   Pope DW, Dansky D: **Hyperosmolar hyperglycemic nonketotic coma.** *Emerg Med Clin North Am* 1989, **7:**849-857.

3.   Williams TF: **Diabetes mellitus.** *Clin Endocrinol Metab* 1981, **10:**179-194.

4.   Owen OE, Reichard GA, Jr., Patel MS, Boden G: **Energy metabolism in feasting and fasting.** *Adv Exp Med Biol* 1979, **111:**169-188.

5.   Hatting M, Tavares CDJ, Sharabi K, Rines AK, Puigserver P: **Insulin regulation of gluconeogenesis.** *Ann N Y Acad Sci* 2017.

6.   Exton JH: **Mechanisms of hormonal regulation of hepatic glucose metabolism.** *Diabetes Metab Rev* 1987, **3:**163-183.

7.   Shimazu T: **Central nervous system regulation of liver and adipose tissue metabolism.** *Diabetologia* 1981, **20 Suppl:**343-356.

8.   Mullur R, Liu YY, Brent GA: **Thyroid hormone regulation of metabolism.** *Physiol Rev* 2014, **94:**355-382.

9.   Umpleby AM, Russell-Jones DL: **The hormonal control of protein metabolism.** *Baillieres Clin Endocrinol Metab* 1996, **10:**551-570.

10.   Cherrington AD, Williams PE, Shulman GI, Lacy WW: **Differential time course of glucagon's effect on glycogenolysis and gluconeogenesis in the conscious dog.** *Diabetes* 1981, **30:**180-187.

11.   Konig M, Bulik S, Holzhutter HG: **Quantifying the contribution of the liver to glucose homeostasis: a detailed kinetic model of human hepatic glucose metabolism.** *PLoS Comput Biol* 2012, **8:**e1002577.

12.   Anstall HB: **Aspects of glycogen synthesis and degradation.** *Am J Clin Pathol* 1968, **50:**3-11.

13.   Kitabchi AE: **Hormonal control of glucose metabolism.** *Otolaryngol Clin North Am* 1975, **8:**335-344.

14.   Peterhoff M, Sieg A, Brede M, Chao CM, Hein L, Ullrich S: **Inhibition of insulin secretion via distinct signaling pathways in alpha2-adrenoceptor knockout mice.** *Eur J Endocrinol* 2003, **149:**343-350.

15.   Goldstein DS: **Adrenal responses to stress.** *Cell Mol Neurobiol* 2010, **30:**1433-1440.

16. Sacca L, Eigler N, Cryer PE, Sherwin RS: **Insulin antagonistic effects of epinephrine and glucagon in the dog.** *Am J Physiol* 1979, **237:**E487-492.

17. Sherwin RS, Shamoon H, Hendler R, Sacca L, Eigler N, Walesky M: **Epinephrine and the regulation of glucose metabolism: effect of diabetes and hormonal interactions.** *Metabolism* 1980, **29:**1146-1154.

18. Bista B, Beck N: **Cushing syndrome.** *Indian J Pediatr* 2014, **81:**158-164.

19. Lee MJ, Pramyothin P, Karastergiou K, Fried SK: **Deconstructing the roles of glucocorticoids in adipose tissue biology and the development of central obesity.** *Biochim Biophys Acta* 2014, **1842:**473-481.

20. Wildbrett J, Nagel M, Theissig F, Gaertner HJ, Gromeier S, Fischer S, Hanefeld M: **[An unusual picture of insulinoma in type-2 diabetes mellitus and morbid obesity].** *Dtsch Med Wochenschr* 1999, **124:**248-252.

21. Friedman JM, Halaas JL: **Leptin and the regulation of body weight in mammals.** *Nature* 1998, **395:**763-770.

22. Montague CT, Farooqi IS, Whitehead JP, Soos MA, Rau H, Wareham NJ, Sewter CP, Digby JE, Mohammed SN, Hurst JA, et al: **Congenital leptin deficiency is associated with severe early-onset obesity in humans.** *Nature* 1997, **387:**903-908.

23. Clement K, Vaisse C, Lahlou N, Cabrol S, Pelloux V, Cassuto D, Gourmelen M, Dina C, Chambaz J, Lacorte JM, et al: **A mutation in the human leptin receptor gene causes obesity and pituitary dysfunction.** *Nature* 1998, **392:**398-401.

24. Ingalls AM, Dickie MM, Snell GD: **Obese, a new mutation in the house mouse.** *J Hered* 1950, **41:**317-318.

25.   Zhang Y, Proenca R, Maffei M, Barone M, Leopold L, Friedman JM: **Positional cloning of the mouse obese gene and its human homologue.** *Nature* 1994, **372:**425-432.

26.   Czech MP: **Insulin action and resistance in obesity and type 2 diabetes.** *Nat Med* 2017, **23:**804-814.

27.   Hardy OT, Czech MP, Corvera S: **What causes the insulin resistance underlying obesity?** *Curr Opin Endocrinol Diabetes Obes* 2012, **19:**81-87.

28.   Ertunc ME, Hotamisligil GS: **Lipid signaling and lipotoxicity in metaflammation: indications for metabolic disease pathogenesis and treatment.** *J Lipid Res* 2016, **57:**2099-2114.

29.   Guilherme A, Virbasius JV, Puri V, Czech MP: **Adipocyte dysfunctions linking obesity to insulin resistance and type 2 diabetes.** *Nat Rev Mol Cell Biol* 2008, **9:**367-377.

30.   Sharma RB, Alonso LC: **Lipotoxicity in the pancreatic beta cell: not just survival and function, but proliferation as well?** *Curr Diab Rep* 2014, **14:**492.

31.   Shimabukuro M, Zhou YT, Levi M, Unger RH: **Fatty acid-induced beta cell apoptosis: a link between obesity and diabetes.** *Proc Natl Acad Sci U S A* 1998, **95:**2498-2502.

32.   Donath MY, Boni-Schnetzler M, Ellingsgaard H, Ehses JA: **Islet inflammation impairs the pancreatic beta-cell in type 2 diabetes.** *Physiology (Bethesda)* 2009, **24:**325-331.

33.   Donath MY, Dalmas E, Sauter NS, Boni-Schnetzler M: **Inflammation in obesity and diabetes: islet dysfunction and therapeutic opportunity.** *Cell Metab* 2013, **17:**860-872.

34.   Mizushima N, Ohsumi Y, Yoshimori T: **Autophagosome formation in mammalian cells.** *Cell Struct Funct* 2002, **27:**421-429.

35. Hung CM, Garcia-Haro L, Sparks CA, Guertin DA: **mTOR-dependent cell survival mechanisms.** *Cold Spring Harb Perspect Biol* 2012, **4**.

36. Mizushima N, Yoshimori T, Ohsumi Y: **The role of Atg proteins in autophagosome formation.** *Annu Rev Cell Dev Biol* 2011, **27:**107-132.

37. Yang Z, Klionsky DJ: **An overview of the molecular mechanism of autophagy.** *Curr Top Microbiol Immunol* 2009, **335:**1-32.

38. Wu X, Won H, Rubinsztein DC: **Autophagy and mammalian development.** *Biochem Soc Trans* 2013, **41:**1489-1494.

39. Devenish RJ, Klionsky DJ: **Autophagy: mechanism and physiological relevance 'brewed' from yeast studies.** *Front Biosci (Schol Ed)* 2012, **4:**1354-1363.

40. Mizushima N, Komatsu M: **Autophagy: renovation of cells and tissues.** *Cell* 2011, **147:**728-741.

41. White E: **The role for autophagy in cancer.** *J Clin Invest* 2015, **125:**42-46.

42. Lavallard VJ, Meijer AJ, Codogno P, Gual P: **Autophagy, signaling and obesity.** *Pharmacol Res* 2012, **66:**513-525.

43. Chen ZF, Li YB, Han JY, Wang J, Yin JJ, Li JB, Tian H: **The double-edged effect of autophagy in pancreatic beta cells and diabetes.** *Autophagy* 2011, **7:**12-16.

44. Singh R, Kaushik S, Wang Y, Xiang Y, Novak I, Komatsu M, Tanaka K, Cuervo AM, Czaja MJ: **Autophagy regulates lipid metabolism.** *Nature* 2009, **458:**1131-1135.

45. Lim YM, Lim H, Hur KY, Quan W, Lee HY, Cheon H, Ryu D, Koo SH, Kim HL, Kim J, et al: **Systemic autophagy insufficiency compromises adaptation to metabolic stress and facilitates progression from obesity to diabetes.** *Nat Commun* 2014, **5:**4934.

46. Kim KH, Jeong YT, Oh H, Kim SH, Cho JM, Kim YN, Kim SS, Kim DH, Hur KY, Kim HK, et al: **Autophagy deficiency leads to protection from**

obesity and insulin resistance by inducing Fgf21 as a mitokine. *Nat Med* 2013, **19:**83-92.

47. Lan T, Morgan DA, Rahmouni K, Sonoda J, Fu X, Burgess SC, Holland WL, Kliewer SA, Mangelsdorf DJ: **FGF19, FGF21, and an FGFR1/beta-Klotho-Activating Antibody Act on the Nervous System to Regulate Body Weight and Glycemia.** *Cell Metab* 2017, **26:**709-718 e703.

48. Staiger H, Keuper M, Berti L, Hrabe de Angelis M, Haring HU: **Fibroblast Growth Factor 21-Metabolic Role in Mice and Men.** *Endocr Rev* 2017, **38:**468-488.

49. Kaushik S, Arias E, Kwon H, Lopez NM, Athonvarangkul D, Sahu S, Schwartz GJ, Pessin JE, Singh R: **Loss of autophagy in hypothalamic POMC neurons impairs lipolysis.** *EMBO Rep* 2012, **13:**258-265.

50. Jung HS, Chung KW, Won Kim J, Kim J, Komatsu M, Tanaka K, Nguyen YH, Kang TM, Yoon KH, Kim JW, et al: **Loss of autophagy diminishes pancreatic beta cell mass and function with resultant hyperglycemia.** *Cell Metab* 2008, **8:**318-324.

51. Ebato C, Uchida T, Arakawa M, Komatsu M, Ueno T, Komiya K, Azuma K, Hirose T, Tanaka K, Kominami E, et al: **Autophagy is important in islet homeostasis and compensatory increase of beta cell mass in response to high-fat diet.** *Cell Metab* 2008, **8:**325-332.

52. Sheng Q, Xiao X, Prasadan K, Chen C, Ming Y, Fusco J, Gangopadhyay NN, Ricks D, Gittes GK: **Autophagy protects pancreatic beta cell mass and function in the setting of a high-fat and high-glucose diet.** *Sci Rep* 2017, **7:**16348.

53. Muller A, Neukam M, Ivanova A, Sonmez A, Munster C, Kretschmar S, Kalaidzidis Y, Kurth T, Verbavatz JM, Solimena M: **A Global Approach for Quantitative Super Resolution and Electron Microscopy on Cryo and Epoxy Sections Using Self-labeling Protein Tags.** *Sci Rep* 2017, **7:**23.

54. Claude-Taupin A, Jia J, Mudd M, Deretic V: **Autophagy's secret life: secretion instead of degradation.** *Essays Biochem* 2017, **61:**637-647.

55. Morrison DK, Davis RJ: **Regulation of MAP kinase signaling modules by scaffold proteins in mammals.** *Annu Rev Cell Dev Biol* 2003, **19:**91-118.

56. Schaeffer HJ, Weber MJ: **Mitogen-activated protein kinases: specific messages from ubiquitous messengers.** *Mol Cell Biol* 1999, **19:**2435-2444.

57. Leng Y, Steiler TL, Zierath JR: **Effects of insulin, contraction, and phorbol esters on mitogen-activated protein kinase signaling in skeletal muscle from lean and ob/ob mice.** *Diabetes* 2004, **53:**1436-1444.

58. Sabio G, Davis RJ: **TNF and MAP kinase signalling pathways.** *Semin Immunol* 2014, **26:**237-245.

59. Prusty D, Park BH, Davis KE, Farmer SR: **Activation of MEK/ERK signaling promotes adipogenesis by enhancing peroxisome proliferator-activated receptor gamma (PPARgamma) and C/EBPalpha gene expression during the differentiation of 3T3-L1 preadipocytes.** *J Biol Chem* 2002, **277:**46226-46232.

60. Ozaki KI, Awazu M, Tamiya M, Iwasaki Y, Harada A, Kugisaki S, Tanimura S, Kohno M: **Targeting the ERK signaling pathway as a potential treatment for insulin resistance and type 2 diabetes.** *Am J Physiol Endocrinol Metab* 2016, **310:**E643-E651.

61. Fernandez-Twinn DS, Blackmore HL, Siggens L, Giussani DA, Cross CM, Foo R, Ozanne SE: **The programming of cardiac hypertrophy in the offspring by maternal obesity is associated with hyperinsulinemia, AKT, ERK, and mTOR activation.** *Endocrinology* 2012, **153:**5961-5971.

62. Matesanz N, Bernardo E, Acin-Perez R, Manieri E, Perez-Sieira S, Hernandez-Cosido L, Montalvo-Romeral V, Mora A, Rodriguez E, Leiva-

Vega L, et al: **MKK6 controls T3-mediated browning of white adipose tissue.** *Nat Commun* 2017, **8:**856.

63.   Hirosumi J, Tuncman G, Chang L, Gorgun CZ, Uysal KT, Maeda K, Karin M, Hotamisligil GS: **A central role for JNK in obesity and insulin resistance.** *Nature* 2002, **420:**333-336.

64.   Boden G, Shulman GI: **Free fatty acids in obesity and type 2 diabetes: defining their role in the development of insulin resistance and beta-cell dysfunction.** *Eur J Clin Invest* 2002, **32 Suppl 3:**14-23.

65.   Boden G: **Role of fatty acids in the pathogenesis of insulin resistance and NIDDM.** *Diabetes* 1997, **46:**3-10.

66.   Arner P: **Insulin resistance in type 2 diabetes: role of fatty acids.** *Diabetes Metab Res Rev* 2002, **18 Suppl 2:**S5-9.

67.   Nguyen MT, Satoh H, Favelyukis S, Babendure JL, Imamura T, Sbodio JI, Zalevsky J, Dahiyat BI, Chi NW, Olefsky JM: **JNK and tumor necrosis factor-alpha mediate free fatty acid-induced insulin resistance in 3T3-L1 adipocytes.** *J Biol Chem* 2005, **280:**35361-35371.

68.   Solinas G, Naugler W, Galimi F, Lee MS, Karin M: **Saturated fatty acids inhibit induction of insulin gene transcription by JNK-mediated phosphorylation of insulin-receptor substrates.** *Proc Natl Acad Sci U S A* 2006, **103:**16454-16459.

69.   Holzer RG, Park EJ, Li N, Tran H, Chen M, Choi C, Solinas G, Karin M: **Saturated fatty acids induce c-Src clustering within membrane subdomains, leading to JNK activation.** *Cell* 2011, **147:**173-184.

70.   Kant S, Barrett T, Vertii A, Noh YH, Jung DY, Kim JK, Davis RJ: **Role of the mixed-lineage protein kinase pathway in the metabolic stress response to obesity.** *Cell Rep* 2013, **4:**681-688.

71.   Jaeschke A, Davis RJ: **Metabolic stress signaling mediated by mixed-lineage kinases.** *Mol Cell* 2007, **27:**498-508.

72.   Gadang V, Kohli R, Myronovych A, Hui DY, Perez-Tilve D, Jaeschke A: **MLK3 promotes metabolic dysfunction induced by saturated fatty acid-enriched diet.** *Am J Physiol Endocrinol Metab* 2013, **305:**E549-556.

73.   Kant S, Standen CL, Morel C, Jung DY, Kim JK, Swat W, Flavell RA, Davis RJ: **A Protein Scaffold Coordinates SRC-Mediated JNK Activation in Response to Metabolic Stress.** *Cell Rep* 2017, **20:**2775-2783.

74.   Hotamisligil GS: **Inflammation and metabolic disorders.** *Nature* 2006, **444:**860-867.

75.   Uysal KT, Wiesbrock SM, Marino MW, Hotamisligil GS: **Protection from obesity-induced insulin resistance in mice lacking TNF-alpha function.** *Nature* 1997, **389:**610-614.

76.   Kant S, Swat W, Zhang S, Zhang ZY, Neel BG, Flavell RA, Davis RJ: **TNF-stimulated MAP kinase activation mediated by a Rho family GTPase signaling pathway.** *Genes Dev* 2011, **25:**2069-2078.

77.   Brancho D, Ventura JJ, Jaeschke A, Doran B, Flavell RA, Davis RJ: **Role of MLK3 in the regulation of mitogen-activated protein kinase signaling cascades.** *Mol Cell Biol* 2005, **25:**3670-3681.

78.   Moxham CM, Tabrizchi A, Davis RJ, Malbon CC: **Jun N-terminal kinase mediates activation of skeletal muscle glycogen synthase by insulin in vivo.** *J Biol Chem* 1996, **271:**30765-30773.

79.   Sabio G, Kennedy NJ, Cavanagh-Kyros J, Jung DY, Ko HJ, Ong H, Barrett T, Kim JK, Davis RJ: **Role of muscle c-Jun NH2-terminal kinase 1 in obesity-induced insulin resistance.** *Mol Cell Biol* 2010, **30:**106-115.

80.   Sabio G, Das M, Mora A, Zhang Z, Jun JY, Ko HJ, Barrett T, Kim JK, Davis RJ: **A stress signaling pathway in adipose tissue regulates hepatic insulin resistance.** *Science* 2008, **322:**1539-1543.

81.   Sabio G, Cavanagh-Kyros J, Barrett T, Jung DY, Ko HJ, Ong H, Morel C, Mora A, Reilly J, Kim JK, Davis RJ: **Role of the hypothalamic-pituitary-**

thyroid axis in metabolic regulation by JNK1. *Genes Dev* 2010, **24:**256-264.

82. Sabio G, Cavanagh-Kyros J, Ko HJ, Jung DY, Gray S, Jun JY, Barrett T, Mora A, Kim JK, Davis RJ: **Prevention of steatosis by hepatic JNK1.** *Cell Metab* 2009, **10:**491-498.

83. Vernia S, Cavanagh-Kyros J, Barrett T, Tournier C, Davis RJ: **Fibroblast Growth Factor 21 Mediates Glycemic Regulation by Hepatic JNK.** *Cell Rep* 2016, **14:**2273-2280.

84. Vernia S, Morel C, Madara JC, Cavanagh-Kyros J, Barrett T, Chase K, Kennedy NJ, Jung DY, Kim JK, Aronin N, et al: **Excitatory transmission onto AgRP neurons is regulated by cJun NH2-terminal kinase 3 in response to metabolic stress.** *Elife* 2016, **5:**e10031.

85. Belgardt BF, Mauer J, Wunderlich FT, Ernst MB, Pal M, Spohn G, Bronneke HS, Brodesser S, Hampel B, Schauss AC, Bruning JC: **Hypothalamic and pituitary c-Jun N-terminal kinase 1 signaling coordinately regulates glucose metabolism.** *Proc Natl Acad Sci U S A* 2010, **107:**6028-6033.

86. Vernia S, Cavanagh-Kyros J, Barrett T, Jung DY, Kim JK, Davis RJ: **Diet-induced obesity mediated by the JNK/DIO2 signal transduction pathway.** *Genes Dev* 2013, **27:**2345-2355.

87. Han MS, Jung DY, Morel C, Lakhani SA, Kim JK, Flavell RA, Davis RJ: **JNK expression by macrophages promotes obesity-induced insulin resistance and inflammation.** *Science* 2013, **339:**218-222.

88. Zeke A, Misheva M, Remenyi A, Bogoyevitch MA: **JNK Signaling: Regulation and Functions Based on Complex Protein-Protein Partnerships.** *Microbiol Mol Biol Rev* 2016, **80:**793-835.

89. Pawson T, Scott JD: **Signaling through scaffold, anchoring, and adaptor proteins.** *Science* 1997, **278:**2075-2080.

90. Bhattacharyya RP, Remenyi A, Yeh BJ, Lim WA: **Domains, motifs, and scaffolds: the role of modular interactions in the evolution and wiring of cell signaling circuits.** *Annu Rev Biochem* 2006, **75:**655-680.

91. Kholodenko BN: **Cell-signalling dynamics in time and space.** *Nat Rev Mol Cell Biol* 2006, **7:**165-176.

92. Scott JD, Pawson T: **Cell signaling in space and time: where proteins come together and when they're apart.** *Science* 2009, **326:**1220-1224.

93. Whitmarsh AJ, Davis RJ: **Structural organization of MAP-kinase signaling modules by scaffold proteins in yeast and mammals.** *Trends Biochem Sci* 1998, **23:**481-485.

94. Zeke A, Lukacs M, Lim WA, Remenyi A: **Scaffolds: interaction platforms for cellular signalling circuits.** *Trends Cell Biol* 2009, **19:**364-374.

95. Good MC, Zalatan JG, Lim WA: **Scaffold proteins: hubs for controlling the flow of cellular information.** *Science* 2011, **332:**680-686.

96. Choi KY, Satterberg B, Lyons DM, Elion EA: **Ste5 tethers multiple protein kinases in the MAP kinase cascade required for mating in S. cerevisiae.** *Cell* 1994, **78:**499-512.

97. Printen JA, Sprague GF, Jr.: **Protein-protein interactions in the yeast pheromone response pathway: Ste5p interacts with all members of the MAP kinase cascade.** *Genetics* 1994, **138:**609-619.

98. Therrien M, Michaud NR, Rubin GM, Morrison DK: **KSR modulates signal propagation within the MAPK cascade.** *Genes Dev* 1996, **10:**2684-2695.

99. Garrenton LS, Young SL, Thorner J: **Function of the MAPK scaffold protein, Ste5, requires a cryptic PH domain.** *Genes Dev* 2006, **20:**1946-1958.

100. Winters MJ, Lamson RE, Nakanishi H, Neiman AM, Pryciak PM: **A membrane binding domain in the ste5 scaffold synergizes with**

gbetagamma binding to control localization and signaling in pheromone response. *Mol Cell* 2005, **20:**21-32.

101. Pryciak PM, Huntress FA: **Membrane recruitment of the kinase cascade scaffold protein Ste5 by the Gbetagamma complex underlies activation of the yeast pheromone response pathway.** *Genes Dev* 1998, **12:**2684-2697.

102. Zhang W, Sloan-Lancaster J, Kitchen J, Trible RP, Samelson LE: **LAT: the ZAP-70 tyrosine kinase substrate that links T cell receptor to cellular activation.** *Cell* 1998, **92:**83-92.

103. Lin J, Weiss A: **Identification of the minimal tyrosine residues required for linker for activation of T cell function.** *J Biol Chem* 2001, **276:**29588-29595.

104. McKay MM, Ritt DA, Morrison DK: **Signaling dynamics of the KSR1 scaffold complex.** *Proc Natl Acad Sci U S A* 2009, **106:**11022-11027.

105. Ducasse R, Wang WA, Navarro MG, Debons N, Colin A, Gautier J, Guigner JM, Guyot F, Gueroui Z: **Programmed Self-Assembly of a Biochemical and Magnetic Scaffold to Trigger and Manipulate Microtubule Structures.** *Sci Rep* 2017, **7:**11344.

106. Dueber JE, Wu GC, Malmirchegini GR, Moon TS, Petzold CJ, Ullal AV, Prather KL, Keasling JD: **Synthetic protein scaffolds provide modular control over metabolic flux.** *Nat Biotechnol* 2009, **27:**753-759.

107. Pryciak PM: **Designing new cellular signaling pathways.** *Chem Biol* 2009, **16:**249-254.

108. Bashor CJ, Helman NC, Yan S, Lim WA: **Using engineered scaffold interactions to reshape MAP kinase pathway signaling dynamics.** *Science* 2008, **319:**1539-1543.

109. Dickens M, Rogers JS, Cavanagh J, Raitano A, Xia Z, Halpern JR, Greenberg ME, Sawyers CL, Davis RJ: **A cytoplasmic inhibitor of the JNK signal transduction pathway.** *Science* 1997, **277:**693-696.

110. Yasuda J, Whitmarsh AJ, Cavanagh J, Sharma M, Davis RJ: **The JIP group of mitogen-activated protein kinase scaffold proteins.** *Mol Cell Biol* 1999, **19:**7245-7254.

111. Ito M, Yoshioka K, Akechi M, Yamashita S, Takamatsu N, Sugiyama K, Hibi M, Nakabeppu Y, Shiba T, Yamamoto KI: **JSAP1, a novel jun N-terminal protein kinase (JNK)-binding protein that functions as a Scaffold factor in the JNK signaling pathway.** *Mol Cell Biol* 1999, **19:**7539-7548.

112. Kelkar N, Gupta S, Dickens M, Davis RJ: **Interaction of a mitogen-activated protein kinase signaling module with the neuronal protein JIP3.** *Mol Cell Biol* 2000, **20:**1030-1043.

113. Lee CM, Onesime D, Reddy CD, Dhanasekaran N, Reddy EP: **JLP: A scaffolding protein that tethers JNK/p38MAPK signaling modules and transcription factors.** *Proc Natl Acad Sci U S A* 2002, **99:**14189-14194.

114. Kelkar N, Standen CL, Davis RJ: **Role of the JIP4 scaffold protein in the regulation of mitogen-activated protein kinase signaling pathways.** *Mol Cell Biol* 2005, **25:**2733-2743.

115. Schoorlemmer J, Goldfarb M: **Fibroblast growth factor homologous factors and the islet brain-2 scaffold protein regulate activation of a stress-activated protein kinase.** *J Biol Chem* 2002, **277:**49111-49119.

116. Buchsbaum RJ, Connolly BA, Feig LA: **Interaction of Rac exchange factors Tiam1 and Ras-GRF1 with a scaffold for the p38 mitogen-activated protein kinase cascade.** *Mol Cell Biol* 2002, **22:**4073-4085.

117. Matsuguchi T, Masuda A, Sugimoto K, Nagai Y, Yoshikai Y: **JNK-interacting protein 3 associates with Toll-like receptor 4 and is involved in LPS-mediated JNK activation.** *EMBO J* 2003, **22:**4455-4464.

118. Verhey KJ, Meyer D, Deehan R, Blenis J, Schnapp BJ, Rapoport TA, Margolis B: **Cargo of kinesin identified as JIP scaffolding proteins and associated signaling molecules.** *J Cell Biol* 2001, **152:**959-970.

119. Whitmarsh AJ, Kuan CY, Kennedy NJ, Kelkar N, Haydar TF, Mordes JP, Appel M, Rossini AA, Jones SN, Flavell RA, et al: **Requirement of the JIP1 scaffold protein for stress-induced JNK activation.** *Genes Dev* 2001, **15:**2421-2432.

120. Bowman AB, Kamal A, Ritchings BW, Philp AV, McGrail M, Gindhart JG, Goldstein LS: **Kinesin-dependent axonal transport is mediated by the sunday driver (SYD) protein.** *Cell* 2000, **103:**583-594.

121. Horiuchi D, Barkus RV, Pilling AD, Gassman A, Saxton WM: **APLIP1, a kinesin binding JIP-1/JNK scaffold protein, influences the axonal transport of both vesicles and mitochondria in Drosophila.** *Curr Biol* 2005, **15:**2137-2141.

122. Nguyen Q, Lee CM, Le A, Reddy EP: **JLP associates with kinesin light chain 1 through a novel leucine zipper-like domain.** *J Biol Chem* 2005, **280:**30185-30191.

123. Mooser V, Maillard A, Bonny C, Steinmann M, Shaw P, Yarnall DP, Burns DK, Schorderet DF, Nicod P, Waeber G: **Genomic organization, fine-mapping, and expression of the human islet-brain 1 (IB1)/c-Jun-amino-terminal kinase interacting protein-1 (JIP-1) gene.** *Genomics* 1999, **55:**202-208.

124. Kim IJ, Lee KW, Park BY, Lee JK, Park J, Choi IY, Eom SJ, Chang TS, Kim MJ, Yeom YI, et al: **Molecular cloning of multiple splicing variants of JIP-1 preferentially expressed in brain.** *J Neurochem* 1999, **72:**1335-1343.

125. Pellet JB, Haefliger JA, Staple JK, Widmann C, Welker E, Hirling H, Bonny C, Nicod P, Catsicas S, Waeber G, Riederer BM: **Spatial, temporal and**

subcellular localization of islet-brain 1 (IB1), a homologue of JIP-1, in mouse brain. *Eur J Neurosci* 2000, **12:**621-632.

126. Bonny C, Nicod P, Waeber G: **IB1, a JIP-1-related nuclear protein present in insulin-secreting cells.** *J Biol Chem* 1998, **273:**1843-1846.

127. Chen ZF, Paquette AJ, Anderson DJ: **NRSF/REST is required in vivo for repression of multiple neuronal target genes during embryogenesis.** *Nat Genet* 1998, **20:**136-142.

128. Abderrahmani A, Steinmann M, Plaisance V, Niederhauser G, Haefliger JA, Mooser V, Bonny C, Nicod P, Waeber G: **The transcriptional repressor REST determines the cell-specific expression of the human MAPK8IP1 gene encoding IB1 (JIP-1).** *Mol Cell Biol* 2001, **21:**7256-7267.

129. Consortium GT: **Human genomics. The Genotype-Tissue Expression (GTEx) pilot analysis: multitissue gene regulation in humans.** *Science* 2015, **348:**648-660.

130. Abe H, Murao K, Imachi H, Cao WM, Yu X, Yoshida K, Wong NC, Shupnik MA, Haefliger JA, Waeber G, Ishida T: **Thyrotropin-releasing hormone-stimulated thyrotropin expression involves islet-brain-1/c-Jun N-terminal kinase interacting protein-1.** *Endocrinology* 2004, **145:**5623-5628.

131. Tawadros T, Formenton A, Dudler J, Thompson N, Nicod P, Leisinger HJ, Waeber G, Haefliger JA: **The scaffold protein IB1/JIP-1 controls the activation of JNK in rat stressed urothelium.** *J Cell Sci* 2002, **115:**385-393.

132. Whitmarsh AJ, Cavanagh J, Tournier C, Yasuda J, Davis RJ: **A mammalian scaffold complex that selectively mediates MAP kinase activation.** *Science* 1998, **281:**1671-1674.

133. Mooney LM, Whitmarsh AJ: **Docking interactions in the c-Jun N-terminal kinase pathway.** *J Biol Chem* 2004, **279:**11843-11852.

134. Gupta S, Barrett T, Whitmarsh AJ, Cavanagh J, Sluss HK, Derijard B, Davis RJ: **Selective interaction of JNK protein kinase isoforms with transcription factors.** *EMBO J* 1996, **15:**2760-2770.

135. Coffey ET: **Nuclear and cytosolic JNK signalling in neurons.** *Nat Rev Neurosci* 2014, **15:**285-299.

136. D'Ambrosio C, Arena S, Fulcoli G, Scheinfeld MH, Zhou D, D'Adamio L, Scaloni A: **Hyperphosphorylation of JNK-interacting protein 1, a protein associated with Alzheimer disease.** *Mol Cell Proteomics* 2006, **5:**97-113.

137. Nihalani D, Wong HN, Holzman LB: **Recruitment of JNK to JIP1 and JNK-dependent JIP1 phosphorylation regulates JNK module dynamics and activation.** *J Biol Chem* 2003, **278:**28694-28702.

138. Morel C, Standen CL, Jung DY, Gray S, Ong H, Flavell RA, Kim JK, Davis RJ: **Requirement of JIP1-mediated c-Jun N-terminal kinase activation for obesity-induced insulin resistance.** *Mol Cell Biol* 2010, **30:**4616-4625.

139. Willoughby EA, Perkins GR, Collins MK, Whitmarsh AJ: **The JNK-interacting protein-1 scaffold protein targets MAPK phosphatase-7 to dephosphorylate JNK.** *J Biol Chem* 2003, **278:**10731-10736.

140. Fayard E, Tintignac LA, Baudry A, Hemmings BA: **Protein kinase B/Akt at a glance.** *J Cell Sci* 2005, **118:**5675-5678.

141. Kim AH, Yano H, Cho H, Meyer D, Monks B, Margolis B, Birnbaum MJ, Chao MV: **Akt1 regulates a JNK scaffold during excitotoxic apoptosis.** *Neuron* 2002, **35:**697-709.

142. Kim AH, Sasaki T, Chao MV: **JNK-interacting protein 1 promotes Akt1 activation.** *J Biol Chem* 2003, **278:**29830-29836.

143. Levresse V, Butterfield L, Zentrich E, Heasley LE: **Akt negatively regulates the cJun N-terminal kinase pathway in PC12 cells.** *J Neurosci Res* 2000, **62:**799-808.

144. Kim JW, Kim MJ, Kim KJ, Yun HJ, Chae JS, Hwang SG, Chang TS, Park HS, Lee KW, Han PL, et al: **Notch interferes with the scaffold function of JNK-interacting protein 1 to inhibit the JNK signaling pathway.** *Proc Natl Acad Sci U S A* 2005, **102:**14308-14313.

145. Hori K, Sen A, Artavanis-Tsakonas S: **Notch signaling at a glance.** *J Cell Sci* 2013, **126:**2135-2140.

146. De Strooper B, Annaert W, Cupers P, Saftig P, Craessaerts K, Mumm JS, Schroeter EH, Schrijvers V, Wolfe MS, Ray WJ, et al: **A presenilin-1-dependent gamma-secretase-like protease mediates release of Notch intracellular domain.** *Nature* 1999, **398:**518-522.

147. Kim MY, Ann EJ, Mo JS, Dajas-Bailador F, Seo MS, Hong JA, Jung J, Choi YH, Yoon JH, Kim SM, et al: **JIP1 binding to RBP-Jk mediates cross-talk between the Notch1 and JIP1-JNK signaling pathway.** *Cell Death Differ* 2010, **17:**1728-1738.

148. Santos CR, Blanco S, Sevilla A, Lazo PA: **Vaccinia virus B1R kinase interacts with JIP1 and modulates c-Jun-dependent signaling.** *J Virol* 2006, **80:**7667-7675.

149. Kristensen O, Guenat S, Dar I, Allaman-Pillet N, Abderrahmani A, Ferdaoussi M, Roduit R, Maurer F, Beckmann JS, Kastrup JS, et al: **A unique set of SH3-SH3 interactions controls IB1 homodimerization.** *EMBO J* 2006, **25:**785-797.

150. Standen CL, Kennedy NJ, Flavell RA, Davis RJ: **Signal transduction cross talk mediated by Jun N-terminal kinase-interacting protein and insulin receptor substrate scaffold protein complexes.** *Mol Cell Biol* 2009, **29:**4831-4840.

151. Nihalani D, Merritt S, Holzman LB: **Identification of structural and functional domains in mixed lineage kinase dual leucine zipper-bearing kinase required for complex formation and stress-activated protein kinase activation.** *J Biol Chem* 2000, **275:**7273-7279.

152. Ikeda A, Hasegawa K, Masaki M, Moriguchi T, Nishida E, Kozutsumi Y, Oka S, Kawasaki T: **Mixed lineage kinase LZK forms a functional signaling complex with JIP-1, a scaffold protein of the c-Jun NH(2)-terminal kinase pathway.** *J Biochem* 2001, **130:**773-781.

153. Kennedy NJ, Martin G, Ehrhardt AG, Cavanagh-Kyros J, Kuan CY, Rakic P, Flavell RA, Treistman SN, Davis RJ: **Requirement of JIP scaffold proteins for NMDA-mediated signal transduction.** *Genes Dev* 2007, **21:**2336-2346.

154. Nihalani D, Wong H, Verma R, Holzman LB: **Src family kinases directly regulate JIP1 module dynamics and activation.** *Mol Cell Biol* 2007, **27:**2431-2441.

155. Xie J, Onnockx S, Vandenbroere I, Degraef C, Erneux C, Pirson I: **The docking properties of SHIP2 influence both JIP1 tyrosine phosphorylation and JNK activity.** *Cell Signal* 2008, **20:**1432-1441.

156. Dajas-Bailador F, Jones EV, Whitmarsh AJ: **The JIP1 scaffold protein regulates axonal development in cortical neurons.** *Curr Biol* 2008, **18:**221-226.

157. Meyer D, Liu A, Margolis B: **Interaction of c-Jun amino-terminal kinase interacting protein-1 with p190 rhoGEF and its localization in differentiated neurons.** *J Biol Chem* 1999, **274:**35113-35118.

158. Ittner LM, Ke YD, Gotz J: **Phosphorylated Tau interacts with c-Jun N-terminal kinase-interacting protein 1 (JIP1) in Alzheimer disease.** *J Biol Chem* 2009, **284:**20909-20916.

159. Chiba K, Araseki M, Nozawa K, Furukori K, Araki Y, Matsushima T, Nakaya T, Hata S, Saito Y, Uchida S, et al: **Quantitative analysis of APP axonal transport in neurons: role of JIP1 in enhanced APP anterograde transport.** *Mol Biol Cell* 2014, **25:**3569-3580.

160. Fu MM, Holzbaur EL: **JIP1 regulates the directionality of APP axonal transport by coordinating kinesin and dynein motors.** *J Cell Biol* 2013, **202:**495-508.

161. Deng CY, Lei WL, Xu XH, Ju XC, Liu Y, Luo ZG: **JIP1 mediates anterograde transport of Rab10 cargos during neuronal polarization.** *J Neurosci* 2014, **34:**1710-1723.

162. Hao Y, Wong R, Feig LA: **RalGDS couples growth factor signaling to Akt activation.** *Mol Cell Biol* 2008, **28:**2851-2859.

163. Gotthardt M, Trommsdorff M, Nevitt MF, Shelton J, Richardson JA, Stockinger W, Nimpf J, Herz J: **Interactions of the low density lipoprotein receptor gene family with cytosolic adaptor and scaffold proteins suggest diverse biological functions in cellular communication and signal transduction.** *J Biol Chem* 2000, **275:**25616-25624.

164. Stockinger W, Brandes C, Fasching D, Hermann M, Gotthardt M, Herz J, Schneider WJ, Nimpf J: **The reelin receptor ApoER2 recruits JNK-interacting proteins-1 and -2.** *J Biol Chem* 2000, **275:**25625-25632.

165. Cai Y, Lechner MS, Nihalani D, Prindle MJ, Holzman LB, Dressler GR: **Phosphorylation of Pax2 by the c-Jun N-terminal kinase and enhanced Pax2-dependent transcription activation.** *J Biol Chem* 2002, **277:**1217-1222.

166. Scheinfeld MH, Roncarati R, Vito P, Lopez PA, Abdallah M, D'Adamio L: **Jun NH2-terminal kinase (JNK) interacting protein 1 (JIP1) binds the cytoplasmic domain of the Alzheimer's beta-amyloid precursor protein (APP).** *J Biol Chem* 2002, **277:**3767-3775.

167. Taru H, Iijima K, Hase M, Kirino Y, Yagi Y, Suzuki T: **Interaction of Alzheimer's beta -amyloid precursor family proteins with scaffold proteins of the JNK signaling cascade.** *J Biol Chem* 2002, **277:**20070-20078.

168. Blanco S, Sanz-Garcia M, Santos CR, Lazo PA: **Modulation of interleukin-1 transcriptional response by the interaction between VRK2 and the JIP1 scaffold protein.** *PLoS One* 2008, **3:**e1660.

169. Fu MM, Nirschl JJ, Holzbaur ELF: **LC3 binding to the scaffolding protein JIP1 regulates processive dynein-driven transport of autophagosomes.** *Dev Cell* 2014, **29:**577-590.

170. Thompson NA, Haefliger JA, Senn A, Tawadros T, Magara F, Ledermann B, Nicod P, Waeber G: **Islet-brain1/JNK-interacting protein-1 is required for early embryogenesis in mice.** *J Biol Chem* 2001, **276:**27745-27748.

171. Im JY, Lee KW, Kim MH, Lee SH, Ha HY, Cho IH, Kim D, Yu MS, Kim JB, Lee JK, et al: **Repression of phospho-JNK and infarct volume in ischemic brain of JIP1-deficient mice.** *J Neurosci Res* 2003, **74:**326-332.

172. Lizio M, Harshbarger J, Shimoji H, Severin J, Kasukawa T, Sahin S, Abugessaisa I, Fukuda S, Hori F, Ishikawa-Kato S, et al: **Gateways to the FANTOM5 promoter level mammalian expression atlas.** *Genome Biol* 2015, **16:**22.

173. Waeber G, Delplanque J, Bonny C, Mooser V, Steinmann M, Widmann C, Maillard A, Miklossy J, Dina C, Hani EH, et al: **The gene MAPK8IP1, encoding islet-brain-1, is a candidate for type 2 diabetes.** *Nat Genet* 2000, **24:**291-295.

174. Jaeschke A, Czech MP, Davis RJ: **An essential role of the JIP1 scaffold protein for JNK activation in adipose tissue.** *Genes Dev* 2004, **18:**1976-1980.

175. Hayashi T, Sakai K, Sasaki C, Zhang WR, Warita H, Abe K: **c-Jun N-terminal kinase (JNK) and JNK interacting protein response in rat brain after transient middle cerebral artery occlusion.** *Neurosci Lett* 2000, **284:**195-199.

176. Franker MA, Hoogenraad CC: **Microtubule-based transport - basic mechanisms, traffic rules and role in neurological pathogenesis.** *J Cell Sci* 2013, **126:**2319-2329.

177. Urnavicius L, Zhang K, Diamant AG, Motz C, Schlager MA, Yu M, Patel NA, Robinson CV, Carter AP: **The structure of the dynactin complex and its interaction with dynein.** *Science* 2015, **347:**1441-1446.

178. Satake T, Otsuki K, Banba Y, Suenaga J, Hirano H, Yamanaka Y, Ohno S, Hirai S: **The interaction of Kinesin-1 with its adaptor protein JIP1 can be regulated via proteins binding to the JIP1-PTB domain.** *BMC Cell Biol* 2013, **14:**12.

179. Waterman-Storer CM, Karki S, Holzbaur EL: **The p150Glued component of the dynactin complex binds to both microtubules and the actin-related protein centractin (Arp-1).** *Proc Natl Acad Sci U S A* 1995, **92:**1634-1638.

180. Matsuda S, Matsuda Y, D'Adamio L: **Amyloid beta protein precursor (AbetaPP), but not AbetaPP-like protein 2, is bridged to the kinesin light chain by the scaffold protein JNK-interacting protein 1.** *J Biol Chem* 2003, **278:**38601-38606.

181. Muresan Z, Muresan V: **Coordinated transport of phosphorylated amyloid-beta precursor protein and c-Jun NH2-terminal kinase-interacting protein-1.** *J Cell Biol* 2005, **171:**615-625.

182. Vagnoni A, Glennon EB, Perkinton MS, Gray EH, Noble W, Miller CC: **Loss of c-Jun N-terminal kinase-interacting protein-1 does not affect axonal transport of the amyloid precursor protein or Abeta production.** *Hum Mol Genet* 2013, **22:**4646-4652.

183. Horiuchi D, Collins CA, Bhat P, Barkus RV, Diantonio A, Saxton WM: **Control of a kinesin-cargo linkage mechanism by JNK pathway kinases.** *Curr Biol* 2007, **17:**1313-1317.

184. Hammond JW, Griffin K, Jih GT, Stuckey J, Verhey KJ: **Co-operative versus independent transport of different cargoes by Kinesin-1.** *Traffic* 2008, **9:**725-741.

185. Ha HY, Cho IH, Lee KW, Lee KW, Song JY, Kim KS, Yu YM, Lee JK, Song JS, Yang SD, et al: **The axon guidance defect of the telencephalic commissures of the JSAP1-deficient brain was partially rescued by the transgenic expression of JIP1.** *Dev Biol* 2005, **277:**184-199.

186. Kawano T, Araseki M, Araki Y, Kinjo M, Yamamoto T, Suzuki T: **A small peptide sequence is sufficient for initiating kinesin-1 activation through part of TPR region of KLC1.** *Traffic* 2012, **13:**834-848.

187. Blasius TL, Cai D, Jih GT, Toret CP, Verhey KJ: **Two binding partners cooperate to activate the molecular motor Kinesin-1.** *J Cell Biol* 2007, **176:**11-17.

188. Morfini GA, You YM, Pollema SL, Kaminska A, Liu K, Yoshioka K, Bjorkblom B, Coffey ET, Bagnato C, Han D, et al: **Pathogenic huntingtin inhibits fast axonal transport by activating JNK3 and phosphorylating kinesin.** *Nat Neurosci* 2009, **12:**864-871.

189. Morfini G, Pigino G, Szebenyi G, You Y, Pollema S, Brady ST: **JNK mediates pathogenic effects of polyglutamine-expanded androgen receptor on fast axonal transport.** *Nat Neurosci* 2006, **9:**907-916.

190. Reed NA, Cai D, Blasius TL, Jih GT, Meyhofer E, Gaertig J, Verhey KJ: **Microtubule acetylation promotes kinesin-1 binding and transport.** *Curr Biol* 2006, **16:**2166-2172.

191. Lanuza-Masdeu J, Arevalo MI, Vila C, Barbera A, Gomis R, Caelles C: **In vivo JNK activation in pancreatic beta-cells leads to glucose intolerance caused by insulin resistance in pancreas.** *Diabetes* 2013, **62:**2308-2317.

192. Kaneto H, Xu G, Fujii N, Kim S, Bonner-Weir S, Weir GC: **Involvement of c-Jun N-terminal kinase in oxidative stress-mediated suppression of insulin gene expression.** *J Biol Chem* 2002, **277:**30010-30018.

193. Wei Y, Pattingre S, Sinha S, Bassik M, Levine B: **JNK1-mediated phosphorylation of Bcl-2 regulates starvation-induced autophagy.** *Mol Cell* 2008, **30:**678-688.

194. Xu P, Das M, Reilly J, Davis RJ: **JNK regulates FoxO-dependent autophagy in neurons.** *Genes Dev* 2011, **25:**310-322.

195. Du L, Lyle CS, Chambers TC: **Characterization of vinblastine-induced Bcl-xL and Bcl-2 phosphorylation: evidence for a novel protein kinase and a coordinated phosphorylation/dephosphorylation cycle associated with apoptosis induction.** *Oncogene* 2005, **24:**107-117.

196. Terrano DT, Upreti M, Chambers TC: **Cyclin-dependent kinase 1-mediated Bcl-xL/Bcl-2 phosphorylation acts as a functional link coupling mitotic arrest and apoptosis.** *Mol Cell Biol* 2010, **30:**640-656.

197. Mellor HR, Rouschop KM, Wigfield SM, Wouters BG, Harris AL: **Synchronised phosphorylation of BNIP3, Bcl-2 and Bcl-xL in response to microtubule-active drugs is JNK-independent and requires a mitotic kinase.** *Biochem Pharmacol* 2010, **79:**1562-1572.

CHAPTER 2: JIP1 Promotes Insulin Secretion by a Kinesin-dependent Mechanism

2.1 INTRODUCTION

Insulin secretion by pancreatic β cells is essential for the normal physiological regulation of glycemia. An increase in intracellular glucose induces insulin secretion by inhibiting potassium channels and increasing calcium flux in β-cells [1] (Figure 2.1.).
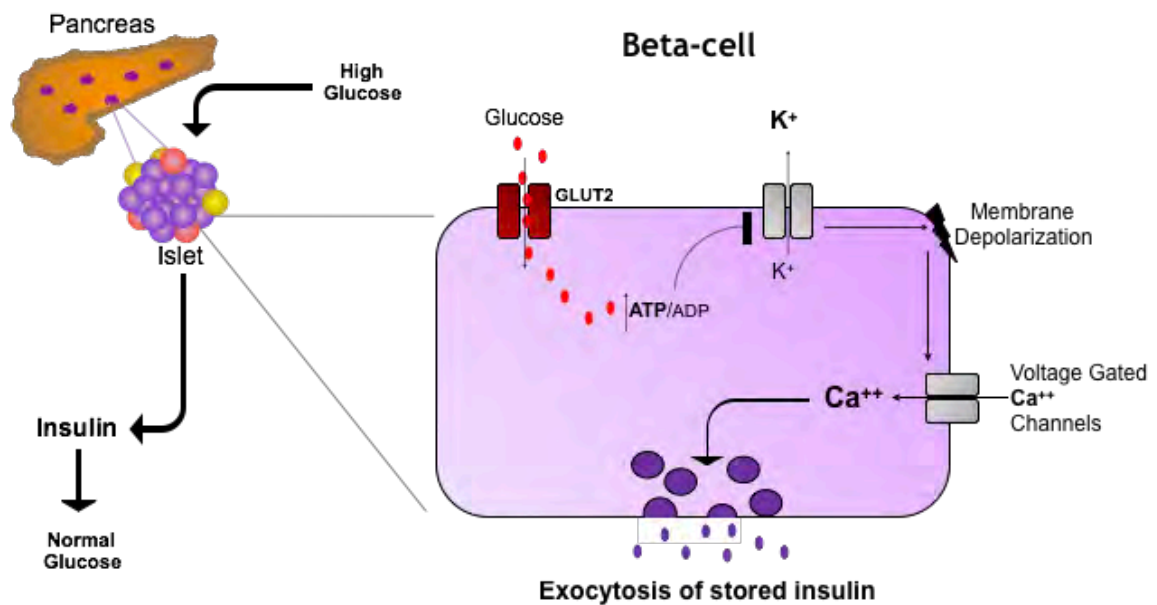
Figure 2.1. Insulin secretion from pancreas beta cells in response to glucose.

Two phases of glucose-stimulated insulin secretion have been identified [2]. An initial acute phase triggered by a rise in cytoplasmic calcium involves the rapid fusion of a readily-releasable pool of insulin granules [3]. In contrast, the second phase of insulin secretion is characterized by the release of a reserve

pool of insulin granules that generates a prolonged and low amplitude response that provides a major contribution to overall insulin secretion [4]. Both of these phases of insulin secretion by vesicle exocytosis are balanced by membrane endocytosis to maintain cellular homeostasis [5]. The movement of insulin granules to the plasma membrane where exocytosis occurs is required for sustained insulin secretion. This movement appears to be mediated by a constrained diffusion mechanism rather than an active transport mechanism [6]. However, remodeling of the actin and microtubule components of the cytoskeleton [7] may contribute to the dynamics of insulin secretion [3].

The microtubules in β cells form a dense multi-directional network that nucleates from the Golgi apparatus rather than the typical radial configuration of orientated microtubules nucleated at the centrosome [8]. Importantly, microtubules are not required for insulin secretion [8, 9]. Nevertheless, microtubule-mediated insulin granule transport by dynein and kinesin motor proteins is implicated as a regulatory mechanism for insulin secretion [10, 11]. Recent studies have demonstrated that this microtubule-mediated insulin granule transport can occur within the sub-plasmalemmal space prior to secretion [12] and that this process may reflect local delivery / removal of insulin granules from docking sites for vesicle fusion on the plasma membrane [8].

Compelling evidence has been reported that demonstrates a role for microtubule-based transport in insulin secretion. Thus, glucose stimulates microtubule-mediated transport of insulin granules [8, 12, 13] by a mechanism

that may involve both kinesin activation [13, 14] and dynamic changes in microtubule nucleation and stability [8]. Moreover, disruption of kinesin-1 function strongly suppresses glucose-stimulated insulin secretion [10, 11, 13-15]. Since microtubule-mediated insulin granule trafficking is mediated by both kinesin and dynein [10], disruption of one of these directional motor proteins may cause sequestration of insulin granules away from docking sites on the plasma membrane and thus suppress insulin secretion [8].

The trafficking function of kinesin-1 is mediated by the interaction of kinesin-1 with adaptor proteins that bind cargos [16]. The adapter protein that is relevant to the requirement of kinesin-1 for insulin secretion has not been identified. Here we tested the role of the JIP1 protein, encoded by the *Mapk8ip1* gene, that is highly expressed in β cells. JIP1 binds kinesin-1 and can function as a cargo adapter [17, 18]. Previous studies have implicated the human *MAPK8IP1* gene in diabetes [19] and the murine JIP1 protein in glycemic regulation [20]. However, the function of JIP1 in β cells has not been defined. We report that JIP1 in β cells is required for normal glucose-stimulated insulin secretion. This role of JIP1 depends on the interaction of JIP1 with the kinesin-1 motor protein. These data demonstrate that JIP1 plays a key role in the physiological regulation of insulin secretion by β cells.

2.2 RESULTS

2.2.1 Ablation of exon2 disrupts JIP1 expression and improves glycemia

We established mice with a *floxed* allele of the *Mapk8ip1* gene to test the role of JIP1 in β cells. The *Mapk8ip1* locus in these mice includes *LoxP* sites that flank exon 2. *Cre*-mediated ablation of exon 2 was confirmed by sequence analysis of mRNA amplified by RT-PCR (Figure 2.2.).
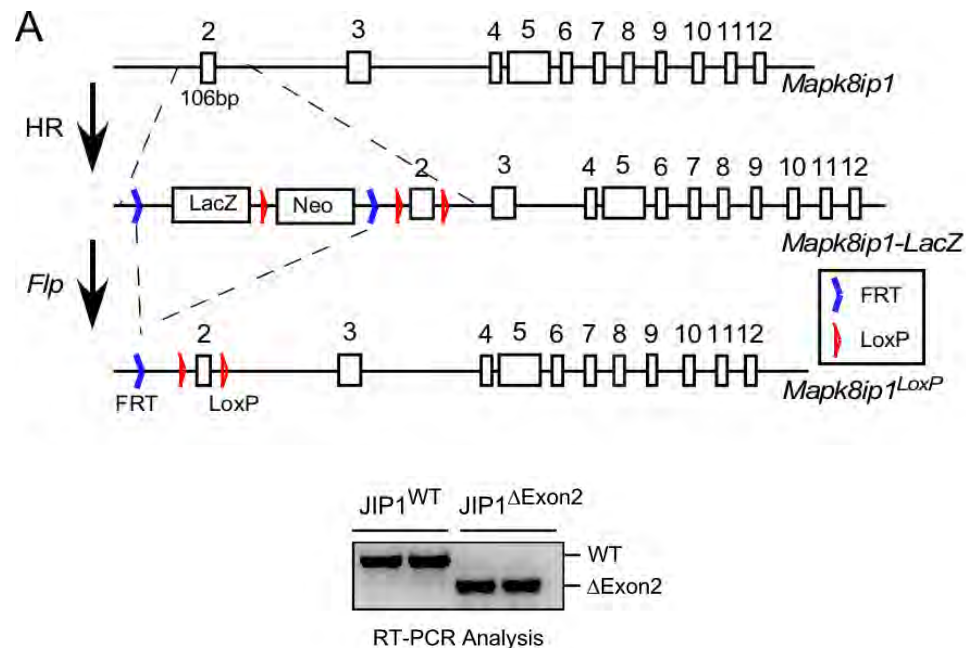
Figure 2.2. Schematic illustration of the Mapk8ip1 genomic locus (exons 2-12), the targeting vector that was used for homologous recombination (HR), the *Mapk8ip1-LacZ* allele, and the conditional allele obtained using *Flp* recombinase (Left panel). RT-PCR analysis of *Mapk8ip1* mRNA expression in the brain of JIP1^{WT} (*Mapk8ip1$^{+/+}$*) mice and JIP1$^{\Delta Exon2}$ (*Mapk8ip1$^{Exon2/\Delta Exon2}$*) was performed using oligos designed based on the sequence of exon 1 (distal) and exon 3 (Right panel).

This analysis identified *Mapk8ip1* mRNA with alternative 3' splicing sites within exon 3 in both JNK^WT and JIP1^ΔExon2 mice. These *Mapk8ip1* mRNA encoded truncated JIP1 proteins with alternative in-frame translational initiation and stop codons (Figure 2.3.).
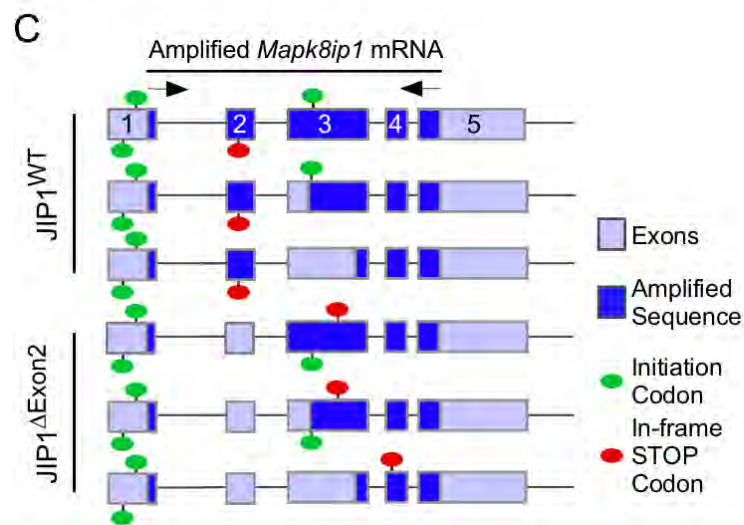
Figure 2.3. RT-PCR analysis of Mapk8ip1 mRNA was performed using primers designed based on the sequence of exon 1 (distal) and exon 5. The amplicons were sequenced and are illustrated schematically using a cartoon of the genomic locus. Arrows indicate the amplified region, gray boxes represent the annotated exons, blue boxes represent PCR product alignments. Green circles indicate in-frame ATG codons. Red circles indicate stop codons that are in-frame with ATG codons *above* or *below* each annotated sequence.

Immunoblot analysis of brain lysates demonstrated the presence of full-length and truncated JIP1 proteins in *Mapk8ip1*^+/+ (JIP1^WT) mice, loss of all JIP1 proteins in *Mapk8ip1*^-/- (JIP1^KO) mice, and loss of only full-length JIP1 in both

66

Mapk8ip1$^{LoxP/LoxP}$ *Nes-Cre*$^{+/-}$ (JIP1$^{\Delta Brain}$) mice and germ-line JIP1$^{\Delta Exon2}$ mice (Figure 2.4.).
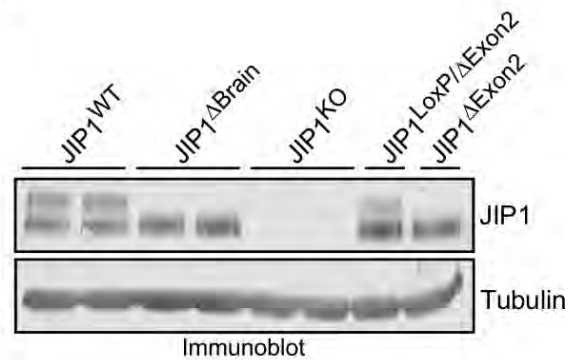
Figure 2.4. Immunoblot analysis of brain lysates prepared from JIP1^{WT} (*Nestin-Cre*$^{+/-}$) mice, JIP1$^{\Delta Brain}$ (*Mapk8ip1*$^{LoxP/LoxP}$ *Nestin-Cre*$^{+/-}$) mice, JIP1^{KO} (*Mapk8ip1*$^{-/-}$) mice, JIP1$^{LoxP/\Delta Exon2}$ (*Mapk8ip1*$^{LoxP/\Delta Exon2}$) mice, and JIP1$^{\Delta Exon2}$ (*Mapk8ip1*$^{\Delta Exon2/\Delta Exon2}$) mice was performed by probing with antibodies to JIP1 and αTubulin.

Previous studies of JIP1^{KO} mice demonstrated that whole body JIP1 deficiency causes improved glycemia [20]. To test whether *Mapk8ip1* exon2 ablation phenocopies the effects the *Mapk8ip1* null allele, we examined germ-line JIP1$^{\Delta exon2}$ mice. These studies demonstrated that JIP1$^{\Delta exon2}$ mice gained less fat mass than WT mice (Figure 2.5.).
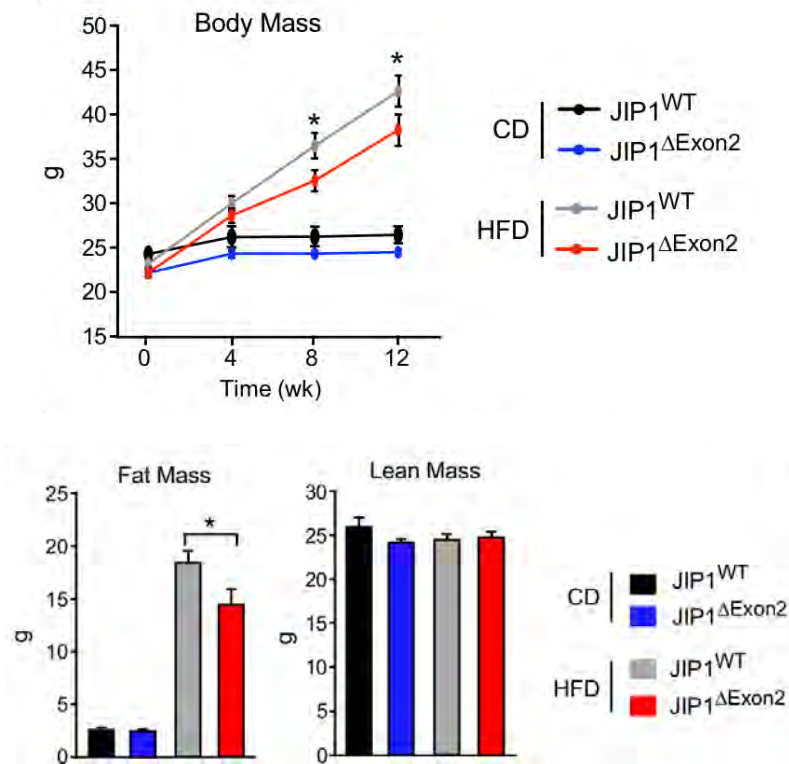
Figure 2.5. The total body mass of 8 wk old JIP1WT and JIP1ΔExon2 mice were fed a CD or a HFD (12 wks) was measured (upper). Fat (lower-left) and lean (lower-right) mass was measured by 1H-MRS. The data represent the mean ± SEM; n=8~9; *, $p<0.05$ (ANOVA).

These mice also exhibited improved glucose tolerance, insulin tolerance, and reduced fed state hyperglycemia (Figure 2.6.).

Collectively, these data demonstrate that *Mapk8ip1*[LoxP/LoxP] (JIP1[LoxP]) mice represent a model that can be used for the examination of the tissue-specific effects of JIP1.
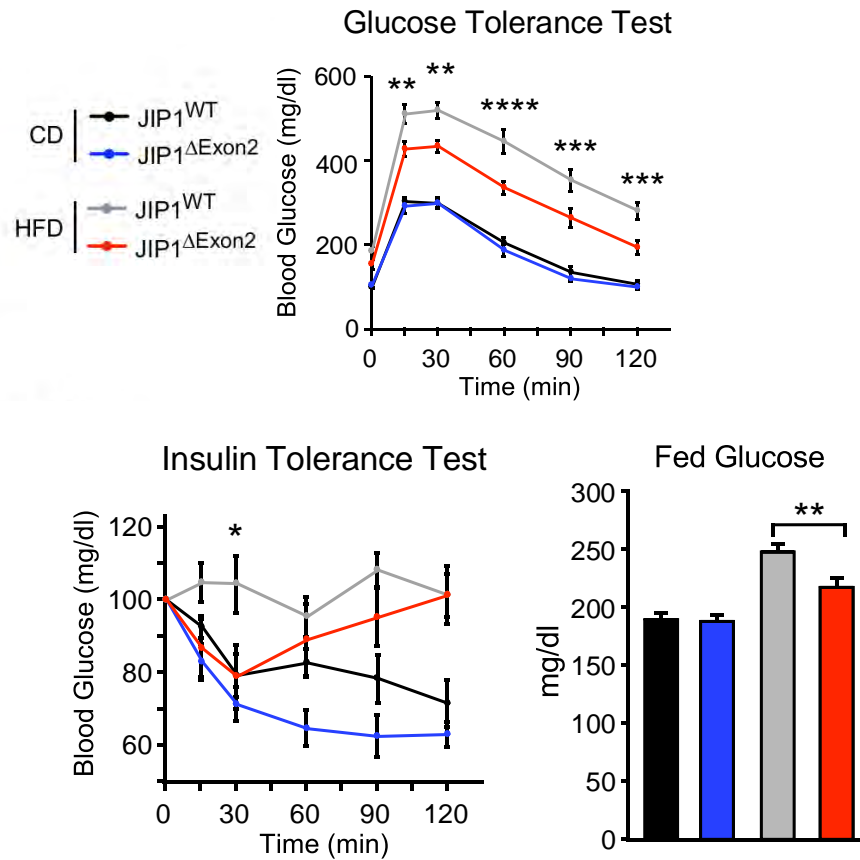
Figure 2.6. Glucose tolerance test (upper) and Insulin Tolerance test were (lower) performed on JIP1^{WT} and JIP1$^{\Delta Exon2}$ mice (age 20 wks) (mean ± SEM; n=7~9; **, $p<0.01$; ***, $p<0.001$; ****, $p<0.0001$; ANOVA).

2.2.2 JIP1 deficiency suppresses glucose-stimulated insulin secretion

To examine the role of JIP1 in β cells, we compared Control JIP1^{WT} (*Mip1-Cre$^{ERT+/-}$*) mice and JIP$^{\Delta ISL}$ (*Mapk8ip1$^{LoxP/LoxP}$ Mip1-Cre$^{ERT+/-}$*) mice with β cell-specific ablation of *Mapk8ip1* exon 2. Genomic PCR analysis demonstrated ablation of exon 2 in islets of JIP$^{\Delta ISL}$ mice and immunoblot analysis confirmed reduced expression of JIP1 compared with Control JIP1^{WT} mice (Figure 2.7.).
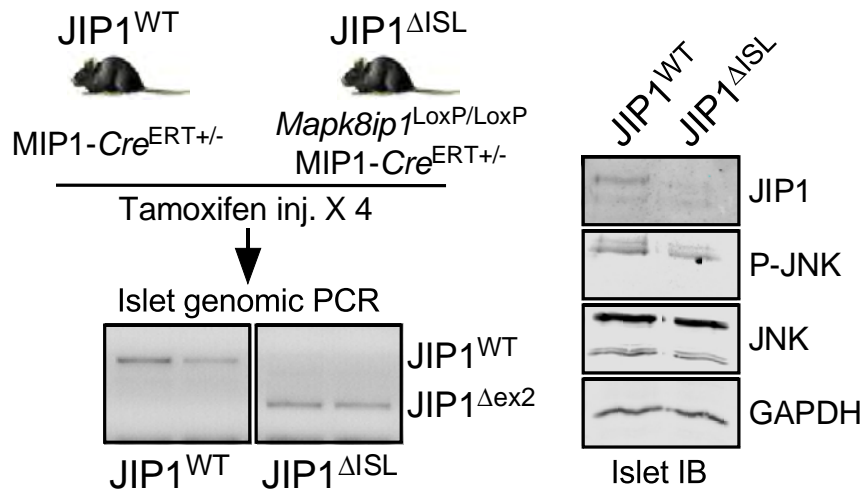
Figure 2.7. Genomic DNA isolated from islets of tamoxifen-treated JIP1WT (Mip1-CreERT+/-) and JIP1ΔISL (Mapk8ip1LoxP/LoxP Mip1-CreERT+/-) mice was examined by PCR to detect *Mapk8ip1* exon2 ablation (left). Isolated islets were cultured overnight and examined by immunoblot analysis by probing with antibodies to JIP1, pJNK, JNK, and GAPDH (right).

No significant differences in body mass, fat mass or lean mass between JIP1^{WT} mice and JIP^{ΔISL} mice were detected (Figure 2.8.). We examined glucose-stimulated insulin secretion in JIP1^{WT} and JIP^{ΔISL} mice. Glucose caused increased amounts of circulating insulin in JIP1^{WT} mice while this effect was blunted in JIP^{ΔISL} mice (Figure 2.9.). However, no significant difference in blood insulin concentration between overnight-fasted JIP1^{WT} and JIP^{ΔISL} mice was detected. These data suggest that JIP1 deficiency may reduce glucose-induced insulin secretion.
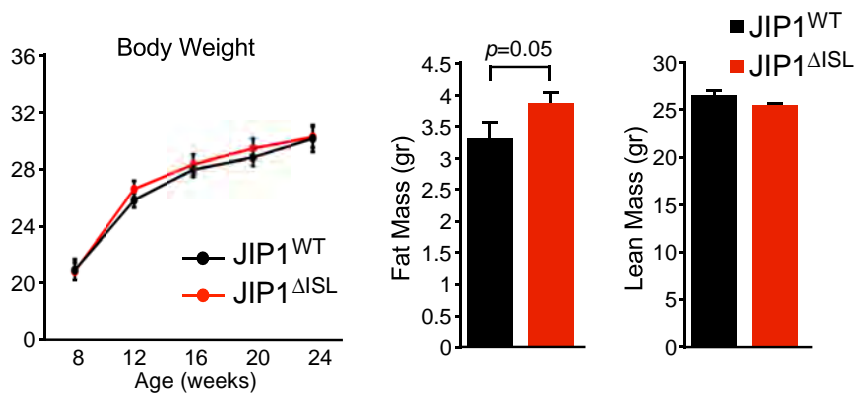
Figure 2.8. Weight gain of mice was examined (left). Fat and lean mass of 24 wk old mice were measured by ^{1}H-MRS analysis. The data presented are the mean ± SEM; n=10~11; $p>0.05$; Student's T-test.
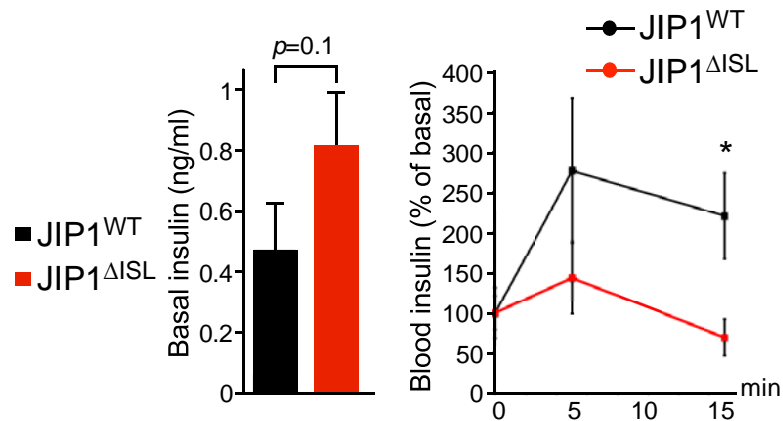
Figure 2.9. Mice (age 24 wk) were fasted overnight and administered 2g/kg glucose by intraperitoneal injection. Plasma insulin was measured by ELISA and presented as the basal fasted insulin (left) and percentage of the basal (right). (mean ± SEM; n=9; *, $p<0.05$; Student's T-test).

We performed perifusion studies using islets isolated from JIP1^{WT} and JIP$^{\Delta ISL}$ mice to directly test the requirement of JIP1 for glucose-stimulated insulin secretion. This analysis demonstrated that JIP1 deficiency caused decreased

secretion of insulin in response to glucose stimulation (Figure 2.10.). We also

found that JIP1 deficiency caused reduced insulin secretion in response to β cell

depolarization with KCl (Figure 2.10.). These secretion defects were not

associated with decreased amounts of total intracellular insulin or *Insulin* and

Slc2a2 (encodes GLUT2) mRNA (Figure 2.11.).
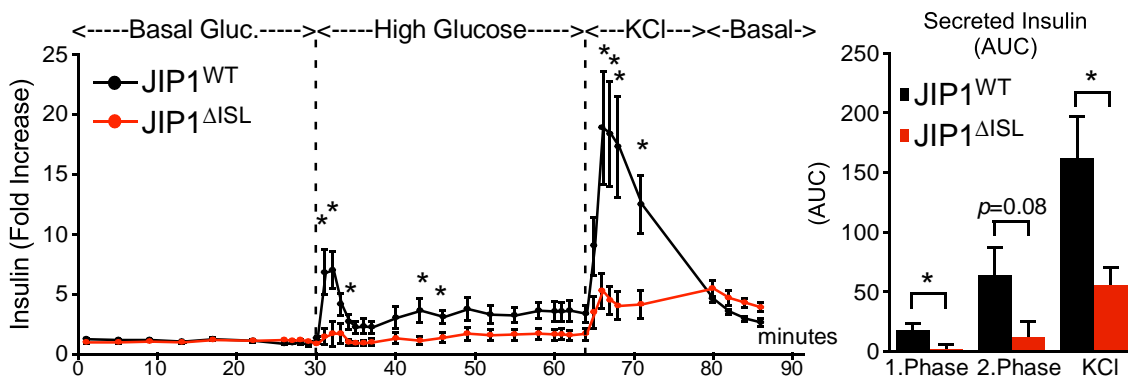
Figure 2.10. Islets isolated from JIP1WT and JIP1ΔISL mice (age 24 wk)
were examined by perifusion analysis to measure insulin secretion. The data
are normalized to the mean basal insulin secretion for each mouse (left). The
area under the curve (AUC) for first phase insulin secretion (30-34min), second
phase insulin secretion (34-64min) and KCl stimulation (64-80min) is presented
(right). (mean ± SEM; n=4~5 mice; *, $p < 0.05$; Student's T-test)

To confirm a physiological role for JIP1 in β cell secretion, we examined

the effect of re-feeding on the concentration of C-peptide in the blood of JIP1[WT]

and JIP[ΔISL] mice. This analysis demonstrated that the increase in circulating C-

peptide caused by re-feeding in JIP1[WT] mice was suppressed in JIP[ΔISL] mice

(Figure 2.12.). These data support the conclusion that JIP1 in β cells plays an

important role in the regulation of glucose-induced insulin secretion.
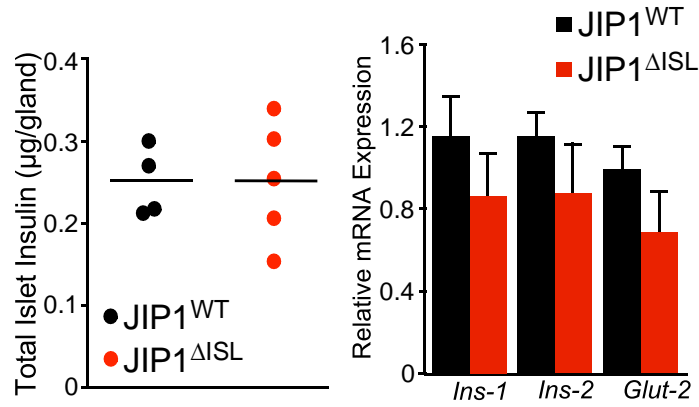
Figure 2.11. The total insulin content of the islets was measured by ELISA (left). Expression of *Insulin-1*, *Insulin-2,* and *Slc2a2* (encodes GLUT2) mRNA by JIP1^{WT} and JIP1$^{\Delta ISL}$ islets was measured by Taqman assays (right) (mean ± SEM; n=5 mice; *p*>0.05; Student's T-test)
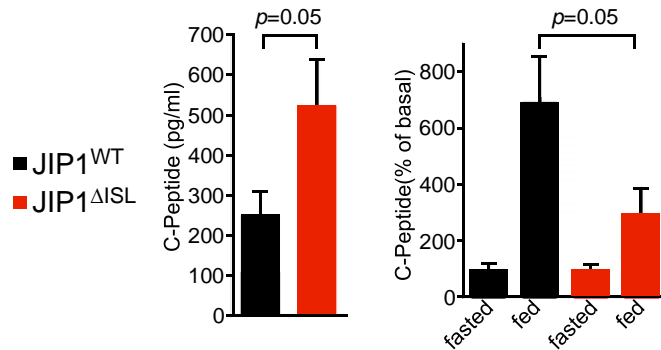
Figure 2.12. Mice (age 24 wk) were fasted overnight and re-fed (1hr). Plasma C-peptide concentration was measured by ELISA and presented as % basal (mean ± SEM; n= 8; *p*<0.05; ANOVA).

2.2.3 JIP1 deficiency is not compensated by JIP2.

The JIP1 and JIP2 proteins are structurally related and both proteins can function as cargo adapters for kinesin-1. JIP1 and JIP2 may therefore serve partially redundant functions. To test whether JIP2 might compensate for JIP1 deficiency in β cells, we studied JIP1,2$^{\Delta ISL}$ mice with dual-deficiency of JIP1 plus JIP2 in β cells. We established *floxed* JIP2 mice and bred these mice to obtain JIP1,2$^{\Delta ISL}$ mice (Figure 2.13.).
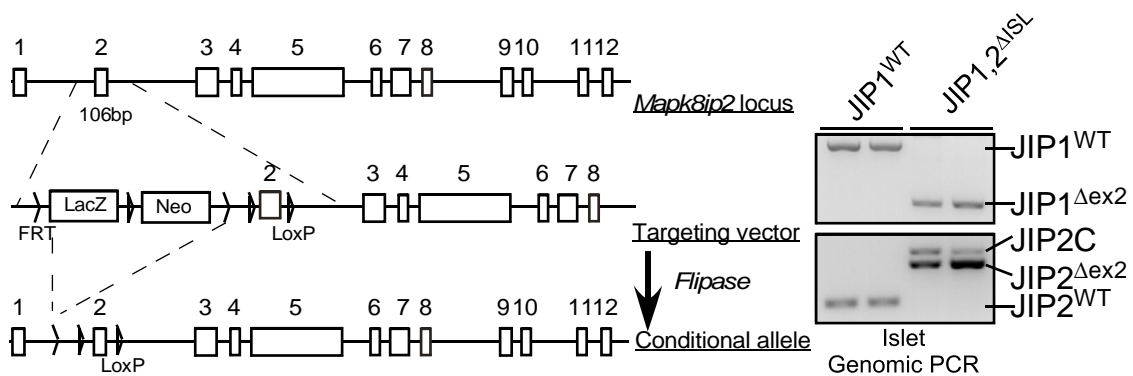
Figure 2.13. Schematic illustration of the Mapk8ip2 genomic locus (exons 1-12), the targeting vector that was used for homologous recombination (HR), the *Mapk8ip2-LacZ* allele, and the conditional allele obtained using *Flp* recombinase (left). Genomic DNA isolated from islets of Tamoxifen-treated JIP1,2^{WT} (*Mip1-Cre*$^{ERT+/-}$) and JIP1,2$^{\Delta ISL}$ (*Mapk8ip1*$^{LoxP/LoxP}$ *Mapk8ip2*$^{LoxP/LoxP}$ *Mip1-Cre*$^{ERT+/-}$) mice was examined by PCR analysis (right).

74

No significant differences in body mass, fat mass, or lean mass were detected between Control JIP1,2^{WT} (*Mip1-Cre$^{ERT+/-}$*) mice and JIP1,2$^{\Delta ISL}$ (*Mapk8ip1$^{LoxP/LoxP}$ Mapk8ip2$^{LoxP/LoxP}$ Mip1-Cre$^{ERT+/-}$*) mice (Figure 2.14.).
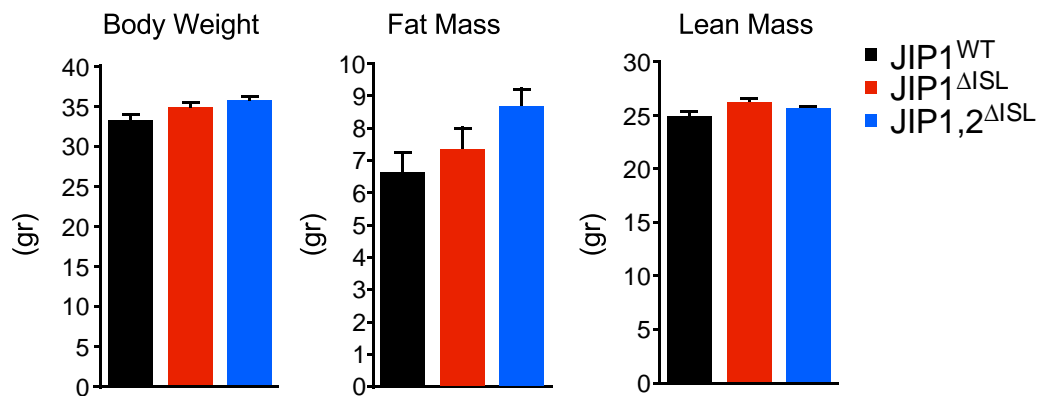
Figure 2.14. JIP1WT, JIP1ΔISL, and JIP1,2ΔISL mice (age 58 wk) were examined by measurement of total body mass, fat mass, and lean mass (mean ± SEM; n=8~9; *, p<0.05; ANOVA)

In contrast, reduced glucose-induced insulin secretion was detected in JIP1,2$^{\Delta ISL}$ mice compared with Control JIP1,2^{WT} mice, although the circulating concentration of insulin in overnight fasted JIP1,2^{WT} and JIP1,2$^{\Delta ISL}$ mice was similar (Figure 2.15.). These data demonstrate that the deficiency of JIP1 or JIP1 plus JIP2 in β cells exhibit a similar insulin secretion defect.
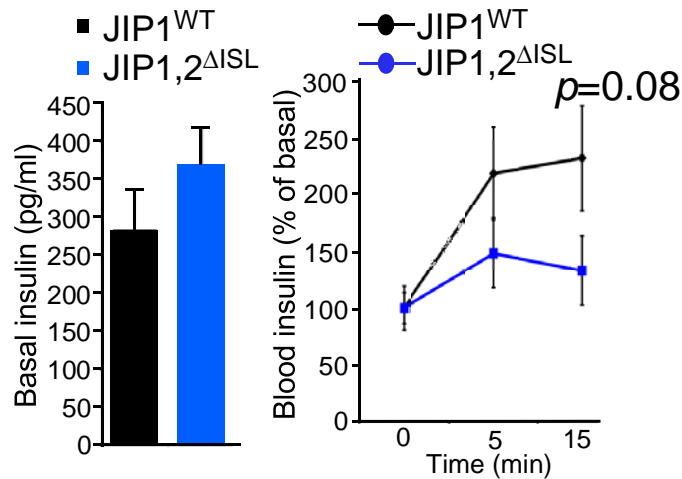
Figure 2.15. Glucose-induced insulin secretion by JIP1,2WT and JIP1,2∆ISL mice (age 26 wk) was examined. Plasma insulin concentration in JIP1,2^{WT} and JIP1,2$^{∆ISL}$ mice (age 26 wk) is presented as fasted basal (left) and percentage of basal (right) (mean ± SEM; n=8~9; p=0.08; ANOVA).

2.2.4 JIP1 deficiency in beta cells causes age-dependent changes in glucose tolerance

JIP1-deficient β cells secrete reduced amounts of insulin. Consequently, we anticipated that JIP1$^{∆ISL}$ mice would exhibit glucose intolerance. Indeed, comparison of mice at 4 wk post-tamoxifen treatment (age 10 wk) demonstrated glucose intolerance in JIP1$^{∆ISL}$ mice compared with JIP1^{WT} mice (Figure 2.16.A). However, studies of older mice indicated that JIP1$^{∆ISL}$ mice subsequently developed improved glucose tolerance compared with JIP1^{WT} mice (Figure 2.16.B-E). The JIP1$^{∆ISL}$ mice also exhibited an age-dependent decrease in fasting blood glucose concentration (Figure 2.16.F).
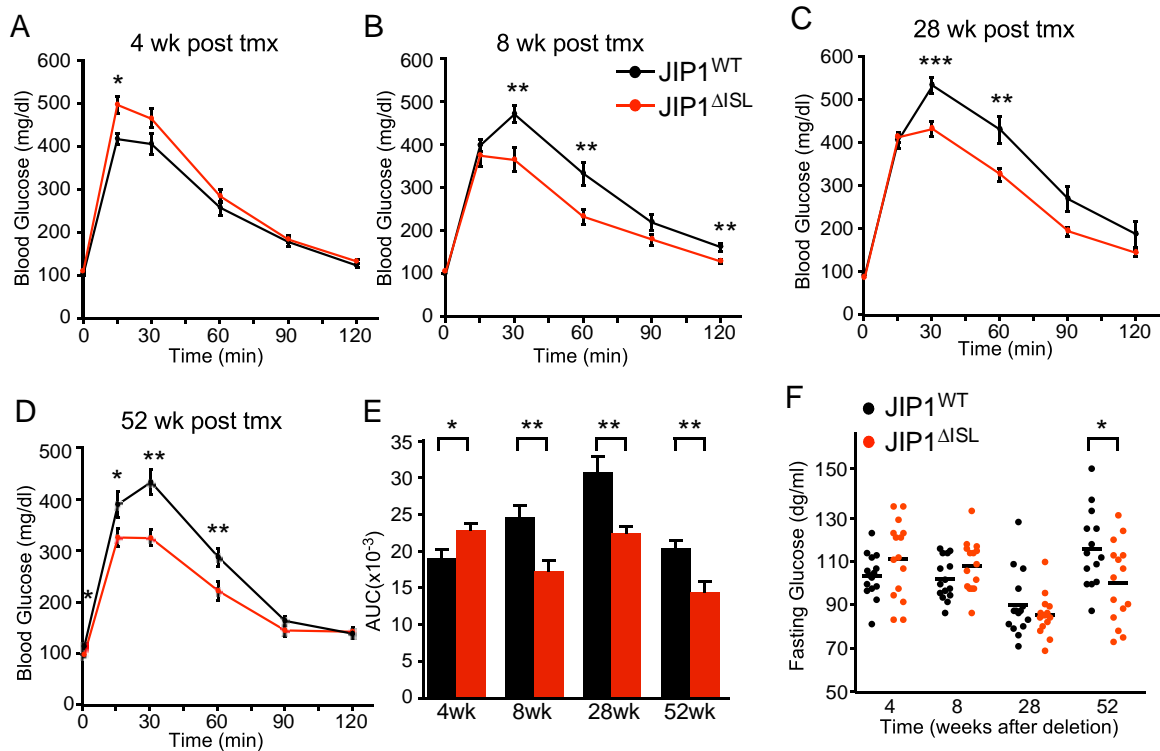
Figure 2.16. Glucose tolerance tests were performed on tamoxifen-treated (at age 5 wk) JIP1WT (Mip1-CreERT+/-) mice and JIP1ΔISL (Mapk8ip1LoxP/LoxP Mip1-CreERT+/-) mice (mean ± SEM; n=14~15; *, $p<0.05$; **, $p<0.01$; ***, $p<0.001$; Student's T-test) (A-D). The time after tamoxifen injection is indicated. The areas under the curve (AUC) for the glucose tolerance tests are presented (mean ± SEM; n=14~15; *, p<0.05; **, p<0.01; Student's T-test) (E). Overnight fasting blood glucose concentration in aging JIP1WT and JIP1ΔISL mice was measured (mean ± SEM; n=14~15; *p<0.05; Student's T-test) (F).

The cause of the age-dependent improvement in glucose tolerance in JIP1ΔISL mice is unclear, but this observation may reflect increased peripheral insulin sensitivity as an age-dependent adaptation to reduced circulating concentrations

of insulin. This potential mechanism is consistent with the proposed role of insulin to promote insulin resistance [21] and the finding that reduced insulin expression increases insulin sensitivity [22]. To test this prediction, we examined insulin-stimulated hepatic AKT activation by monitoring AKT phosphorylation on Thr[308] and Ser[473] by immunoblot analysis. This analysis demonstrated that JIP1$^{\Delta ISL}$ mice exhibited significantly greater insulin-stimulated AKT activation than JIP1^{WT} mice (Figure 2.17.).

Together, these data suggest that a defect in insulin secretion may contribute to the reported increase in peripheral insulin sensitivity detected in whole body JIP1^{KO} mice [20].
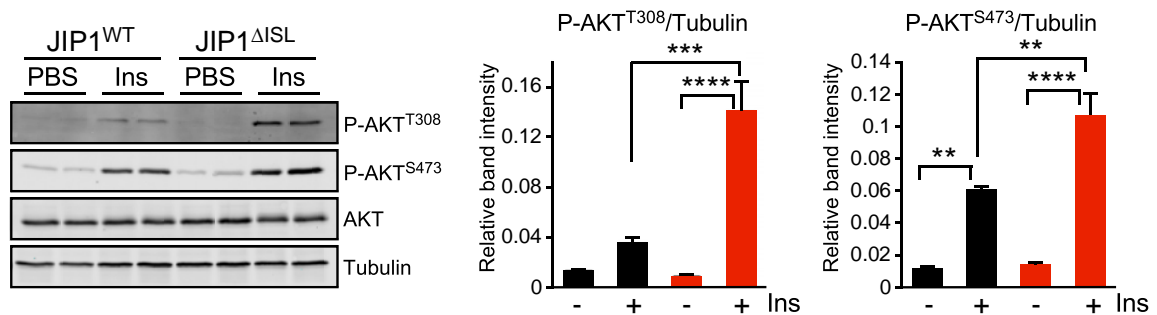
Figure 2.17. Insulin stimulated hepatic AKT activation in JIP1WT and JIP1ΔISL mice (age 24 wk) was examined by immunoblot analysis by probing with antibodies to pThr[308]AKT, pSer[473]AKT, AKT, and α Tubulin (left). Intensity of the pThr[308]AKT, pSer[473]AKT bands relative to tubulin was quantified and presented as bar graphs (right). (mean ± SEM; n=4; *, $p < 0.05$; ANOVA).

2.2.5 JIP1 deficiency causes defects in sub-cellular distribution of insulin vesicles in β cells

The mechanism that accounts for the defect in insulin secretion caused by JIP1 deficiency in β cells is unclear. We therefore examined the morphology of islets and β cells in JIP1^{WT} and JIP$^{\Delta ISL}$ mice. Total β cell mass is one factor that can limit overall insulin secretion. However, we found that islet size and mass, as well as pancreas mass, were similar in JIP1^{WT} and JIP$^{\Delta ISL}$ mice (Figure 2.18. and 2.19.).
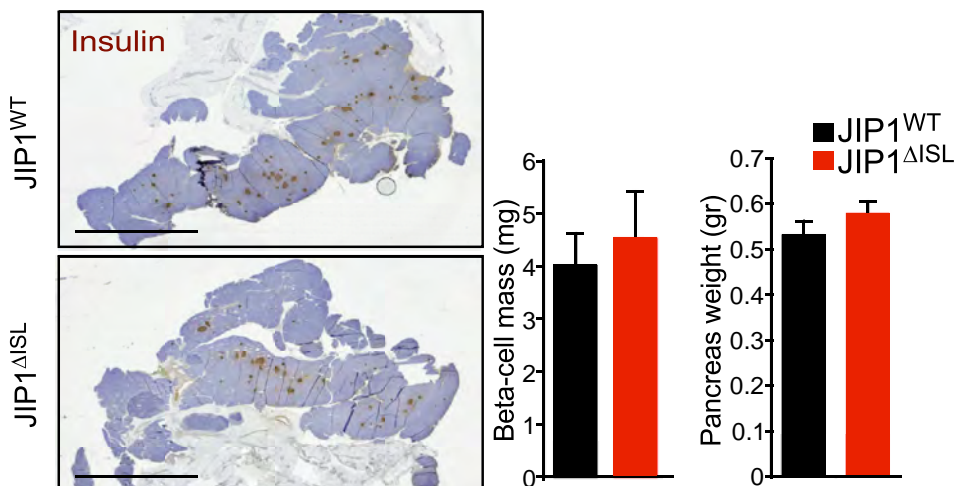
Figure 2.18. Representative whole slide scans of insulin (DAB/brown) and hematoxylin-stained pancreas sections from JIP1WT (Mip1-CreERT+/-) and JIP1ΔISL (Mapk8ip1LoxP/LoxP Mip1-CreERT+/-) mice (age 60 wk). (upper panel) Whole pancreas of the mice were dissected out and their weight were measured (lower right panel). The β cell mass of mice were calculated by multiplying the percentage insulin stained pancreas area (quantified by Photoshop using whole slide scans) and whole pancreas mass (lower left panel) (mean ± SEM; n=8; *p*>0.05; Student's T-test). Scale bar=5mm
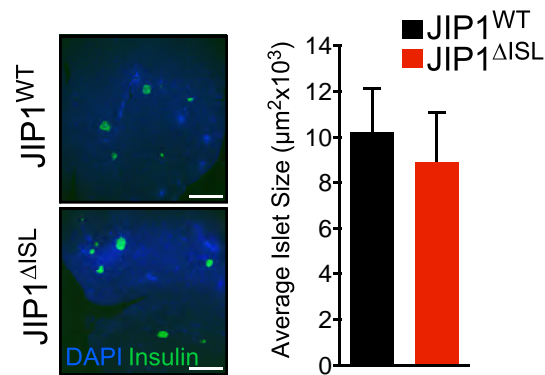
Figure 2.19. JIP1WT and JIP1ΔISL pancreas sections stained with an antibody to insulin (green) and DAPI (blue) were imaged by confocal fluorescence microscopy. Scale bar=300μm. The area of 15-25 islets was quantitated for each mouse (age 24 wk). The data are presented as mean ± SEM; n=7~8 mice; $p>0.05$; Student's T-test.

Transmission electron microscopy demonstrated that pancreatic islets of JIP1^{WT} and JIP^{ΔISL} mice exhibited similar overall morphology (Figure 2.20.). Quantitative analysis of insulin granules indicated a small, but significant ($p<0.05$), reduction in both total granule number and the number of granules apposed to the cell surface membrane (Figure 2.20.), although total insulin content was unchanged (Figure 2.10.).

Since docked vesicles represent only part of the readily releasable pool of insulin granules [3], the modest decrease in granules apposed to the cell surface in JIP^{ΔISL} β cells most likely does not make a major contribution to the severe defect in insulin secretion caused by JIP1 deficiency (Figure 2.10.).
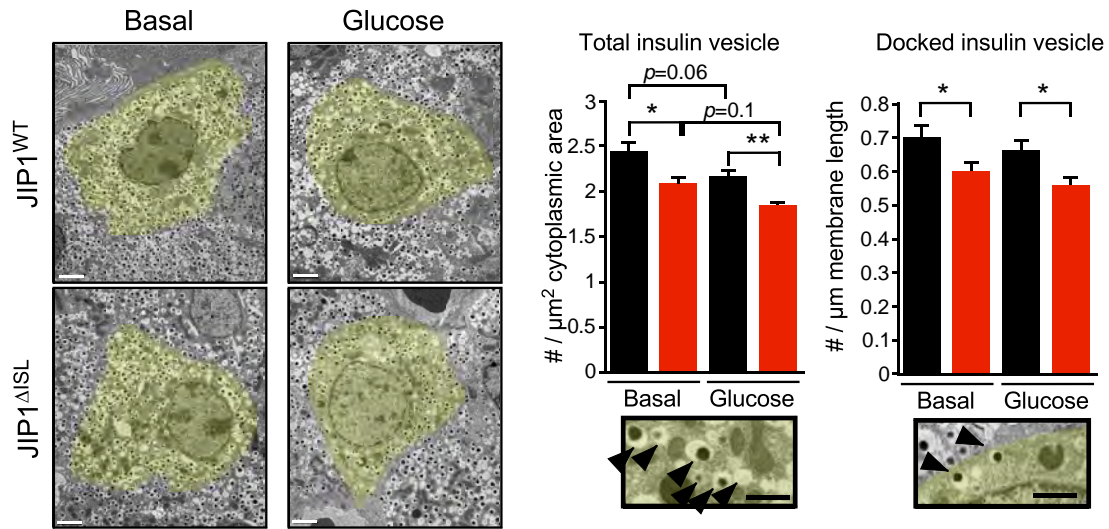
Figure 2.20. Transmission electron microscope images of pancreas tissue from overnight-fasted mice (age 58 wks) following intraperitoneal injection (2 min) of 2mg/kg glucose or solvent (PBS). Highlighted regions (false color) indicate the cellular margins. Scale bar=2µm (E). Total insulin vesicle number per $µm^2$ cytoplasmic area (F) and docked insulin vesicles per µm cell membrane (G) was quantitated. Arrowheads indicate insulin vesicles. The data presented are the mean ± SEM; n=29~48 β cells; *$p<0.05$; **, $p<0.01$; ANOVA. Scale bar=1µm.

One possible explanation for the insulin secretion defect (Figure 2.10.) is that the insulin granules in JIP^{ΔISL} β cells, unlike similar granules in JIP1^{WT} mice, may not localize effectively to active sites for secretion. This hypothesis is consistent with the proposal that kinesin-mediated trafficking may contribute to the appropriate localization of insulin granules to sites of active secretion rather than simple localization to the plasma membrane [8]. Indeed, studies of kinesin-1 knockout mice, like JIP^{ΔISL} mice, demonstrate profound defects in insulin

secretion in the absence of changes in insulin granule localization to the plasma membrane [15]. Together, these data suggest that the requirement for the JIP1 adapter protein for insulin secretion may be related to the function of the kinesin-1 motor protein.

2.2.6 JIP1 binding to kinesin 1 is required for glucose-stimulated insulin secretion

The primary site of JIP1 interaction with kinesin-1 is mediated by the COOH-terminus of JIP1 and the tetratricopeptide repeat domain of kinesin light chain [17, 18, 23]. Kinesin-1 light chain interactions with other regions of JIP1 have also been detected [24] and an additional interaction of JIP1 with kinesin heavy chain has also been reported [25]. These secondary interactions serve to regulate the motor function of kinesin-1 [24, 25].

To test the role of the JIP1 interaction with kinesin-1, we examined the effect of a point mutation in the COOH terminus of JIP1 (Y705A) that disrupts the interaction of JIP1 with kinesin-1 *in vitro*. We established *Mapk8ip1*$^{Y705A/Y705A}$ (JIP1^{Y705A}) mice (Figure 2.21.).

We demonstrated that JIP1, but not JIP1^{Y705A}, co-immunoprecipitated with kinesin-1. In contrast, both JIP1 and JIP1^{Y705A} were found to similarly co-immunoprecipitate with JNK (Figure 2.22.). These data confirm that the JIP1^{Y705A} mutation causes a selective defect in JIP1 interaction with kinesin-1.

Exon 12

```
ACA GAA GAT ATC TAC TTG GAG TAG CAG   MAPK8IP1 (JIP1^WT)
 T   E   D   I   Y   L   E   *

--- --- --- --T GC- --- --- --- ---   MAPK8IP1^Y705A (JIP1^YA)
        ΔEcoRV  A
```
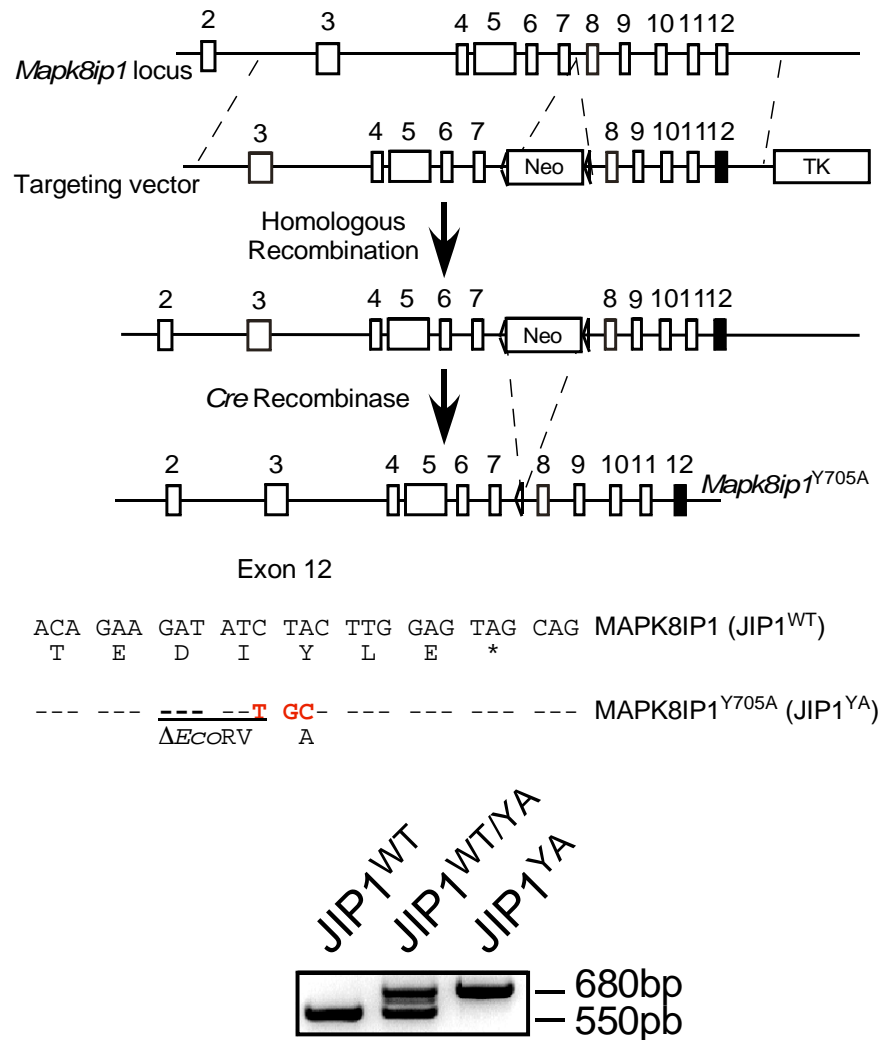
Figure 2.21. Schematic illustration of the Mapk8ip1 genomic locus (exons 2-12), the targeting vector, and the Mapk8ip1Y705A allele. The DNA and amino acid sequence of exon 12 showing the Y705A mutation is presented. Homozygous wild-type and mutant mice were designated JIP1^WT mice and JIP1^Y705A mice, respectively. (upper panel) PCR analysis of genomic DNA identifies the wild-type and *Mapk8ip1*^Y705A alleles (lower panel).
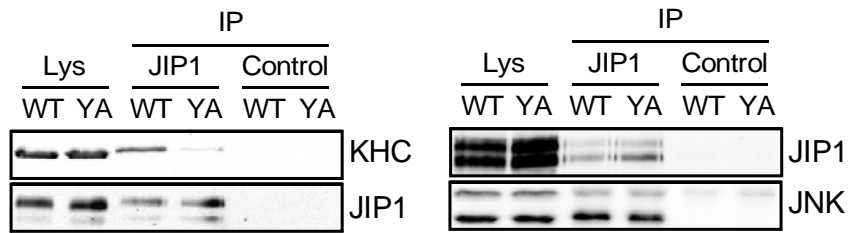
Figure 2.22. Immunoprecipitates (IP) were prepared from brain lysates using an antibody to JIP1 or non-immune antibody (Control). The lysate and the immunoprecipitates were examined by immunoblot analysis using antibodies to kinesin heavy chain (KHC) and JIP1 (left) or JIP1 and JNK (right).

JIP1, β-Tubulin, DAPI
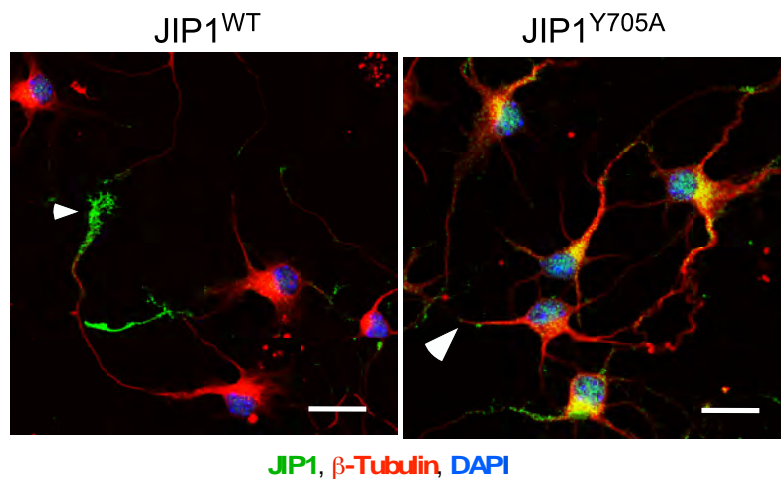
Figure 2.23. Immunofluorescence images of cultured primary neurons stained for JIP1 (green), βIII Tubulin (red), and DAPI (blue). White arrowheads indicate growth cones located at the ends of axons. Scale bar=20μm.

We examined the localization of JIP1 in primary hippocampal neurons to test if this interaction defect is functionally significant. Studies of wild-type neurons demonstrated that JIP1 was localized to neuronal growth cones. In contrast, JIP1^{Y705A} was localized to the soma of hippocampal neurons (Figure

2.23.). These data are consistent with the hypothesis that kinesin-mediated

trafficking drives the accumulation of JIP1 in growth cones and that, in the

absence of kinesin-mediated trafficking, JIP1^{Y705A} remains localized to the soma.

These data indicate that JIP1^{Y705A} represent a model for the analysis of JIP1-

mediated kinesin trafficking. We compared insulin secretion by islets isolated

from JIP1^{WT} and JIP1^{Y705A} mice. Perifusion studies demonstrated that the Y705A

mutation in JIP1 strongly suppressed glucose-induced insulin secretion by β cells

(Figure 2.24.). Control studies demonstrated that the total islet insulin content of

JIP1^{WT} and JIP1^{Y705A} mice was similar (Figure 2.24.). These data demonstrate

that the JIP1 interaction with kinesin-1 is critically required for normal glucose-

induced insulin secretion.
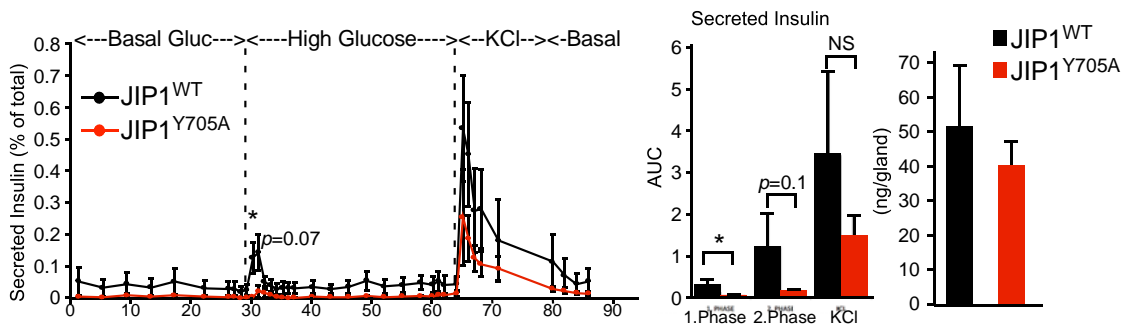
Figure 2.24. Islets isolated from JIP1WT and JIP1YA mice (age 24 wks) were
examined by perifusion analysis to measure insulin secretion. The data are
normalized to total insulin content of the islets (mean ± SEM; n=4~5 mice; *,
$p<0.05$; Students' T-test) (left). The islet perifusion data are presented as the
area under the curve (AUC) for first phase insulin secretion (29-32 min) and
second phase insulin secretion (32-64min) (mean ± SEM; n=4~5 mice; *, $p<0.05$;
Student's T-test) (G). Insulin content of islets was measured by ELISA (mean ±
SEM; n=4~5 mice; $p>0.05$; Student's T-test) (H).

2.2.7 JNK signaling plays a regulatory role in insulin secretion

The JIP1 adapter protein interacts with both kinesin-1 and a MAP kinase signaling module consisting of mixed-lineage protein kinases, MAP2K7, and JNK [26]. This observation suggests that JNK signaling may play a role in JIP1-mediated cargo trafficking by kinesin-1. Indeed, JIP1 deficiency in β cells caused reduced JNK activation (Figure 2.7.). We therefore tested the role of JNK in insulin secretion by β cells.

Initial studies were performed using the drug JNK-in-8 [27] that inhibits JNK signaling. Perifusion experiments demonstrated that JNK-in-8 inhibited glucose-induced insulin secretion by β cells (Figure 2.25.). To associate this role of JNK with the JIP1 adapter protein, we examined JIP1$^{\Delta JBD}$ mice with point mutations in the JNK binding site (replacement of Leu^{160}-Asn^{161}-Leu^{162} with Gly^{160}-Arg^{161}-Gly^{162}) that prevent JIP1-mediated JNK activation [28]. This analysis demonstrated that, like the drug JNK-in-8, mutation of the JNK binding site on JIP1 suppresses glucose-induced insulin secretion (Figure 2.25). However, control studies demonstrated that the total islet insulin content of JIP1^{WT} and JIP1$^{\Delta JBD}$ mice was similar (Figure 2.25.).

These data indicate that JNK may play a regulatory role in insulin secretion mediated by the JIP1 adapter protein.
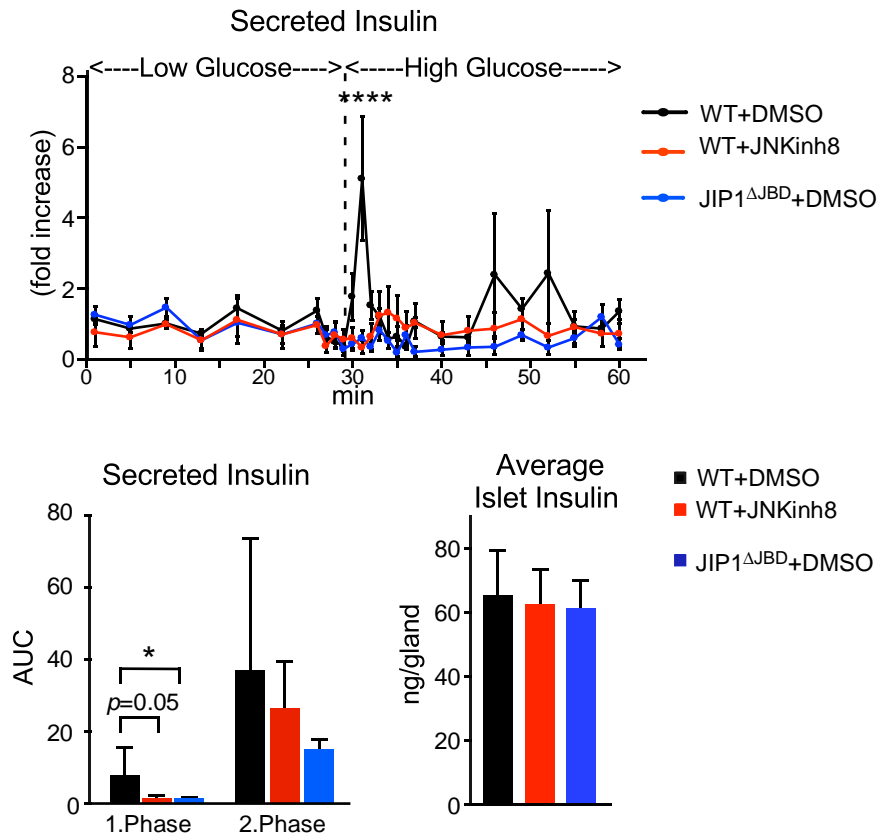
Figure 2.25. Islets isolated from JIP1WT (Mapk8ip1+/+) mice and JIP1ΔJBD (Mapk8ip1ΔJBD/ΔJBD) mice (age 24 wks) were examined by perifusion analysis using low and high concentrations of glucose. The effects of treatment with JNK-in-8 or solvent (DMSO) were examined. The concentration of insulin in the perifusate was measured by ELISA. The data presented are normalized to basal insulin secretion for each mouse (mean ± SEM; n=3~4 mice; ****, $p<0.0001$; ANOVA) (upper panel). Islet perifusion data are presented as the area under the curve (AUC) for first-phase insulin secretion (29-32min), and second-phase insulin secretion (32-64min) (mean ± SEM; n=3~4 mice; *, $p<0.05$; ANOVA) (lower left panel). The total amount of islet insulin was measured by ELISA (mean ± SEM; n=3~4; $p>0.05$; ANOVA) (lower right panel).

2.2.8 Role of JIP1 in hormone secretion

The role of JIP1 in insulin secretion may represent a specialized function of JIP1 in β cells. Alternatively, JIP1 may contribute to hormone secretion by other cells. To explore this question, we examined the secretion of Thyroid-stimulating hormone (TSH) by anterior pituitary gland thyrotrophs in response to Thyrotopin-releasing hormone (TRH). TRH acts to increase cAMP in thyrotrophs and triggers a pulsatile pattern of TSH secretion [29]. Whole mount staining demonstrates that the *Mapk8ip1* gene is expressed in the pituitary gland (Figure 2.26.). We used *Cga-Cre* to establish mice with JIP1 deficiency in cells that express the glycoprotein hormone α-subunit in the anterior pituitary gland.

JIP1-LacZ$^+$ WT
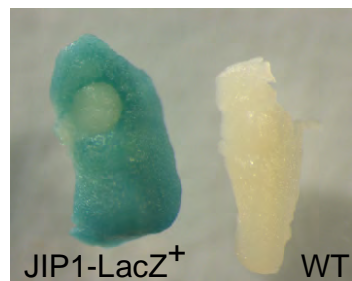
X-Gal Staining

Figure 2.26. Whole mount staining of pituitary glands for LacZ expression was performed using X-Gal. Representative images of pituitary glands isolated from 24 wk old wild-type mice (WT) and mice that express *LacZ* under the control of the *Mapk8ip1* promoter (*Mapk8ip1-LacZ*$^+$ mice) are presented.

Comparison of JIP1^{WT} (*Cga-Cre$^{+/-}$*) mice and JIP1$^{\Delta PIT}$ (*Mapk8ip1$^{LoxP/LoxP}$*

Cga-Cre$^{+/-}$) mice by PCR analysis of genomic DNA demonstrated *Mapk8ip1* exon

2 ablation in the anterior pituitary gland of JIP1$^{\Delta PIT}$ mice (Figure 2.27.).

Immunoblot analysis confirmed that JIP1 protein expression was decreased in

the pituitary glands of JIP1$^{\Delta PIT}$ mice compared with JIP1^{WT} mice (Figure 2.27.).
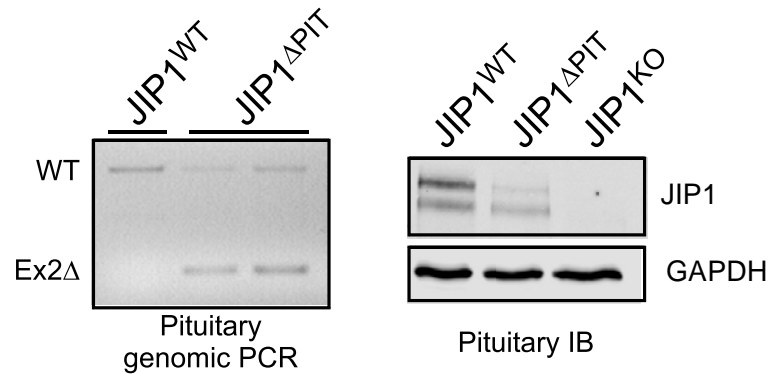
Figure 2.27. Genomic DNA isolated from the pituitary glands of JIP1^{cond}
(*Mapk8ip$^{LoxP/LoxP}$*) mice and JIP1$^{\Delta PIT}$ (*Mapk8ip$^{LoxP/loxP}$ Cga-Cre$^{+/-}$*) mice (age 24 wks)
was examined by PCR analysis using amplimers designed based on the
sequence of introns 1 and 2. (left). Pituitary glands from JIP1^{WT} (CGA-*Cre$^{+/-}$*),
JIP1$^{\Delta PIT}$, and JIP1^{KO} (*Mapk8ip1$^{-/-}$*) mice were examined by immunoblot analysis
using antibodies to JIP1 and GAPDH (right).

Analysis of blood hormones in overnight fasted mice demonstrated

reduced amounts of circulating TSH and T4, but no change in T3, in JIP1$^{\Delta PIT}$

mice compared with JIP1^{WT} mice (Figure 2.28.).
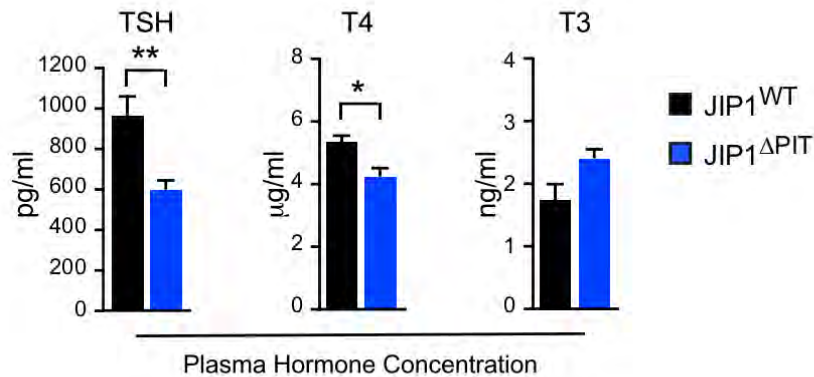
Figure 2.28. The concentration of circulating TSH, T4, and T3 in JIP1WT and JIP1ΔPIT mice (age 24 wks) was measured by ELISA (mean ± SEM; n=16 (TSH) and n=8 (T3/T4); *, $p<0.05$; **, $p<0.01$; Student's T-test).
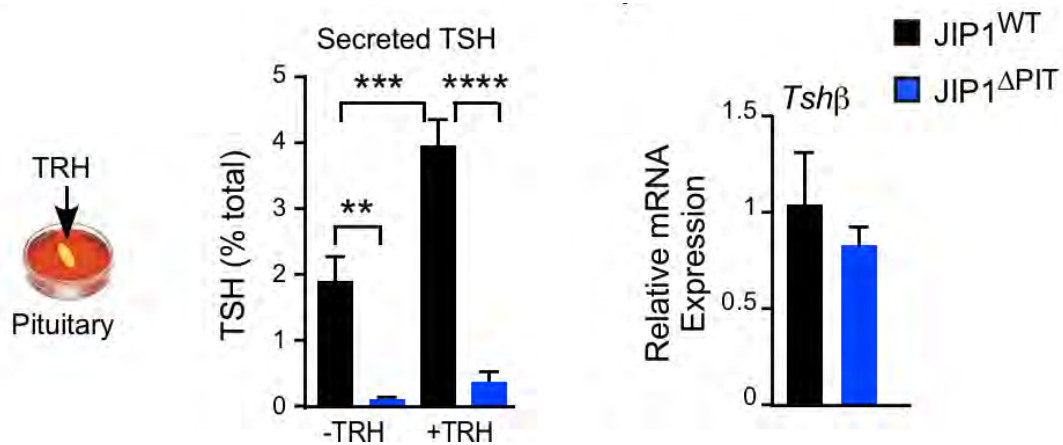
Figure 2.29. Explant cultures of pituitary glands (1 h) from JIP1WT and JIP1ΔPIT mice (age 24 wks) were treated without or with 300 nM TRH (60 mins). The concentration of TSH in the medium was measured by ELISA and is presented as % of total TSH (mean ± SEM; n=4~5; **, $p<0.01$; ***, $p<0.001$; ****, $p<0.0001$; ANOVA) (left). Pituitary gland expression of

Tsh mRNA was measured by qRT-PCR analysis (mean ± SEM; n=7~8, *,
p>0.05; Student's T-test) (right).

Since TSH secretion *in vivo* is positively regulated by TRH and negatively

regulated by T4/3, we examined TSH secretion using pituitary gland explants *in*

vitro. These studies demonstrated that JIP1 deficiency caused reduced TRH-

stimulated secretion of TSH (Figure 2.29.). This defect in secretion was not

associated with a change in the expression of *Tshβ* mRNA (Figure 2.29.).

To test the role of the interaction of JIP1 with kinesin-1 in thyrotrophs, we

examined TRH-induced TSH secretion from the anterior pituitary glands of

JIP1^{WT} and JIP1^{YA} mice. This analysis demonstrated that the Y705A mutation in

JIP1 strongly suppressed TRH-induced TSH secretion (Figure 2.30.). Thus, like

insulin secretion from β cells, TSH secretion from thyrotrophs requires the

interaction of JIP1 with kinesin-1.
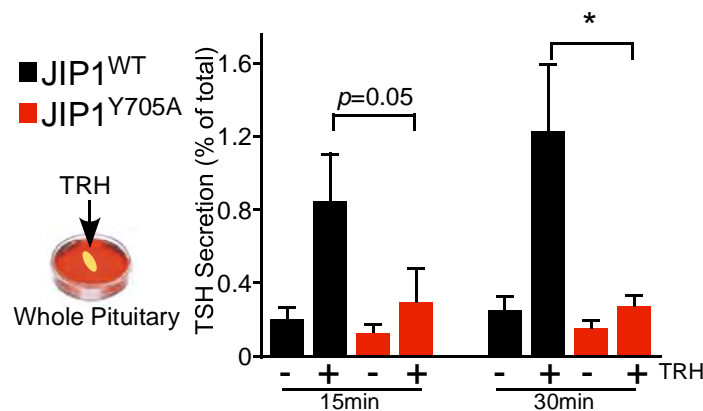
Figure 2.30. Explant cultures of pituitary glands were treated with TRH (30
min) and the concentration of TSH in the medium was measured by ELISA.
Secreted TSH is presented as the percentage of total pituitary TSH content
(mean ± SEM; n=4; *, *p*<0.05; ANOVA).

2.3 DISCUSSION

Our data demonstrate that the kinesin-1 adapter protein JIP1 plays a key role in hormone secretion, including the release of insulin from β cells. JIP1 deficiency in β cells reduces glucose-induced insulin secretion (Figure 1). Importantly, a mutation in JIP1 (Y705A) that prevents the interaction of JIP1 with kinesin-1 suppresses glucose-induced insulin secretion (Figure 4). Similarly, disruption of kinesin-1 function in β cells also causes reduced glucose-induced insulin secretion [10, 11, 13-15]. Together, these data demonstrate that the JIP1 adapter protein is important for kinesin-regulated insulin secretion. This function may be mediated by a role for kinesin-mediated trafficking to increase the dwell time of insulin granules at sites of membrane fusion at the cell surface by opposing dynein-mediated trafficking [8].

A goal for future studies will be to examine regulatory mechanisms mediated by JIP1 that influence insulin secretion by directly visualizing insulin granule dynamics. One example of a potential regulatory mechanism is the JNK pathway that is tethered as a signaling module to JIP1 [30]. Genetic analysis indicates that JNK potently stimulates kinesin-mediated cargo transport [31] and biochemical studies demonstrate that this role of JNK is mediated, in part, by kinesin-1 phosphorylation [32, 33]. This established knowledge is consistent with the observations that JIP1 deficiency in β cells causes reduced JNK activation (Figure 1B), that pharmacological inhibition of JNK causes reduced insulin secretion (Figure S3), and that mutation of the JNK binding site on JIP1

suppresses insulin secretion (Figure S3). Together, these data suggest that local

control of JNK signaling by JIP1 that targets the kinesin-1 motor protein may

represent a key mechanism for the physiological control of insulin secretion.

2.4 METHODS

2.4.1 Animal Models

2.4.1.1 Mouse husbandry

The mice were housed with *ad libitum* access to food and water with a

12:12-hr dark-light cycle, in a specific pathogen-free facility accredited by the

American Association for Laboratory Animal Care. The Institutional Animal Care

and Use Committee of the University of Massachusetts approved all studies

using animals. All studies were performed using C57BL/6J background, age-

matched, male mice. Littermate mice were randomly assigned to groups.

Mice (aged 8 wk) were fed a chow diet (Iso Pro 3000, Purina) or high fat

diet (S3282, Bioserve). Body mass was measured with a scale. Fat mass and

lean mass were non-invasively measured using ^{1}H-MRS (Echo Medical

Systems).

2.4.1.2 Previously published mouse models

We have previously described *Mapk8ip1$^{-/-}$* (JIP1 knockout) mice [17] and

JIP1$^{\Delta JBD}$ mice [28]. C57BL/6J mice (stock# 000664), B6.Cg-Tg(Ins1-

cre/ERT)1Lphi/J (*Mip1-Cre^{ERT}*) mice (stock# 024709) [34], B6;SJL-Tg(Cga-

cre)3Sac/J (*Cga-Cre*) mice (stock#004426) [35], B6.Cg-Tg(Nes-cre)1Kln/J

(*Nes-Cre*) mice (stock# 003771) [36], B6.Cg-Tg(Syn1-cre)671Jxm/J (Syn1-*Cre*) mice (stock# 003966) [37], and 129S4/SvJaeSor-*Gt(ROSA)26Sor*[tm1(FLP)Dym]/J (FLPeR) mice (stock# 003946) [38] were obtained from The Jackson Laboratory.

2.4.1.3 Establishment of *Mapk8ip1*[Y705A/Y705A] mice

Mice with the point mutation Tyr705Ala in JIP1 were constructed by homologous recombination in embryonic stem (ES) cells using standard methods. Briefly, a targeting vector was constructed (Figure 4A). This targeting vector was designed to introduce point mutations in exon 12 of the *Mapk8ip1* gene that create the Tyr705Ala mutation and, the loss of an EcoRV restriction site (Figure 4A). The targeting vector was also designed to introduce a floxed Neo^R cassette in intron 7 (Figure 4A). TC1 embryonic stem cells (strain 129svev) were electroporated with this vector and selected with 200 µg/ml G418 (Thermo Fisher Cat#10131035) and 2 µM ganciclovir (Syntex). ES cell clones with the floxed Neo^R cassette correctly inserted in intron 7 were identified by Southern blot analysis. ES cells were injected into C57BL/6J blastocysts to create chimeric mice that were bred to obtain germ-line transmission of the targeted *Mapk8ip1* allele. The floxed Neo^R cassette was excised using *Cre* recombinase. These mice were backcrossed to the C57BL/6J strain.

2.4.1.4 Establishment of *Mapk8ip1*[LoxP/LoxP] and *Mapk8ip2*[LoxP/LoxP] mice

A *Frt-LacZ-LoxP-Neo*^{R}*-Frt-LoxP* cassette was inserted by homolgous recombination in intron 1 and a *LoxP* site was inserted into intron 2 of the

Mapk8ip1 gene (Figure S1A) and *Mapk8ip2* gene (Figure S2A). We used

JM8A3.N1 ES cells (strain C57BL/6N-A/a; Mapk8ip1[tm1a(EUCOMM)Wtsi]) and

JM8A3.N1 ES cells (strain C57BL/6N; Mapk8ip2[tm1a(EUCOMM)Wtsi]) to create

chimeric mice that were bred to obtain germ-line transmission of the mutated

Mapk8ip1-LacZ and *Mapk8ip2-LacZ* alleles using standard procedures. The *Frt-*

LacZ-LoxP-Neo[R]-Frt cassette was excised by crossing with *FLPeR* mice to

obtain mice with the *Mapk8ip1*[LoxP] and *Mapk8ip2*[LoxP] alleles. These mice were

backcrossed to the C57BL/6J strain.

2.4.1.5 Establishment of *Mapk8ip1*[ΔExon2/ΔExon2] mice

Mapk8ip1[LoxP/LoxP] mice were bred with Synapsin1-*Cre*^{+/-} mice to obtain

male *Mapk8ip1*[+/LoxP] *Synapsin1-Cre*^{+/-} mice that were bred with female C57BL/6J

mice. *Cre* expression in the male germ-line resulted in the generation of

Mapk8ip1[+/ΔExon2] mice that were bred to obtain *Mapk8ip1*[ΔExon2/ΔExon2] mice.

2.4.1.6 Establishment of tissue-specific JIP-deficient mice

We bred *floxed* mice and *Cre*^{+/-} mice to generate mice with the following

genotypes for analysis: Control and JIP1[ΔISL] mice (*Mip1- Cre*[ERT +/-] and

Mapk8ip1[LoxP/LoxP] *Mip1- Cre*[ERT +/-] mice); Control and JIP1,2[ΔISL] mice (*Mip1-*

Cre[ERT +/-] and *Mapk8ip1*[LoxP/LoxP] *Mapk8ip2*[LoxP/LoxP] *Mip1- Cre*[ERT +/-] mice); Control

and JIP1[ΔPIT] mice (*Cga-Cre*^{+/-} and *Mapk8ip1*[LoxP/LoxP] *Cga-Cre*^{+/-} mice); and Control

and JIP1[ΔBrain] mice (*Nestin-Cre*^{+/-} and *Mapk8ip1*[LoxP/LoxP] *Nestin-Cre*^{+/-} mice).

Cre[ERT] mice (age 5 wks) were injected with 1.5mg tamoxifen (Millipore Sigma

Cat#T5648-16) in 100μl sunflower seed oil every other day for 8 days (4

injections).

2.4.1.7 Genotype analysis

Genomic DNA was isolated from mouse tissues (brain, islets, and pituitary gland) using the DNeasy Blood and Tissue Kit (Qiagen cat#69506). PCR analysis of genomic DNA using amplimers 5'- TCCCAGGTCTCCTTCACTGT-3' and 5'-CGGCTCTATTGGAGAGATGC-3' detected the $Mapk8ip1^+$ (202bp) and $Mapk8ip1^{LoxP}$ (366bp) alleles. Amplimers 5'-TGTAGTTGAAGAGATGACACCAAGA-3' and 5'-CTGAGAGGCCCTTCTCTTAACTCT-3' detected the $Mapk8ip1^+$ (926bp), $Mapk8ip1^{LoxP}$ (1,137bp), and $Mapk8ip1^{\Delta exon2}$ (335bp) alleles. PCR analysis using primers 5'-GACGGCAGAGAGTGAAATC-3', 5'-ATACCTTGAACCAACGGGG-3', and 5'-GGCATTTCCTCAAAACAAGC-3' detected the $Mapk8ip2^+$ (188bp), $Mapk8ip2^{LoxP}$ (392bp), and $Mapk8ip2^{\Delta exon2}$ (325bp) alleles. Amplimers 5'-ACACACACCCCAGGTCTTAG-3' and 5'-TCAGCTTTGACGCCTATCTTGAC-3' detected the $Mapk8ip1^+$ (550bp) and $Mapk8ip1^{Y705A}$ alleles (680bp). Methods for genotyping JIP1 knockout mice [17], JIP1$^{\Delta JBD}$ mice [28], Cre mice [36], and Flp mice [38] have been reported previously.

2.4.1.8 Sequencing of *Mapk8ip1* mRNA

Brain RNA from WT and JIP1$^{\Delta Exon2}$ mice was amplified by RT-PCR using primers designed based on the sequence of distal exon 1 (5'-CATTCCTGGGACTGCACAT-3') or proximal exon 1 (5'-AGCTGGTTGGAGGATCAGTG-3') together with exon 5 (5'-

CACATCTGCCTGGTAGTGGA-3') (Figure S1C). Amplicons were purified

using 1.8X AMPure XP reagent (Fisher Scientific Cat#A63880). The purified

amplicons were incubated (50 μL) with 1mM dATP (Thermo Fisher Cat#R0141)

and 15U Klenow 3'->5' exo- (New England Biolabs Cat#M0212) in 1X NEB

buffer 2.1 (New England Biolabs Cat#B7202) at 37°C (30 mins). The A-tailed

amplicons were purified using 1.8X AMPure XP reagents and then incubated (50

μL) at 25°C (2 h) with 25U T4 ligase (Thermo Fisher, Cat#15224041) plus 20nM

indexed adapters (TrueSeq RNA Single Indexes Set-A (Cat# 20020492) and Set-

B (Cat# 20020493)) in 1X T4 ligase buffer (New England Biolabs), followed by

1.8X AMPure XP purification. The libraries were mixed (4:1) with a PhiX Control

v3 library (Illumina Cat#FC-110-3001) and sequenced using an Illumina MiSeq

(300bp paired-end reads, 300,000 mean reads per library). Reads were aligned

to the mouse reference genome mm10 using Tophat2 [39] and visualized using

the Integrative Genomics Viewer [40].

2.4.1.9 Blood Analysis

Blood glucose was measured with an Ascensia Breeze 2 glucometer

(Bayer). Multiplexed ELISA (Luminex 200 machine, Millipore Sigma) was used

to measure the concentration of insulin with the Mouse Adipokine Magnetic Bead

Panel (Millipore Sigma Cat#MADKMAG-71K), C-Peptide was measured with the

Mouse Metabolic Magnetic Bead Panel (Millipore Sigma Cat#MMHMAG-44K),

and TSH / GH were measured with the Mouse Pituitary Magnetic Bead Panel

(Millipore Sigma Cat#MPTMAG-49K-03). ELISA was used to measure the

concentration of T4 (Calbiotech Cat#T4224T) and T3 (Calbiotech Cat#T3225T).

2.4.1.10 Glucose Stimulated Insulin Secretion *in vivo*

Mice were starved overnight (16 h) and injected with 2g/kg glucose. Blood

was collected at 0, 5 and 15 mins post-injection. The concentration of insulin

was measured by multiplexed ELISA.

2.4.1.11 Glucose Tolerance Test

Glucose tolerance tests were performed using mice starved overnight (16

h) and intraperitoneally injected with 2g/kg glucose. However, glucose tolerance

studies using old mice (≥60 wks) were performed using 1.5 g/kg glucose and

HFD studies were performed using 1.0 g/kg glucose.

2.4.1.12 Insulin Stimulated AKT Phosphorylation

Mice were starved overnight and intraperitoneally injected with 1U/kg

insulin or solvent (phosphate-buffered saline). The mice were euthanized at 15

mins post-injection and liver tissue was flash-frozen in liquid nitrogen. Tissues

lysates were examined by immunoblot analysis.

2.4.1.13 Immunoprecipitation

Extracts of murine cerebral cortex were prepared in Triton lysis buffer

[20 mM Tris (pH 7.4), 1% Triton X-100, 10% glycerol, 137 mM NaCl, 2 mM

EDTA, 25 mM β-glycerophosphate, 1 mM sodium orthovanadate, 1 mM

phenylmethylsulfonyl fluoride, and 10 μg/mL of aprotinin plus leupeptin].

Immunoprecipitation was performed using a rabbit antibody to JIP1 [41], a rabbit

antibody to JNK (Santa Cruz; cat#sc474), and non-immune rabbit IgG (Millipore Sigma cat#I5006) pre-bound to protein A Sepharose (Millipore Sigma cat#P3391). The immunoprecipitates were examined by immunoblot analysis.

2.4.1.14 Immunoblot Analysis

Tissue extracts from brain, isolated islets, and pituitary gland were prepared using Triton lysis buffer. Extracts (20–50 µg protein) were examined by immunoblot analysis by probing with antibodies to JIP1 (Fisher Scientific Cat#BDB611890), pJNK1/2 (Cell Signaling Cat#4668), JNK1/2 (Fisher Scientific Cat#BDB554285), AKT (Cell Signaling Cat#9272), pAKT^{T308} (Cell Signaling Cat#5106), pAKT^{S473} (Cell Signaling Cat#9271), Kinesin Heavy Chain (Millipore Cat#MAB1614), GAPDH (Santa Cruz Cat#sc-25778), and ✔Tubulin (Sigma-Aldrich Cat#T5168). Immunocomplexes were detected by enhanced chemiluminescence (New England Nuclear) or by fluorescence using anti-mouse and anti-rabbit secondary IRDye antibodies (LI-COR Biosciences Cat#925-68070 and Cat#925-32211) and quantitated using the LI-COR Imaging system.

2.4.1.15 Primary Islet Isolation and Perifusion Analysis

Islets were isolated by collagenase digestion of pancreas [42] and used for perifusion studies [43] using methods described previously. Islets were cultured overnight in CMRL media (Thermo Fisher Cat#11530037) with 5.5 mM glucose supplemented with 10% FBS (Atlanta Biologicals Cat#S11150H), 1x Pen/Strep/Glutamine (Thermo Fisher Cat# 10378016) and 1x MEM Non Essential amino acids (Thermo Fisher Cat# 11140-076). Similar-sized islets from

each mouse preparation were hand-picked and 25 islets were examined using a

Biorep Technologies (Miami, FL) perifusion system. Islets were perifused with

Kreb's buffer [115mM NaCl, 5mM KCl, 24mM $NaHCO_3$, 1mM $MgCl_2$, 2.2mM

$CaCl_2$ at pH 7.4] supplemented with 0.17% bovine serum albumin and 2.5 mM

glucose (90 min), followed by 20 mM glucose (35 min), 20 mM KCl plus 3mM

glucose (10 min) and finally 2.5 mM glucose (15 min). Medium was collected at

a flow rate 100 µl/min to assess insulin secretion. Insulin concentration was

measured using an Insulin ELISA kit (Alpco cat#80-INSMSU-E01). The islets

were collected at the end of the study and placed in acidified ethanol overnight to

determine total insulin levels.

2.4.1.16 Gene Expression Analysis

Isolated islets and tissues were used to prepare RNA using an RNAeasy

mini kit (Qiagen Cat#74106). 0.5-1µg RNA was converted into cDNA using the

high-capacity cDNA reverse transcription kit (Thermo Fisher Cat#4368813).

TaqMan assays were used to quantify *Ins1* (Assay ID: Mm01259683-g1), *Ins2*

(Assay ID: Mm00731595-gH), *Slc2a2* (Assay ID: Mm00446229_m1), and *Tsh*🚲

(Assay ID: Mm03990915-g1) genes using a Quantstudio PCR machine (Thermo

Fisher). The relative mRNA expression was normalized by measurement of the

amount of *18S* RNA in each sample using Taqman assays (Thermo Fisher

Cat#4308329).

Mapk8ip1 mRNA from JIP1^{WT} and JIP1$^{\Delta Exon2}$ mice was examined by RT-PCR

assays of total RNA using primers designed based on the sequence of distal

exon 1 (5'-CATTCCTGGGACTGCACAT-3') and exon 3 (5'-CTCTTGGGTCGGTAGGTGTC-3') (Figure S1B).

2.4.1.17 Measurement of β cell mass

We measured islet area within pancreas sections using procedures we have reported previously [44]. Briefly, pancreas tissue was fixed in 10% formalin (24 h), dehydrated, and embedded in paraffin. Sections (7µm) were cut and stained using Insulin antibody (Dako Cat#A0564). Immune complexes were detected using peroxidase-conjugated AffiniPure donkey anti-guinea pig antibody (Jackson ImmununoResearch Cat#706-035-148) and the staining was developed with 3,3'diaminobenzidine (Vector Laboratories, DAB peroxidase substrate kit, Cat#SK-4100). The slides were counter-stained with hematoxylin (Fisher Cat#50-823-93) and scanned (Nikon CoolScan). The images were color-separated (red/blue) and converted to gray scale and thresholded using Adobe Photoshop software (Adobe San Jose, CA). Pancreas and β cell areas were quantified using Image J (National Institutes of Health, Bethesda, MD). The β cell mass was calculated as pancreas mass x (β cell area / pancreas area). The quantitation of β cell mass was performed in a blinded manner with respect to genotype identity.

2.4.1.18 Immunofluorescence Staining of Insulin

Immunofluorescence staining of insulin was performed using 7µm thick paraffin embedded pancreas sections stained with an antibody to Insulin (DAKO Cat#A0564) plus a goat anti-guinea pig Alexa-Fluor-488 antibody (Invitrogen

Cat#A-11073). DNA was detected by staining with DAPI (Life Technologies).

Fluorescence was visualized using a Leica TCS SP2 confocal microscope

equipped with a 405-nm diode laser. Quantitation of islet size was performed in

a blinded manner with respect to genotype identity.

2.4.1.19 TRH-induced TSH secretion

Pituitary gland explant cultures have been previously reported [45]. Briefly,

dissected pituitary glands were cultured in 1 ml DMEM (Thermo Fisher

Cat#11960-051) supplemented with 10% bovine growth serum (Fisher Scientific

Cat#SH3054103), 1x L-glutamine (Thermo Fisher cat#25030081), 1x

Penicillin/Streptomycin (Thermo Fisher cat#15140122), and 1x protease inhibitor

cocktail (Millipore Sigma Cat#P1860). The glands were cultured (1h) and then

transferred to fresh culture medium (1 ml) supplemented without or with 300nM

TRH (Millipore Sigma Cat#P1319). Medium (50 µL) was collected at 30 and 60

mins. The pituitary glands were then homogenized in PBS supplemented with 1x

protease inhibitor cocktail.

2.4.1.20 X-Gal histochemistry

Whole pituitary glands were dissected and fixed in fresh 4%

paraformaldehyde (1h). The glands were incubated (3 times, 30 min, 25°C) in

Rinse Buffer (100 mM sodium phosphate (pH 7.3), 2 mM $MgCl_2$, 0.01% sodium

deoxycholate, 0.02% NP-40). The glands were then stained overnight (4°C) in

Rinse Buffer supplemented with 5 mM potassium ferricyanide, 5 mM potassium

ferrocyanide, 1 mg/ml X-gal). The glands were post-fixed overnight in

10%formalin (4°C).

2.4.1.21 Electron Microscopy

The methods used for sample preparation and electron microscopy were

described previously [46] by the UMASS Electron Microscopy Core. Briefly, mice

were starved overnight and injected with 2gr/kg glucose or solvent (phosphate-

buffered saline). The mice were euthanized at 2 min post-injection. The

pancreas was immediately dissected, cut in 1-2mm^3 cubes, and immersed in

fixation solution (2.5% glutaraldehyde in 100 mM cacodylate pH 7.2). The tissue

was fixed overnight, rinsed in cacodylate buffer and then incubated with 1%

osmium tetroxide (1 hr, 25°C). The samples were rinsed with cacodylate buffer

and then dehydrated through a graded ethanol series (20% increments) before

two changes in 100% ethanol. The samples were then infiltrated with two

changes of 100% propylene oxide and then with 50%/50% propylene oxide / SPI-

Pon 812 resin. On the next day, three changes of fresh 100% SPI-Pon 812 resin

were performed before the samples were polymerized at 68°C in plastic

capsules. The samples were then sectioned (1 µm) and stained with toluidine

blue to locate the islets. The tissue was then re-trimmed with islets in the center

and thin sections (approx. 70 nm) were prepared and placed on copper support

grids and contrasted with lead citrate and uranyl acetate. The sections were

examined using FEI Tecani 12 BT microscope with 80Kv accelerating voltage,

and images were captured using a Gatan TEM CCD camera. The images were

false-colored to highlight individual cells using Adobe Photoshop software.

Quantitation of insulin granules was performed in a blinded manner with respect to genotype identity.

2.4.1.22 Primary Neuron Assays

Hippocampal neurons were cultured from E17.5 mouse embryos [17]. The neurons were maintained in serum-free Neurobasal medium (Thermo Fisher Cat#21103049) with the addition of B27 supplement (Thermo Fisher cat#17504044). The neurons were fixed by incubation with 4% paraformaldehyde in PBS. After permeabilization with 0.1% Triton X-100, the cells were incubated in blocking buffer (1% BSA, 2% normal goat serum in phosphate-buffered saline) for 1 h, and then incubated in blocking buffer with primary antibodies to JIP1 (Santa Cruz Biotechnology Cat#sc-15353) and β3-Tubulin (Biolegend Cat#TUBB3). The primary antibodies were detected by incubation with anti-mouse and anti-rabbit Ig conjugated to Alexa Fluor 488 or 633 (Thermo Fisher Cat#A-11029 and Thermo Fisher Cat# A-21071) DNA was detected by staining with DAPI (Thermo Fisher Cat#D1306)). Fluorescence was visualized using a Leica TCS SP2 confocal microscope equipped with a 405-nm diode laser.

2.4.1.23 Quantification and statistical analysis

Immunoblots were quantitated using Image Studio software (https://www.licor.com/bio/products/software/image_studio/) (LICOR-Biosciences). Images were quantitated using Image J64 software

(https://imagej.nih.gov/ij/) (National Institutes of Health). Differences between

two group were examined for statistical significance using the two-tailed

Student's test with Microsoft Excel software (https://products.office.com/en-us/excel). Multiple comparisons were examined by ANOVA using GraphPad

Prism software (http://www.graphpad.com/scientific-software/prism). Statistical

details are presented in the Figure legends.

2.5 References for Chapter 2

1.   Hou JC, Min L, Pessin JE: **Insulin granule biogenesis, trafficking and exocytosis.** *Vitam Horm* 2009, **80:**473-506.

2.   Boland BB, Rhodes CJ, Grimsby JS: **The dynamic plasticity of insulin production in beta-cells.** *Mol Metab* 2017, **6:**958-973.

3.   Seino S, Shibasaki T, Minami K: **Dynamics of insulin secretion and the clinical implications for obesity and diabetes.** *J Clin Invest* 2011, **121:**2118-2125.

4.   Curry DL, Bennett LL, Grodsky GM: **Dynamics of insulin secretion by the perfused rat pancreas.** *Endocrinology* 1968, **83:**572-584.

5.   Orci L, Malaisse-Lagae F, Ravazzola M, Amherdt M, Renold AE: **Exocytosis-endocytosis coupling in the pancreatic beta cell.** *Science* 1973, **181:**561-562.

6.   Tabei SM, Burov S, Kim HY, Kuznetsov A, Huynh T, Jureller J, Philipson LH, Dinner AR, Scherer NF: **Intracellular transport of insulin granules is a subordinated random walk.** *Proc Natl Acad Sci U S A* 2013, **110:**4911-4916.

7.   Wang Z, Thurmond DC: **Mechanisms of biphasic insulin-granule exocytosis - roles of the cytoskeleton, small GTPases and SNARE proteins.** *J Cell Sci* 2009, **122:**893-903.

8.   Zhu X, Hu R, Brissova M, Stein RW, Powers AC, Gu G, Kaverina I: **Microtubules Negatively Regulate Insulin Secretion in Pancreatic beta Cells.** *Dev Cell* 2015, **34:**656-668.

9.   Mourad NI, Nenquin M, Henquin JC: **Metabolic amplification of insulin secretion by glucose is independent of beta-cell microtubules.** *Am J Physiol Cell Physiol* 2011, **300:**C697-706.

10.   Varadi A, Tsuboi T, Johnson-Cadwell LI, Allan VJ, Rutter GA: **Kinesin I and cytoplasmic dynein orchestrate glucose-stimulated insulin-containing vesicle movements in clonal MIN6 beta-cells.** *Biochem Biophys Res Commun* 2003, **311:**272-282.

11.   Meng YX, Wilson GW, Avery MC, Varden CH, Balczon R: **Suppression of the expression of a pancreatic beta-cell form of the kinesin heavy chain by antisense oligonucleotides inhibits insulin secretion from primary cultures of mouse beta-cells.** *Endocrinology* 1997, **138:**1979-1987.

12.   Heaslip AT, Nelson SR, Lombardo AT, Beck Previs S, Armstrong J, Warshaw DM: **Cytoskeletal dependence of insulin granule movement dynamics in INS-1 beta-cells in response to glucose.** *PLoS One* 2014, **9:**e109082.

13.   Donelan MJ, Morfini G, Julyan R, Sommers S, Hays L, Kajio H, Briaud I, Easom RA, Molkentin JD, Brady ST, Rhodes CJ: **Ca2+-dependent dephosphorylation of kinesin heavy chain on beta-granules in pancreatic beta-cells. Implications for regulated beta-granule transport and insulin exocytosis.** *J Biol Chem* 2002, **277:**24232-24242.

14.   McDonald A, Fogarty S, Leclerc I, Hill EV, Hardie DG, Rutter GA: **Control of insulin granule dynamics by AMPK dependent KLC1 phosphorylation.** *Islets* 2009, **1:**198-209.

15.   Cui J, Wang Z, Cheng Q, Lin R, Zhang XM, Leung PS, Copeland NG, Jenkins NA, Yao KM, Huang JD: **Targeted inactivation of kinesin-1 in**

pancreatic beta-cells in vivo leads to insulin secretory deficiency. *Diabetes* 2011, **60:**320-330.

16. Fu MM, Holzbaur EL: **Integrated regulation of motor-driven organelle transport by scaffolding proteins.** *Trends Cell Biol* 2014, **24:**564-574.

17. Whitmarsh AJ, Kuan CY, Kennedy NJ, Kelkar N, Haydar TF, Mordes JP, Appel M, Rossini AA, Jones SN, Flavell RA, et al: **Requirement of the JIP1 scaffold protein for stress-induced JNK activation.** *Genes Dev* 2001, **15:**2421-2432.

18. Verhey KJ, Meyer D, Deehan R, Blenis J, Schnapp BJ, Rapoport TA, Margolis B: **Cargo of kinesin identified as JIP scaffolding proteins and associated signaling molecules.** *J Cell Biol* 2001, **152:**959-970.

19. Waeber G, Delplanque J, Bonny C, Mooser V, Steinmann M, Widmann C, Maillard A, Miklossy J, Dina C, Hani EH, et al: **The gene MAPK8IP1, encoding islet-brain-1, is a candidate for type 2 diabetes.** *Nat Genet* 2000, **24:**291-295.

20. Jaeschke A, Czech MP, Davis RJ: **An essential role of the JIP1 scaffold protein for JNK activation in adipose tissue.** *Genes Dev* 2004, **18:**1976-1980.

21. Liu HY, Cao SY, Hong T, Han J, Liu Z, Cao W: **Insulin is a stronger inducer of insulin resistance than hyperglycemia in mice with type 1 diabetes mellitus (T1DM).** *J Biol Chem* 2009, **284:**27090-27100.

22. Templeman NM, Flibotte S, Chik JHL, Sinha S, Lim GE, Foster LJ, Nislow C, Johnson JD: **Reduced Circulating Insulin Enhances Insulin Sensitivity in Old Mice and Extends Lifespan.** *Cell Rep* 2017, **20:**451-463.

23. Horiuchi D, Barkus RV, Pilling AD, Gassman A, Saxton WM: **APLIP1, a kinesin binding JIP-1/JNK scaffold protein, influences the axonal transport of both vesicles and mitochondria in Drosophila.** *Curr Biol* 2005, **15:**2137-2141.

24. Chiba K, Araseki M, Nozawa K, Furukori K, Araki Y, Matsushima T, Nakaya T, Hata S, Saito Y, Uchida S, et al: **Quantitative analysis of APP axonal transport in neurons: role of JIP1 in enhanced APP anterograde transport.** *Mol Biol Cell* 2014, **25:**3569-3580.

25. Fu MM, Holzbaur EL: **JIP1 regulates the directionality of APP axonal transport by coordinating kinesin and dynein motors.** *J Cell Biol* 2013, **202:**495-508.

26. Morrison DK, Davis RJ: **Regulation of MAP kinase signaling modules by scaffold proteins in mammals.** *Annu Rev Cell Dev Biol* 2003, **19:**91-118.

27. Zhang T, Inesta-Vaquera F, Niepel M, Zhang J, Ficarro SB, Machleidt T, Xie T, Marto JA, Kim N, Sim T, et al: **Discovery of potent and selective covalent inhibitors of JNK.** *Chem Biol* 2012, **19:**140-154.

28. Kant S, Standen CL, Morel C, Jung DY, Kim JK, Swat W, Flavell RA, Davis RJ: **A Protein Scaffold Coordinates SRC-Mediated JNK Activation in Response to Metabolic Stress.** *Cell Rep* 2017, **20:**2775-2783.

29. Roelfsema F, Veldhuis JD: **Thyrotropin secretion patterns in health and disease.** *Endocr Rev* 2013, **34:**619-657.

30. Whitmarsh AJ, Cavanagh J, Tournier C, Yasuda J, Davis RJ: **A mammalian scaffold complex that selectively mediates MAP kinase activation.** *Science* 1998, **281:**1671-1674.

31. Horiuchi D, Collins CA, Bhat P, Barkus RV, Diantonio A, Saxton WM: **Control of a kinesin-cargo linkage mechanism by JNK pathway kinases.** *Curr Biol* 2007, **17:**1313-1317.

32. Morfini G, Pigino G, Szebenyi G, You Y, Pollema S, Brady ST: **JNK mediates pathogenic effects of polyglutamine-expanded androgen receptor on fast axonal transport.** *Nat Neurosci* 2006, **9:**907-916.

33. Morfini GA, You YM, Pollema SL, Kaminska A, Liu K, Yoshioka K, Bjorkblom B, Coffey ET, Bagnato C, Han D, et al: **Pathogenic huntingtin inhibits fast axonal transport by activating JNK3 and phosphorylating kinesin.** *Nat Neurosci* 2009, **12:**864-871.

34. Wicksteed B, Brissova M, Yan W, Opland DM, Plank JL, Reinert RB, Dickson LM, Tamarina NA, Philipson LH, Shostak A, et al: **Conditional gene targeting in mouse pancreatic ss-Cells: analysis of ectopic Cre transgene expression in the brain.** *Diabetes* 2010, **59:**3090-3098.

35. Cushman LJ, Burrows HL, Seasholtz AF, Lewandoski M, Muzyczka N, Camper SA: **Cre-mediated recombination in the pituitary gland.** *Genesis* 2000, **28:**167-174.

36. Tronche F, Kellendonk C, Kretz O, Gass P, Anlag K, Orban PC, Bock R, Klein R, Schutz G: **Disruption of the glucocorticoid receptor gene in the nervous system results in reduced anxiety.** *Nat Genet* 1999, **23:**99-103.

37. Zhu Y, Romero MI, Ghosh P, Ye Z, Charnay P, Rushing EJ, Marth JD, Parada LF: **Ablation of NF1 function in neurons induces abnormal development of cerebral cortex and reactive gliosis in the brain.** *Genes Dev* 2001, **15:**859-876.

38. Farley FW, Soriano P, Steffen LS, Dymecki SM: **Widespread recombinase expression using FLPeR (flipper) mice.** *Genesis* 2000, **28:**106-110.

39. Kim D, Pertea G, Trapnell C, Pimentel H, Kelley R, Salzberg SL: **TopHat2: accurate alignment of transcriptomes in the presence of insertions, deletions and gene fusions.** *Genome Biol* 2013, **14:**R36.

40. Thorvaldsdottir H, Robinson JT, Mesirov JP: **Integrative Genomics Viewer (IGV): high-performance genomics data visualization and exploration.** *Brief Bioinform* 2013, **14:**178-192.

41. Yasuda J, Whitmarsh AJ, Cavanagh J, Sharma M, Davis RJ: **The JIP group of mitogen-activated protein kinase scaffold proteins.** *Mol Cell Biol* 1999, **19:**7245-7254.

42. Parker DC, Greiner DL, Phillips NE, Appel MC, Steele AW, Durie FH, Noelle RJ, Mordes JP, Rossini AA: **Survival of mouse pancreatic islet allografts in recipients treated with allogeneic small lymphocytes and antibody to CD40 ligand.** *Proc Natl Acad Sci U S A* 1995, **92:**9560-9564.

43. Jurczyk A, Nowosielska A, Przewozniak N, Aryee KE, DiIorio P, Blodgett D, Yang C, Campbell-Thompson M, Atkinson M, Shultz L, et al: **Beyond the brain: disrupted in schizophrenia 1 regulates pancreatic beta-cell function via glycogen synthase kinase-3beta.** *FASEB J* 2016, **30:**983-993.

44. Alonso LC, Yokoe T, Zhang P, Scott DK, Kim SK, O'Donnell CP, Garcia-Ocana A: **Glucose infusion in mice: a new model to induce beta-cell replication.** *Diabetes* 2007, **56:**1792-1801.

45. Roper LK, Briguglio JS, Evans CS, Jackson MB, Chapman ER: **Sex-specific regulation of follicle-stimulating hormone secretion by synaptotagmin 9.** *Nat Commun* 2015, **6:**8645.

46. Pearring JN, San Agustin JT, Lobanova ES, Gabriel CJ, Lieu EC, Monis WJ, Stuck MW, Strittmatter L, Jaber SM, Arshavsky VY, Pazour GJ: **Loss of Arf4 causes severe degeneration of the exocrine pancreas but not cystic kidney disease or retinal degeneration.** *PLoS Genet* 2017, **13:**e1006740.

CHAPTER 3: Role of the cJun NH$_2$-Terminal Kinase (JNK) signaling pathway in starvation-induced autophagy

3.1 INTRODUCTION

Autophagy is a cellular mechanism that enables recycling of cytoplasmic content and plays an important role in cellular homeostasis [1, 2]. Autophagy is initiated with the formation of the phagophore, a double membrane structure that surrounds a portion of cytoplasm [3]. These structures progress to the development of autophagosomes that fuse with lysosomes to form autophago-lysosomes that release nutrients to the cytoplasm(Figure 3.1.) [3].
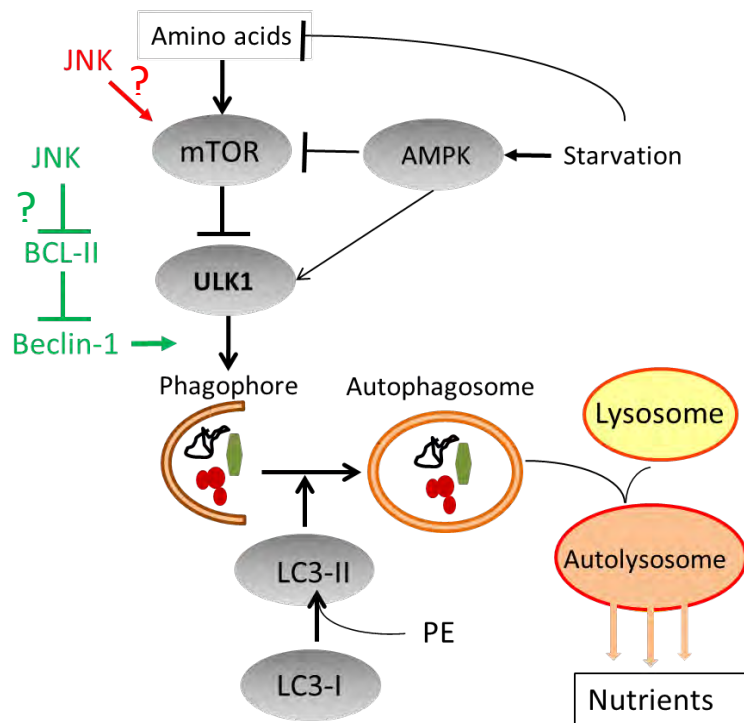
Figure 3.1. Cartoon represents the recycle of cytoplasmic components by autophagy. Previously suggested role of JNK in autophagy pathway is highlighted by red, where JNK has an inhibitory role on autophagy through mTOR, and green, where JNK has an inducer role on autophagy through Beclin-1.

A major regulator of autophagy is established to be the Mechanistic Target of Rapamycin (mTOR) pathway that can sense cellular energy and amino acid levels [4]. TORC1 is activated when cells are in a nutrient rich environment, which leads to inhibition of autophagy [4]. However, suppression of TORC1 activity in response to low energy balance or amino acid starvation causes increased autophagy [4].

It was recently reported that MAPK8/JNK1 (but not MAPK9/JNK2) is required for the induction of autophagy by starvation [5]. This mechanism of MAPK8 signaling is mediated by BCL2 phosphorylation (on Thr-69, Ser-70, and Ser-87) that disrupts BCL2/BECN1 interactions and initiates BECN1-dependent autophagy [5]. Subsequent studies have provided strong support for this role of MAPK8 in autophagy [6-19], although contributing roles for MAPK9 [20-23] and alternative potential functions of MAPK8 related to autophagy have also been reported [24-29].

The MAPK8-promoted autophagy pathway raises several questions. First, what is the mechanistic relationship between the MAPK8 and mTOR pathways in the regulation of autophagy by starvation? Second, since MAPK8 exhibits functional redundancy as a BCL2 kinase [20, 30-34], what mechanism accounts for the requirement of MAPK8 for starvation-induced autophagy? The purpose of this study was to examine these two questions in the context of starvation-induced autophagy. We show that the role of MAPK8/9 in autophagy may be context-dependent and substantially more complex than previously considered.

3.2 Results

3.2.1 mTOR-regulated autophagy does not require MAPK8/9 (JNK)

It is established that mTOR is a master regulator of starvation-induced autophagy [4]. The requirement of MAPK8 for starvation-induced autophagy [5] may therefore reflect a role for MAPK8 upstream or down-stream of mTOR. Indeed, previous studies have demonstrated that MAPK8/9 can be activated in response to TORC1 signaling [35] and that TORC1 activation can require MAPK8/9 signaling [28]. Alternatively, MAPK8/9 and TORC1 may function in parallel pathways that control autophagy.

To test whether MAPK8/9 plays a role in autophagy induction downstream of mTOR, we examined the effect of Torin1, a small molecule inhibitor of mTOR. Control studies demonstrated that Torin1 prevented the phosphorylation of the mTOR substrate Thr-389 RPS6KB1/p70-S6K1 in both wild-type (WT) and *Mapk8*$^{-/-}$ *Mapk9*$^{-/-}$ (JNK$^{\Delta1,2}$) immortalized MEF (Figure 3.2.).
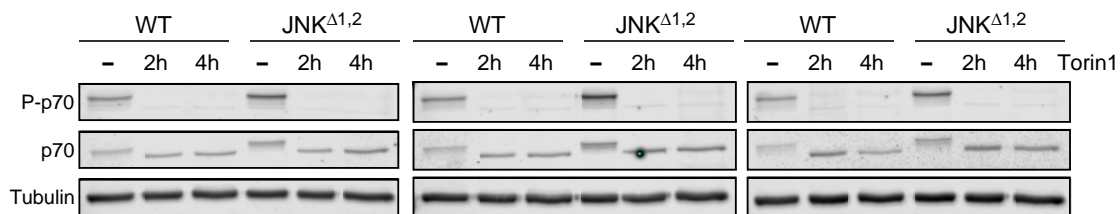
Figure 3.2. The amount of RPS6KB1 (p70), pThr-389 RPS6KB1 (p-p70), and ✔-Tubulin in WT and JNKΔ1, 2 immortalized MEF after incubation without or with 250nM Torin1 (2 or 4 h) was examined by immunoblot analysis.

To assess the effect of Torin1 on autophagy, we initially examined the formation of MAP1LC3B /LC3B puncta in the cytoplasm by fluorescence microscopy. We found that Torin1 caused similar MAP1LC3B puncta in both WT and JNK$^{\Delta1,2}$ immortalized MEF (Figure 3.3.).
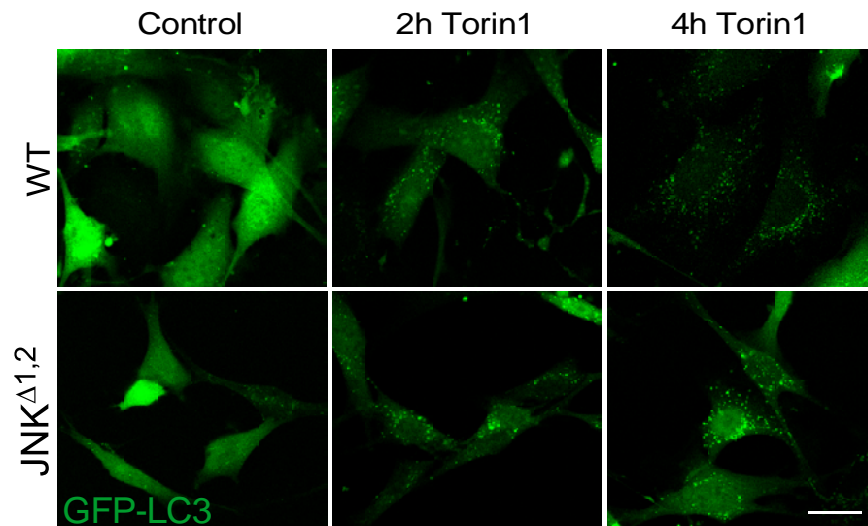
Figure 3.3. WT and JNK$^{\Delta1, 2}$ immortalized MEF were transduced with a lentivirus vector that expresses eGFP- MAP1LC3B (eGFP-LC3B). Puncta formation following incubation of the cells with 250 nM Torin1 (2h and 4h) was examined by fluorescence microcopy. Scale bar = 30 μm.

This observation suggested that MAPK8/9 deficiency caused no major change in autophagy as a result of mTOR inhibition. This conclusion was confirmed by measurement of autophagic flux by monitoring the formation of MAP1LC3B-II in response to mTOR inhibition in the presence of a lysosomal inhibitor [36] (Figure 3.4.) and reduced accumulation of the autophagic substrate SQSTM1/p62 (Figure 3.5.).
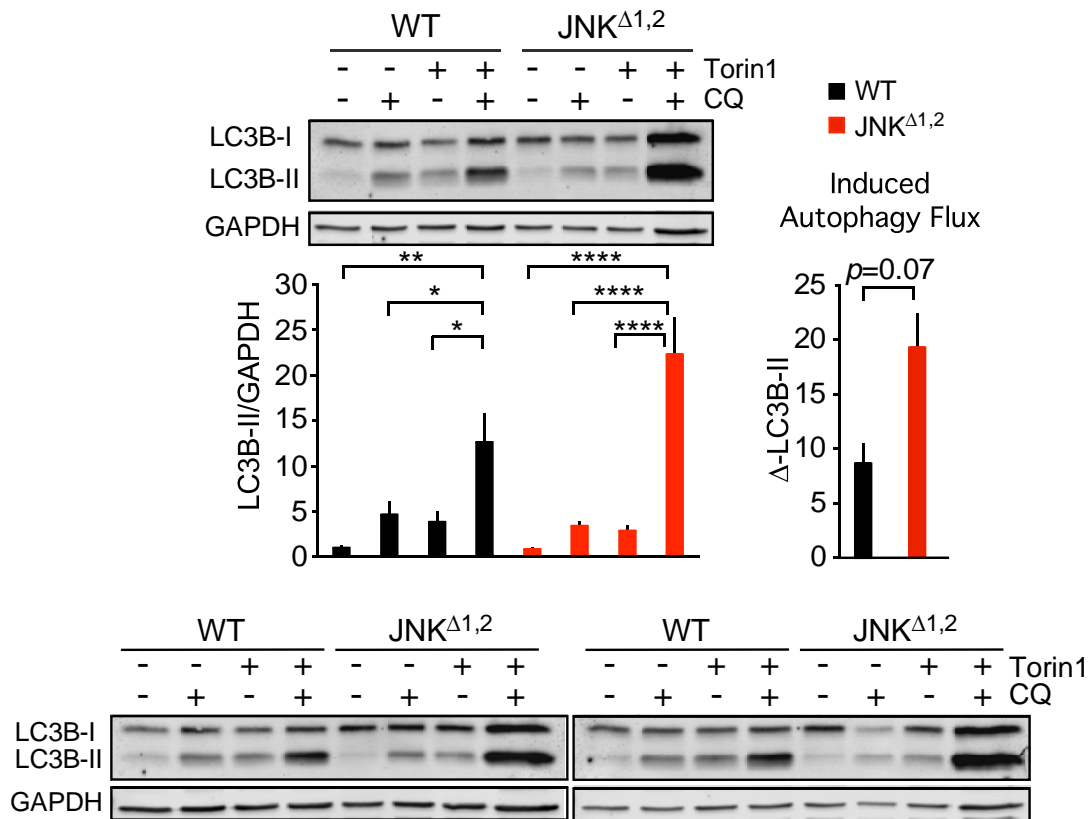
Figure 3.4. MAP1LC3B (LC3B) and GAPDH expression by WT and JNK[Δ1, 2] immortalized MEF after incubation (2 h) without or with 250 nM Torin1 in the absence or presence of 25 µM chloroquine (CQ) was examined by immunoblot analysis. The LC3B-II/GAPDH ratios were normalized to the mean of WT control condition (first lane). The data presented represent the mean ± SEM; n=3 independent experiments; *, $p<0.05$; **, $p<0.01$; ***, $p<0.001$; ****, $p<0.0001$. Two-way ANOVA was used for the analysis of LC3B-II expression and Student's T test is used for the flux analysis.

Figure 3.5. The amount of SQSTM1 (p62) and ✔-Tubulin in WT and JNK$^{\Delta 1, 2}$ immortalized MEF after incubation with 250 nM Torin1 (2 or 4 h) was examined by immunoblot analysis. The p62/Tubulin ratio was quantitated and normalized to p62 expression in WT cells treated without Torin1 (mean ± SEM; n=3 independent experiments; **, $p<0.01$ (two-way ANOVA).

Torin1 is an active site-directed inhibitor of mTOR and therefore inhibits both mTOR complexes TORC1 and TORC2 [37]. To test the role of TORC1, we used low dose Rapamycin to selectively block TORC1 [37]. Control studies

demonstrated that Rapamycin inhibited phosphorylation of the TORC1 substrate

Thr-389 RPS6KB1, but not the TORC2 substrate Ser-473 AKT (Figure 3.6.).
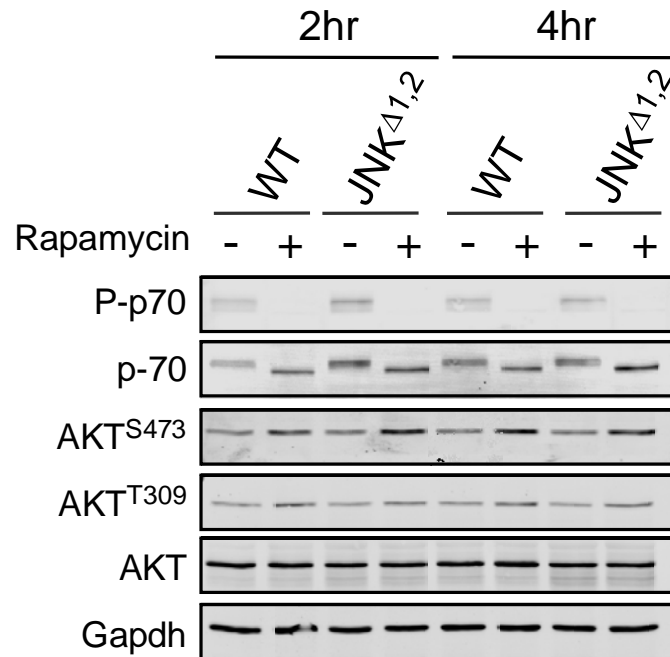
Figure 3.6. RPS6KB1 (p70), pThr-389 RPS6KB1 (P-p70), AKT, pThr-308 AKT, pSer-473 AKT, and GAPDH expression by WT and JNK$^{\Delta 1, 2}$ immortalized MEF after incubation (2 h) without or with 200 nM Rapamycin was examined by immunoblot analysis.

We found that treatment of WT and JNK$^{\Delta 1,2}$ immortalized MEF with rapamycin

caused a similar increase in autophagic flux that was measured by monitoring

the accumulation of MAP1LC3B-II in the presence of a lysosomal inhibitor [36]

(Figure 3.7.).
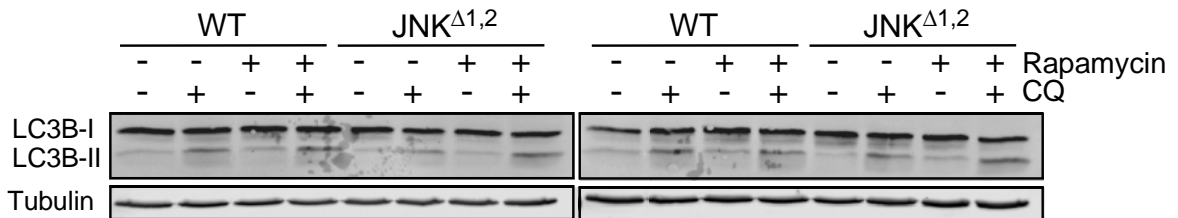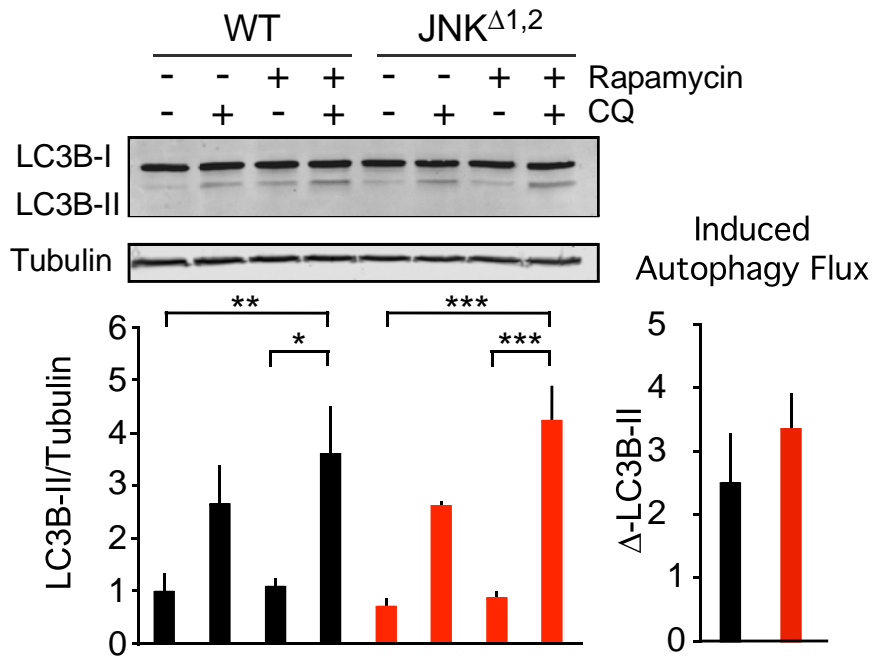
Figure 3.7. MAP1LC3B (LC3B) and α-Tubulin expression by WT and JNK$^{\Delta 1, 2}$ immortalized MEF after incubation (2 h) without or with 200 nM Rapamycin in the presence or absence of 25 µM chloroquine (CQ) was examined by immunoblot analysis. The LC3B-II/Tubulin ratios were normalized to the mean of WT control (first lane). The data presented represent the mean ± SEM; n=3 independent experiments; *, $p<0.05$; **, $p<0.01$; ***, $p<0.001$. Two-way ANOVA was used for the analysis of LC3B-II expression and Student's T test was used for the flux analysis.

Collectively, these data demonstrate that MAPK8/9 are not required for autophagy induced in response to inhibition of TORC1 (by Rapamycin) and inhibition of TORC1 plus TORC2 (by Torin1).

3.2.2 Starvation-induced autophagy does not require MAPK8/9

Our analysis of the effects of mTOR on autophagy in immortalized MEF demonstrated that MAPK8/9 does not regulate autophagy down-stream of mTOR (Figure 3.2.). It was therefore possible that MAPK8/9 functions upstream of mTOR in the regulation of autophagy by starvation [28]. To test this hypothesis, we examined TORC1 signaling in response to starvation.
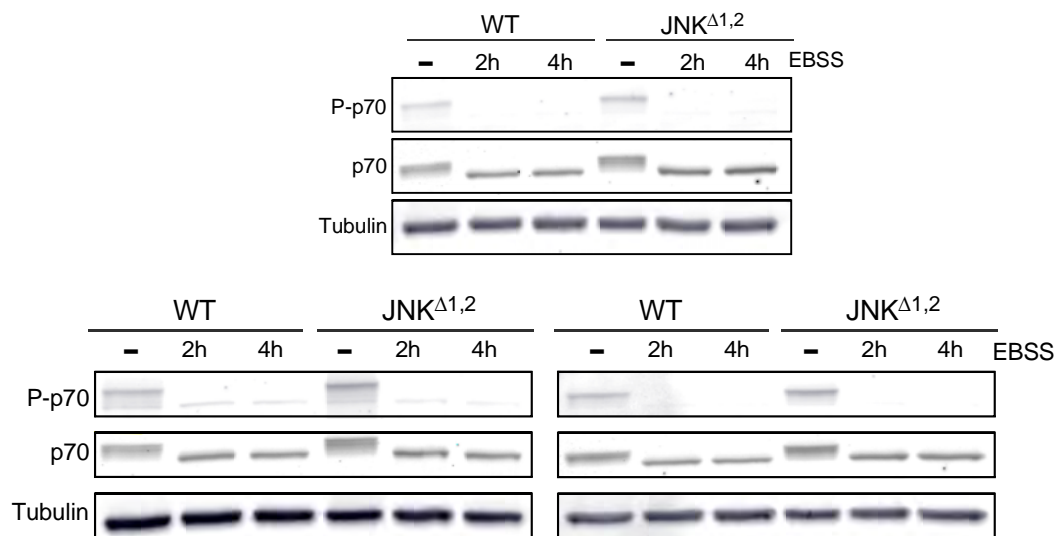
Figure 3.8. RPS6KB1 (p70), pThr-389 RPS6KB1 (P-p70), and GAPDH expression by WT and JNK$^{\Delta1, 2}$ immortalized MEF after incubation with EBSS/5mM glucose (2 or 4h) was examined by immunoblot analysis.

We found that starvation prevented the phosphorylation of the TORC1 substrate Thr-389 RPS6KB1 in both WT and JNK$^{\Delta1,2}$ immortalized MEF (Figure 3.8.). MAPK8/9 are therefore not required for suppression of TORC1 signaling by starvation. Studies of autophagy demonstrated similar MAP1LC3B puncta formation following starvation of WT and JNK$^{\Delta1,2}$ immortalized MEF (Figure 3.9.).

Similarly, no differences in autophagic flux (Figure 3.10.) or accumulation of the autophagic substrate SQSTM1 (Figure 3.11.) were detected between WT and JNK$^{\Delta1,2}$ immortalized MEF. This analysis suggests that MAPK8/9 in immortalized MEF play no required role in starvation-induced autophagy.

Figure 3.9. WT and JNK$^{\Delta1, 2}$ immortalized MEF were transduced with a lentivirus vector that expresses eGFP- MAP1LC3B (eGFP-LC3B). Puncta formation following incubation with EBSS/5 mM glucose (2h) was examined by fluorescence microcopy. Scale bar = 30 μm.

Figure 3.10. MAP1LC3B (LC3B) and GAPDH in WT and JNK[Δ1, 2] immortalized MEF after incubation (2 h) in medium or with EBSS/5 mM glucose in the presence or absence of 25µM chloroquine (CQ) was examined by immunoblot analysis. The LC3B-II/GapDH ratios were normalized to the average of WT control condition (first lane). The data presented represent the mean ± SEM; n=3 independent experiments; *, $p<0.05$; **, $p<0.01$; ***; $p<0.001$; ****; $p<0.0001$. Two-way ANOVA was used for the analysis of LC3B-II expression and Student's T test was used for the flux analysis.
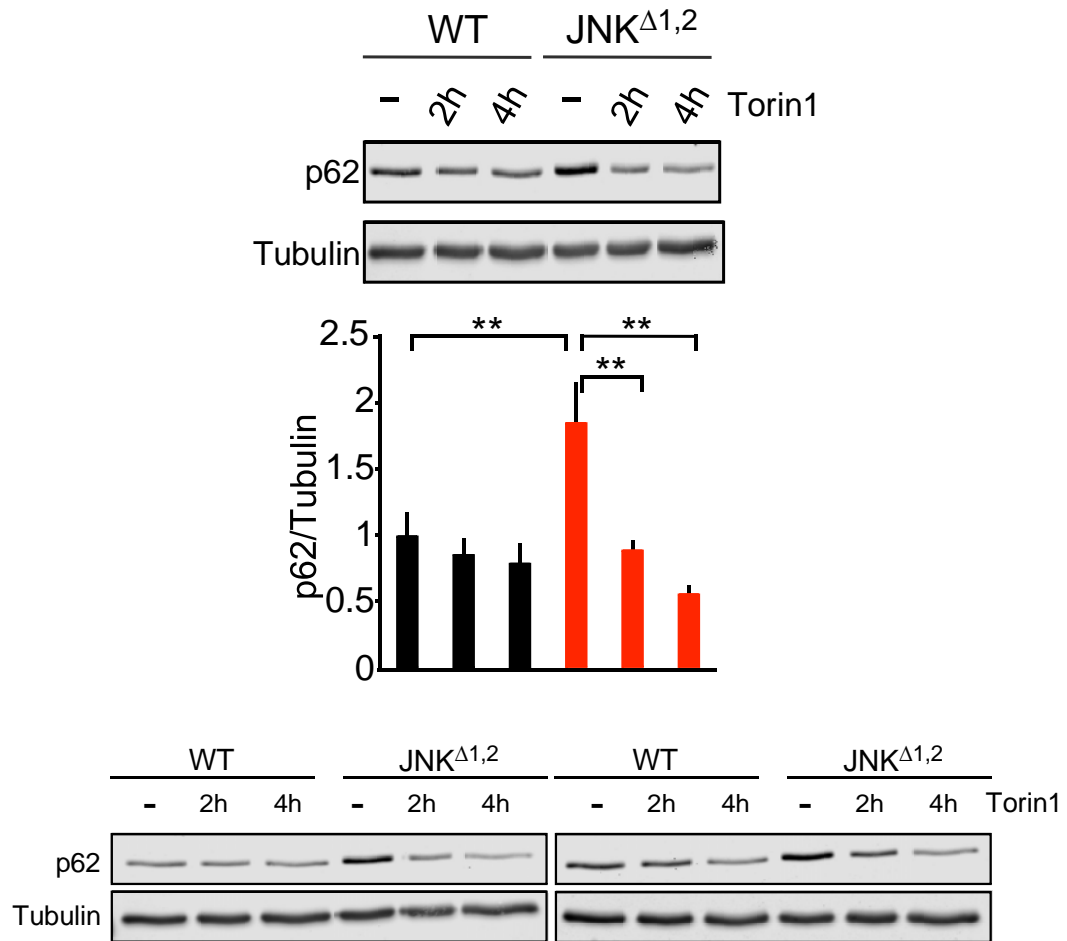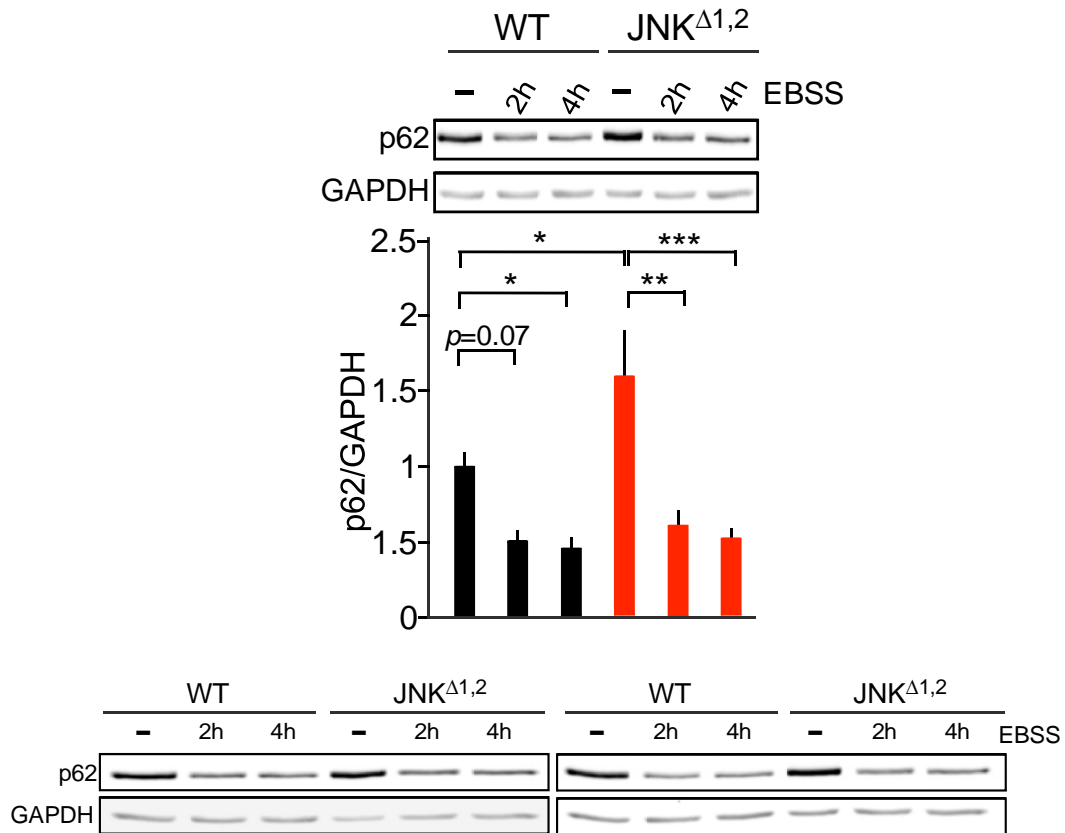
Figure 3.11. The amount of SQSTM1 (p62) and GAPDH in WT and JNK[Δ1, 2] immortalized MEF after incubation with EBSS/5 mM glucose (2 or 4h) was examined by immunoblot analysis. The p62/GAPDH ratio was quantitated and normalized to WT cells treated without EBSS (mean ± SEM; n=3 independent experiments; *, $p<0.05$; **, $p<0.01$; ***; $p<0.001$ (two-way ANOVA).

3.2.3 MAPK8/9 activation and mTOR inhibition

Our inability to detect a difference in autophagy between WT and JNK[Δ1,2] immortalized MEF was not anticipated. One explanation for this finding is that MAPK8/9 is not regulated under the conditions that we employed for these experiments. Indeed, we found that mTOR inhibition caused by starvation or

treatment with Torin1 (Figure 3.12.) under the conditions of the autophagy
assays did not lead to MAPK8/9 activation.
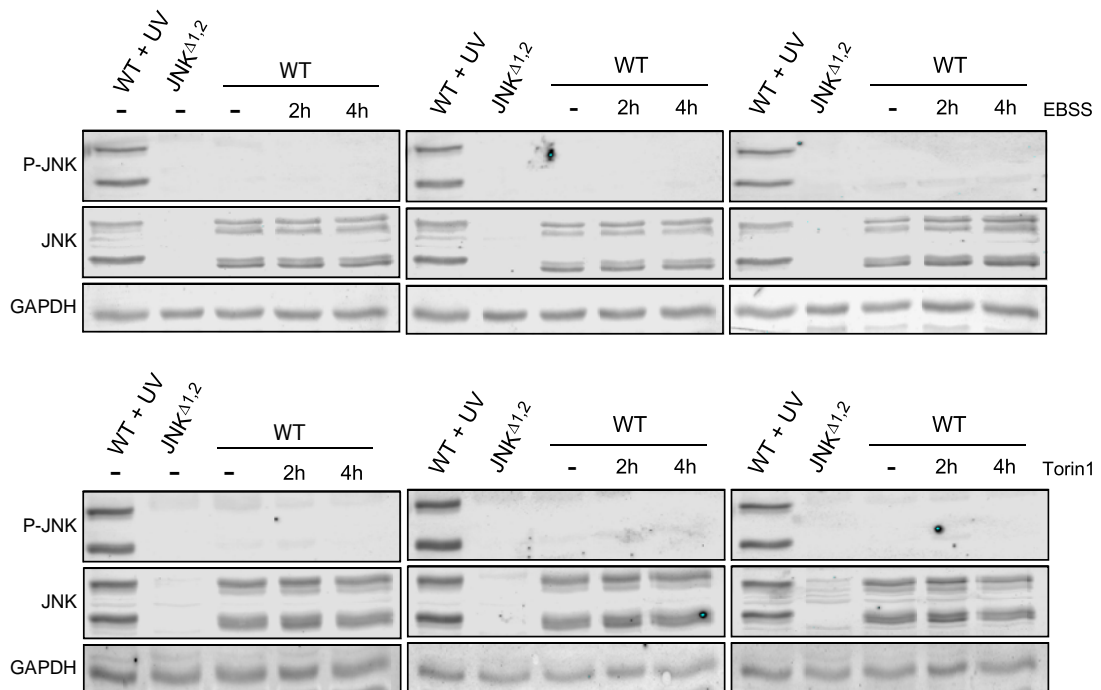
Figure 3.12. MAPK8/9 (JNK) activation in immortalized MEF was examined by
immunoblot analysis of phospho-JNK (P-JNK), JNK, and GAPDH in cells after
incubation (2 or 4h) with EBSS/5 mM glucose (upper panel) or 250 nM Torin1
(lower panel). Lanes 1 & 2 represent positive and negative controls: lysates of
WT MEF exposed to 60J/m^2 UV and JNK$^{\Delta1,\,2}$ MEF.

It is therefore possible that in a different cell type, or under different culture
conditions, MAPK8/9 could be activated and thus may contribute to the
regulation of autophagy during starvation or Torin1 treatment.

To test whether MAPK8/9 activation is sufficient for the induction of autophagy, we examined the effect of MAPK8/9 activation on the conversion of MAP1LC3B-I to MAP1LC3B-II by immunoblot analysis using WT and JNK$^{\Delta 1,2}$ immortalized MEF. We found that activated MAPK8/9 caused no change in MAP1LC3B-II formation (Figure 3.13.).

WT JNK$^{\Delta 1,2}$ WT JNK$^{\Delta 1,2}$ WT JNK$^{\Delta 1,2}$ WT JNK$^{\Delta 1,2}$ WT JNK$^{\Delta 1,2}$ WT JNK$^{\Delta 1,2}$

− − + +   − − + +   − − + +   UV

LC3B-I
LC3B-II
P-JNK
JNK
GAPDH
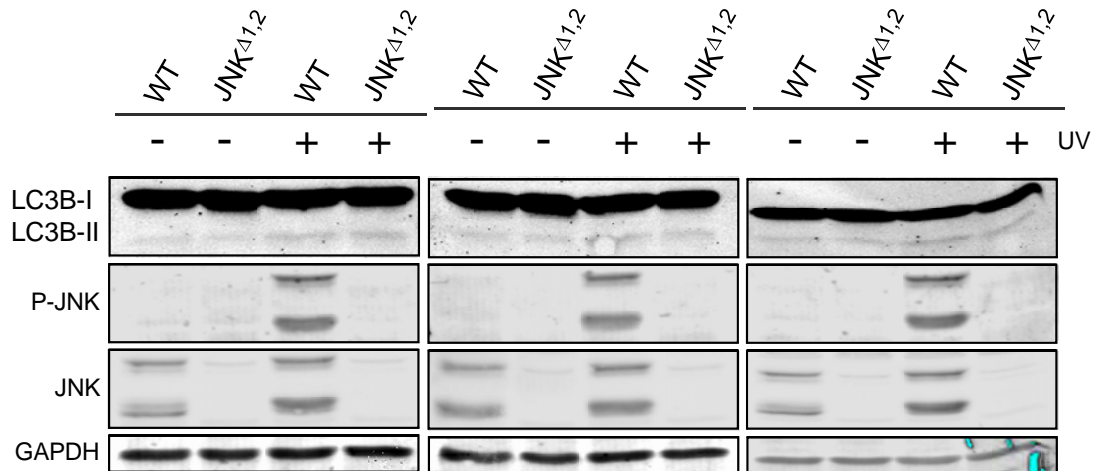
Figure 3.13. WT and JNK$^{\Delta 1, 2}$ immortalized MEF were exposed to UV radiation (60J/m^2) and cell extracts were prepared at 45 min post-irradiation. The expression of MAP1LC3B (LC3B), phospho-JNK (P-JNK), JNK and GAPDH was examined by immunoblot analysis.

These data suggest that MAPK8/9 activation is not sufficient for autophagy and that MAPK8/9-promoted autophagy likely involves interactions between MAPK8/9 and other pro-autophagic signaling pathways.

3.2.4 MAPK8/9 is not required for starvation or Torin1-induced autophagy in primary MEF

Our initial studies of immortalized MEF may be compromised by the loss of TRP53 function in these cells, which may change autophagic responses [38]. We therefore repeated our studies using early passage primary WT and JNK$^{\Delta 1,2}$ MEF. The primary MEF exhibited reduced autophagy flux compared with immortalized MEF. We found that MAPK8/9 deficiency caused no change in MAP1LC3B puncta formation in response to starvation (Figure 3.14.).
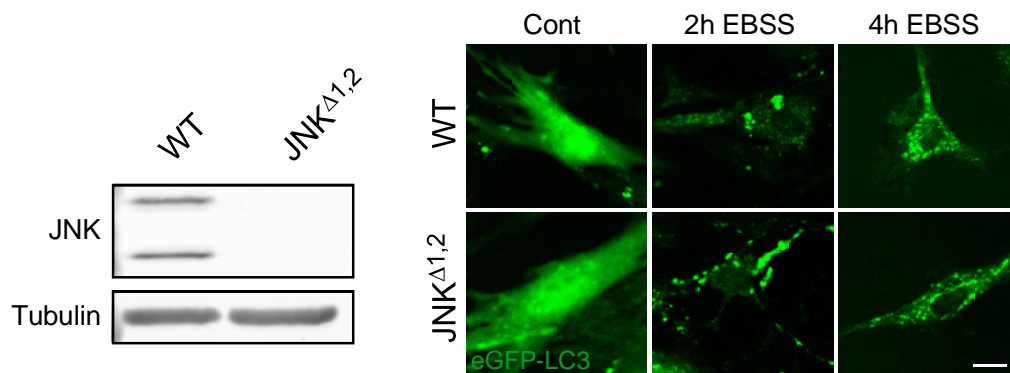
Figure 3.14. 4-Hydroxytamoxifen-treated primary *Rosa*-Cre^{ERT} (WT) MEF and *Rosa*-Cre^{ERT} *Mapk8*$^{LoxP/LoxP}$ *Mapk9*$^{-/-}$ (JNK$^{\Delta 1, 2}$) MEF were examined by immunoblot analysis by probing with antibodies to MAPK8/9 (JNK) and α-Tubulin (right). WT and JNK$^{\Delta 1, 2}$ primary MEF were transduced with a lentivirus vector that expresses eGFP- MAP1LC3B (eGFP-LC3B). Puncta formation following incubation with EBSS/5 mM glucose (2h and 4h) was examined by fluorescence microcopy (right). Scale bar = 25 µm.

Similarly, MAPK8/9-deficiency caused no change in starvation-induced autophagic flux (Figure 3.15) or accumulation of the autophagic substrate SQSTM1 (Figure 3.16).
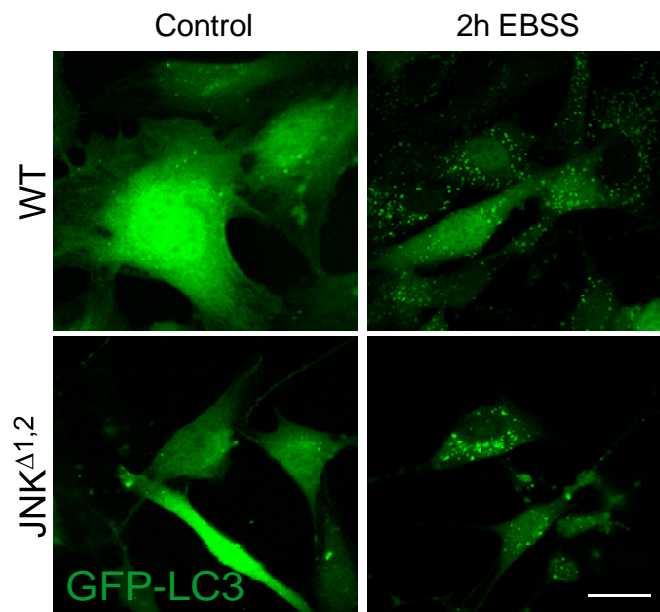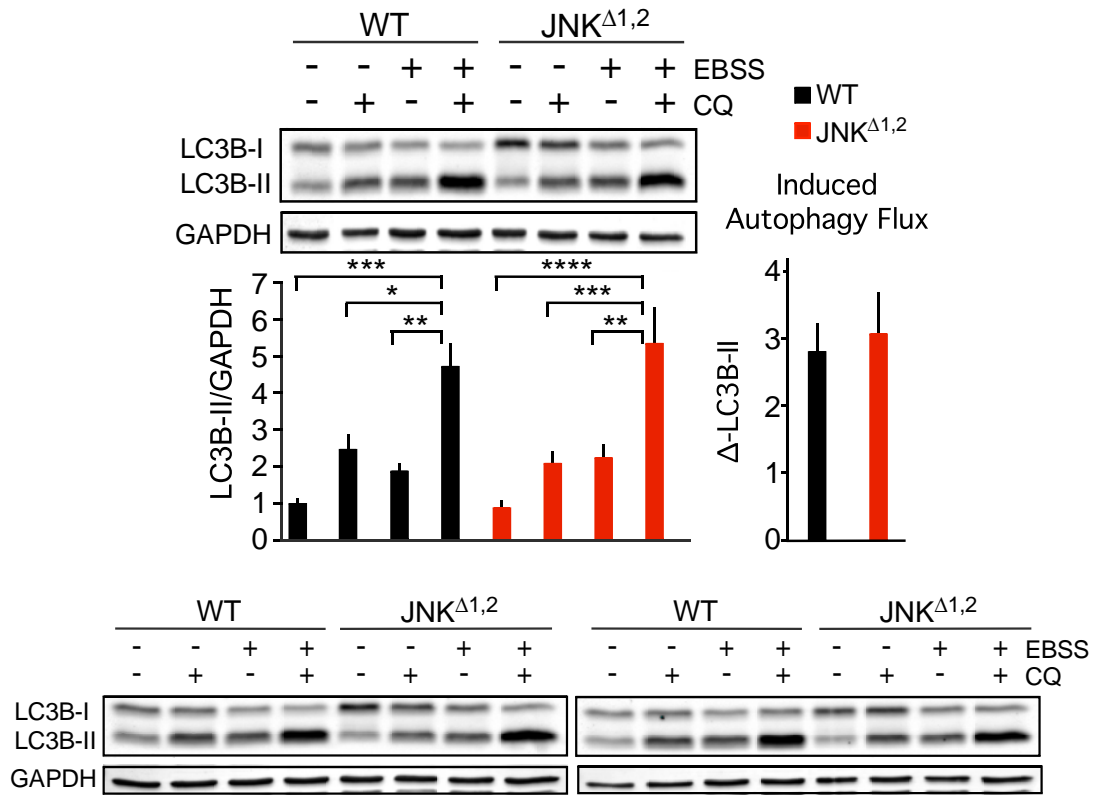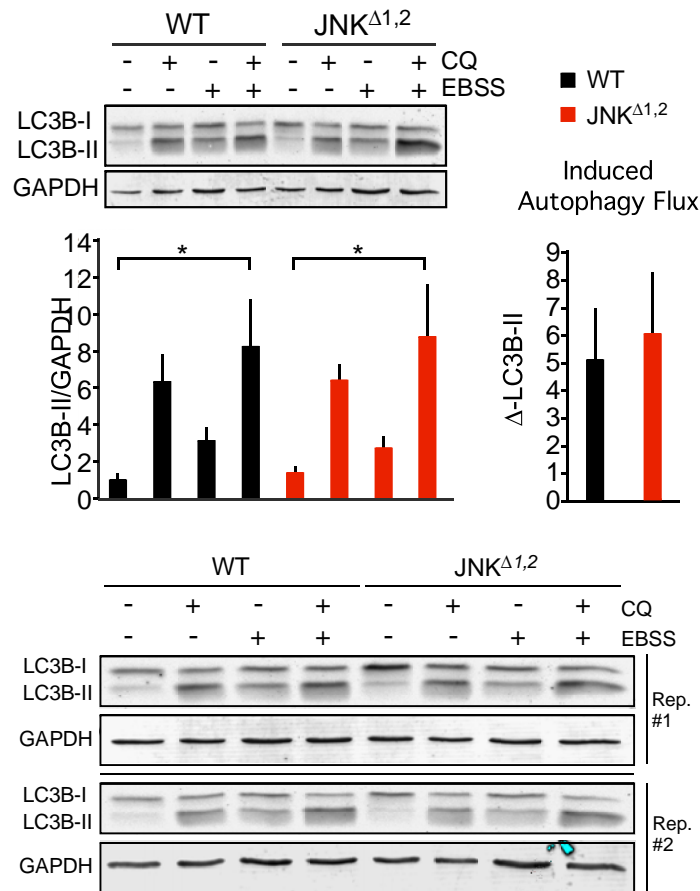

Figure 3.15. MAP1LC3B (LC3B) and GAPDH expression by WT and JNK[Δ1, 2] primary MEF after incubation (2h) in medium or with EBSS/5 mM glucose in the presence or absence of 25 µM chloroquine (CQ) was examined by immunoblot analysis. The LC3B-II/GAPDH ratios were normalized to the mean of WT control (first lane). The data presented represent the mean ± SEM; n=3 independent experiments; *, $p < 0.05$. Two-way ANOVA was used for the analysis of LC3B-II expression and Student's T test was used for the flux analysis.
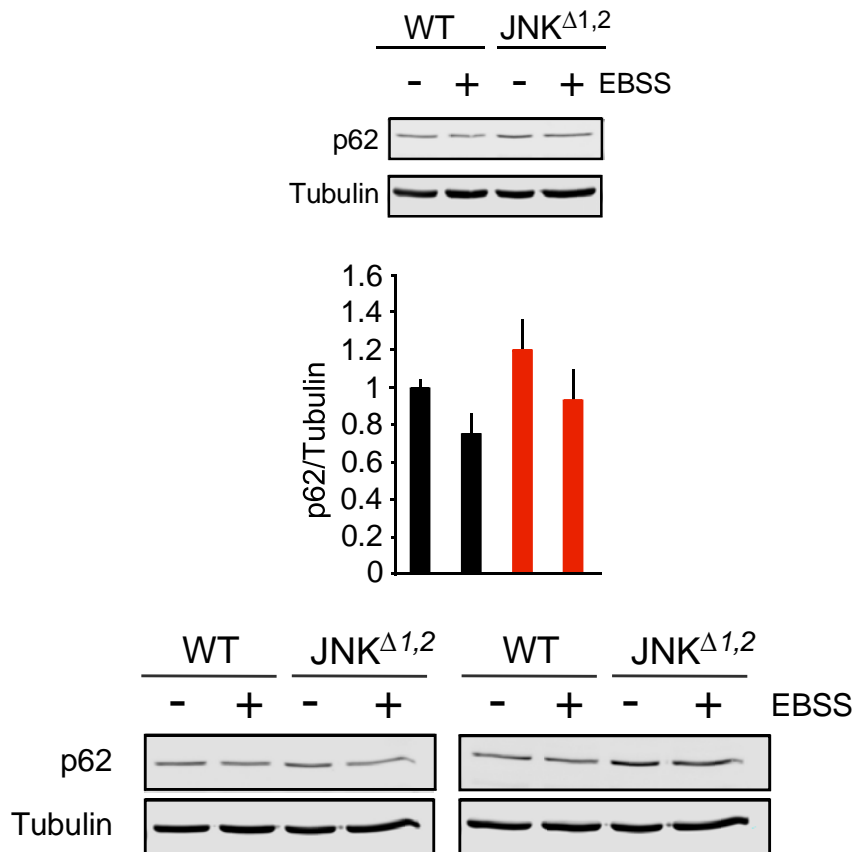
Figure 3.16. The amount of SQSTM1 (p62) and α-Tubulin in WT and JNK[Δ1, 2] primary MEF after incubation with EBSS/5mM glucose (2h) was examined by immunoblot analysis. The p62/Tubulin ratio was quantitated and normalized to p62 expression in WT non-starved cells (mean ± SEM; n=3 independent experiments).

Control studies demonstrated that starvation under these conditions did not activate MAPK8/9, but did prevent phosphorylation of the TORC1 substrate Thr-389 RPS6KB1 (Figure 3.17).
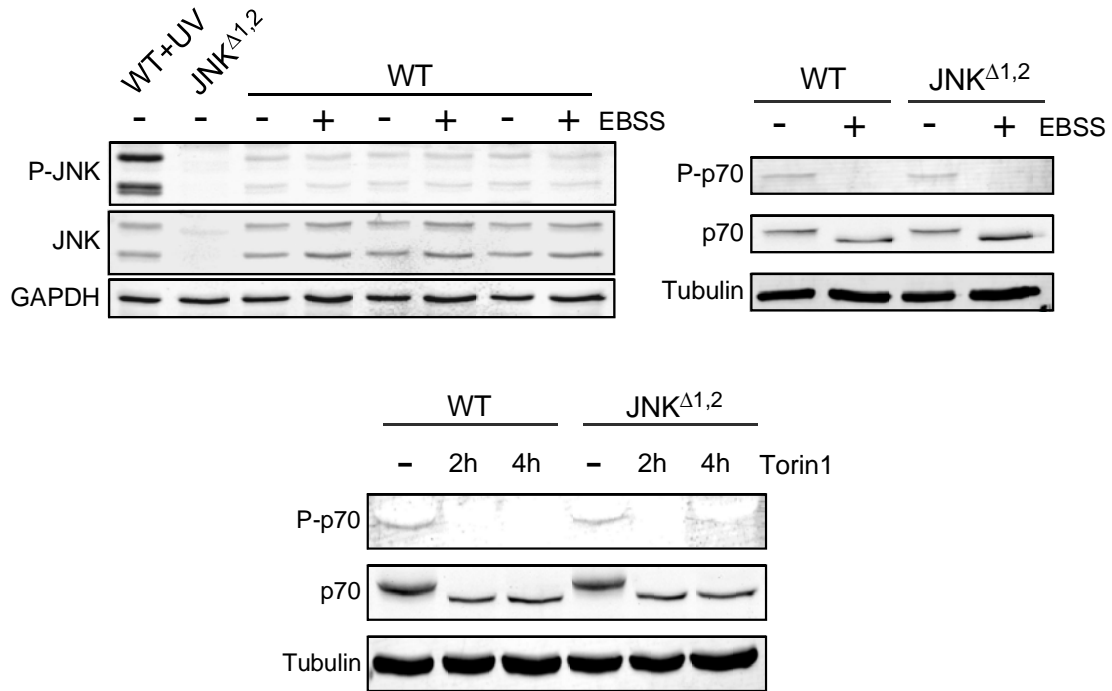
Figure 3.17. MAPK8/9 (JNK) activation in WT and JNK$^{\Delta 1, 2}$ primary MEF was examined by immunoblot analysis of phospho-MAPK8/9 (P-JNK), MAPK8/9 (JNK), and GAPDH after incubation (2h) with media or EBSS/5mM glucose. WT MEF exposed to UV (60J/m^2) and JNK$^{\Delta 1, 2}$ MEF represent positive and negative controls (left). RPS6KB1 (p70), pThr-389 RPS6KB1 (P-p70), and ✔-Tubulin in WT and JNK$^{\Delta 1, 2}$ primary MEF after incubation (2h) with EBSS/5mM glucose was examined by immunoblot analysis (upper panel). The amount of p70-S6K1 (p70), pThr-389 p70-S6K1 (P-p70), and ✔-Tubulin in WT and JNK$^{\Delta 1, 2}$ primary MEF after incubation with 250 nM Torin1 (2 or 4 h) was examined by immunoblot analysis (lower panel).

Studies of Torin1-induced autophagy demonstrated similar inhibition of the phosphorylation of the TORC1 substrate Thr-389 RPS6KB1 in primary WT and

129

JNK$^{\Delta1,2}$ MEF (Figure 3.17.). These cells showed similar Torin1-induced

MAP1LC3B puncta formation (Figure 3.18.).
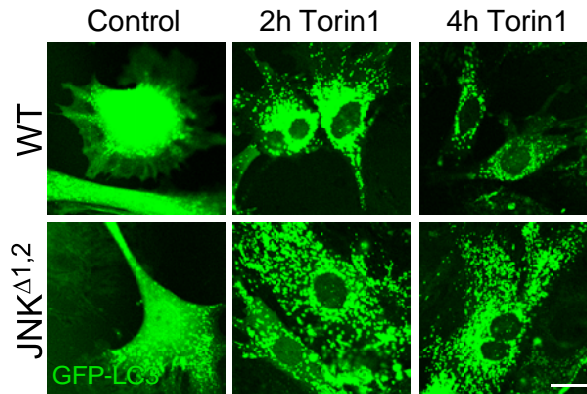
Figure 3.18. WT and JNK$^{\Delta1, 2}$ primary MEF were transduced with a lentivirus vector that expresses GFP-LC3. Puncta formation following incubation with 250nM Torin1 (2h and 4h) was examined by fluorescence microcopy. Scale bar = 25 µm.

A modest decrease in autophagic flux and modestly increased accumulation of the autophagic substrate SQSTM1 was detected in JNK$^{\Delta1,2}$ primary MEF compared with WT primary MEF (Figure 3.19.). Together, these data indicate that MAPK8/9 play no required role in starvation-induced autophagy in primary MEF.

3.2.5 Requirement of MAPK8 and MAPK9 for starvation-induced autophagy in primary MEF

It is possible that our analysis of compound MAPK8 plus MAPK9-deficiency in MEF is compromised by compensatory mechanisms that are

engaged in these cells. Indeed, the role of MAPK8/9 in starvation-induced autophagy was first established in studies using *Mapk8$^{-/-}$* (JNK$^{\Delta 1}$) and *Mapk9$^{-/-}$* (JNK$^{\Delta 2}$) primary MEF [5]. We therefore examined the effects of starvation on WT, JNK$^{\Delta 1}$, and JNK$^{\Delta 2}$ primary MEF. Starvation prevented the phosphorylation of the TORC1 substrate Thr-389 RPS6KB1 in these cells (Figure 3.20.).
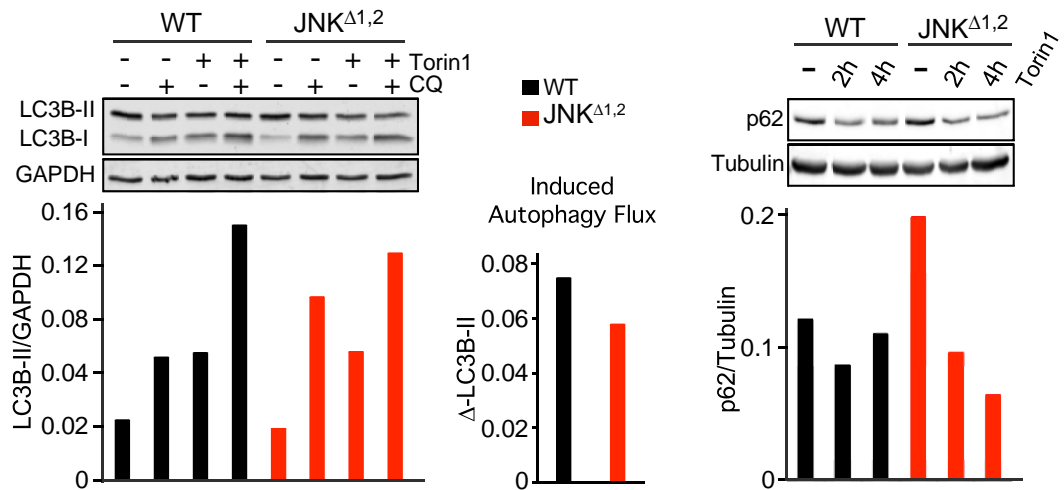
Figure.3.19. LC3B and GAPDH expression by WT and JNK$^{\Delta 1, 2}$ primary MEF after incubation (2 h) with 250nM Torin1 without and with 25µM chloroquine (CQ) was examined by immunoblot analysis. Protein band intensity is quantified and LC3B-II/GAPDH ratios are graphed (left). Autophagy flux is calculated by subtracting LC3B-II/GAPDH ratio in Torin1 condition from Torin1+CQ condition (middle). The amount of p62/SQSTM1 and ✔-Tubulin in WT and JNK$^{\Delta 1, 2}$ primary MEF after incubation with 250 nM Torin1 (2 or 4h) was examined by immunoblot analysis. The p62/Tubulin ratio was quantitated (right).
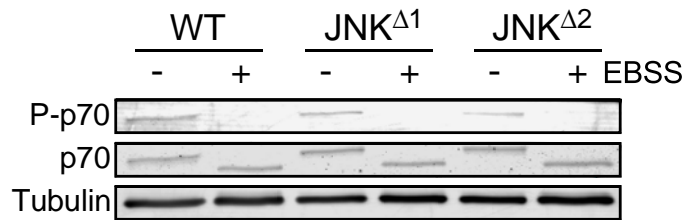
Figure 3.20. The amount of p70-S6K1 (p70), pThr-389 p70-S6K1 (P-p70), and α-Tubulin in WT, JNK$^{\Delta 1}$ and JNK$^{\Delta 2}$ primary MEF after incubation in culture media or EBSS/5 mM glucose (2h) was examined by immunoblot analysis.
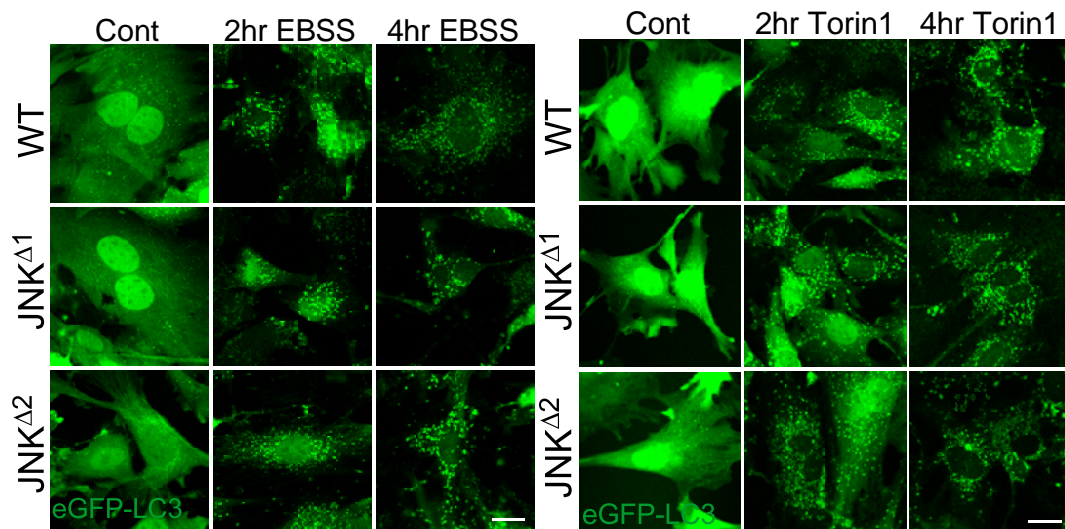
Figure 3.21. WT, JNK$^{\Delta 1}$ and JNK$^{\Delta 2}$ primary MEF were transduced with a lentivirus vector that expresses GFP-LC3B. Puncta formation following incubation of the cells in EBSS/5 mM glucose *(left panels)* or in media with 250 nM Torin1 *(right panels)* was examined by fluorescence microcopy. Scale bar = 25 μm.

Studies of WT, JNK$^{\Delta 1}$, and JNK$^{\Delta 2}$ primary MEF identified similar MAP1LC3B puncta formation (Figure 3.21). Accumulation of the autophagic substrate SQSTM1 (Figure 3.22.), and autophagic flux (Figure 3.23.) were also

similar. These data demonstrate that MAPK8-deficiency and MAPK9-deficiency cause no major defects in starvation-induced autophagy.
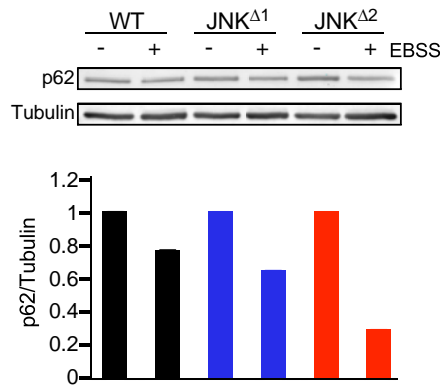
Figure 3.22. The amount of p62/SQSTM1 and α-Tubulin in WT, JNK$^{\Delta 1}$ and JNK$^{\Delta 2}$ primary MEF after incubation in culture media or EBSS/5 mM glucose (2 h) was examined by immunoblot analysis.

Figure 3.23. LC3B and GAPDH expression by WT, JNK$^{\Delta 1}$ and JNK$^{\Delta 2}$ primary MEF after incubation (2 h) in culture media or EBSS/5 mM glucose without and with 25μM chloroquine (CQ) was examined by immunoblot analysis. Protein band intensity is quantified and LC3B-II/Gapdh ratios are graphed.

3.2.6 Requirement of MAPK8/9 for starvation-induced autophagy in primary epithelial cells

Our analysis of primary and immortalized MEF suggests that MAPK8/9 plays no required role in starvation-induced autophagy. However, studies of a different cell type may lead to a different conclusion. We therefore examined starvation-induced autophagic flux in primary kidney epithelial cells.
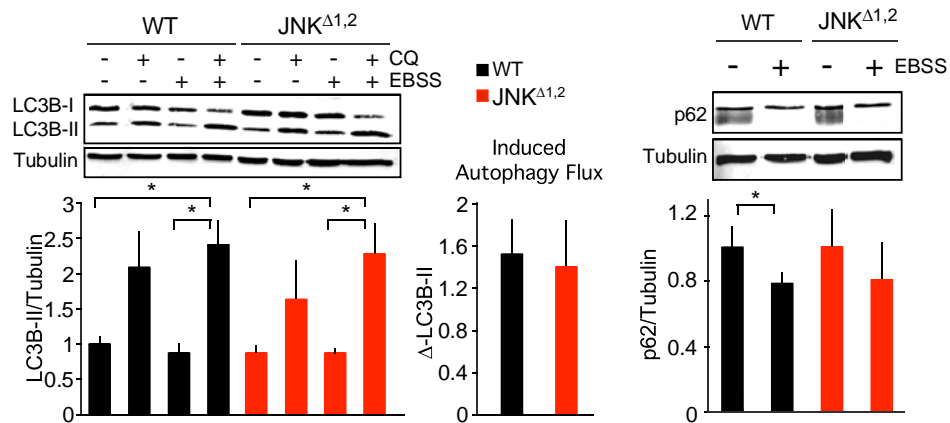
Figure 3.24. LC3B and GAPDH expression by WT and JNK[Δ1, 2] primary epithelial cells after incubation (2h) without or with EBSS/5 mM glucose in the presence or presence of 25 µM chloroquine (CQ) was examined by immunoblot analysis. Protein band intensity is quantified and LC3B-II/Tubulin ratios are normalized to the average of the control (first panel). Autophagy flux is calculated by subtracting LC3B-II/Tubulin ratio in EBSS condition from EBSS+CQ condition. (middle panel) The amount of p62/SQSTM1 and α-Tubulin in WT and JNK[Δ1, 2] primary epithelial cells after incubation with EBSS/5 mM glucose (2h) was examined by immunoblot analysis. The p62/Tubulin ratio was quantitated (right panel). (mean ± SEM; n=3 independent experiments) *$p<0.05$ Two-way ANOVA is used for LC3B-II/Tubulin analysis and p62/Tubulin analysis, Student's T test is used for the flux analysis.)

We found that MAPK8/9 deficiency caused no difference in autophagic flux in these epithelial cells, and no difference in the accumulation of the autophagic substrate SQSTM1 (Figure 3.24.) in response to starvation. These data demonstrate that MAPK8/9 has no required role in primary kidney epithelial cells for starvation-induced autophagy.

3.2.7 Requirement of MAPK8/9 for autophagy in response to Ras and hypoxia

If MAPK8/9 are not required for autophagy in response to starvation or mTOR inhibition, it is possible that MAPK8/9 may be required for autophagy in response to other stimuli. JNK activation is increased in Ras transformed MEFs compared to controls (Figure 3.25.)
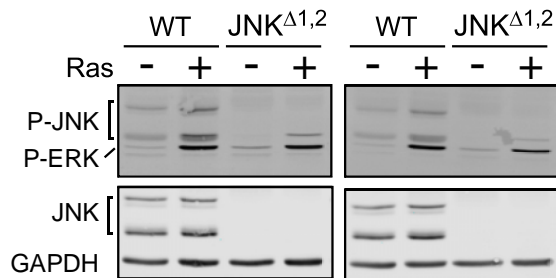
Figure 3.25. P-JNK, JNK, and GAPDH expression by WT-Puro, WT-HRAS, $Jnk^{\Delta 1,2}$-Puro and $Jnk^{\Delta 1,2}$-HRas immortalized (p53-/-) MEFs (P12).

We therefore examined $Trp53^{-/-}$ MEF (-Ras) and H-Ras transformed (+Ras) $Trp53^{-/-}$ MEF without (WT) and with ablation of the $Mapk8$ plus $Mapk9$ genes (JNK$^{\Delta 1,2}$) (Figure S8A). Autophagic flux studies demonstrated no

significant effects of MAPK8/9 deficiency (Figure 3.26). These data indicate that

MAPK8/9 are not required for autophagy in Control or *H-Ras*-transformed *Trp53*^{-/-}

MEF.
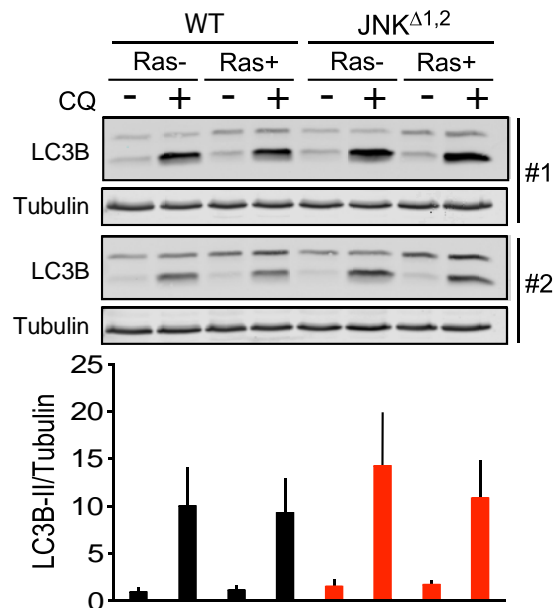
Figure 3.26. LC3B and GAPDH expression by MEFs after 24 h incubation in the
presence or absence of 25 µM chloroquine (CQ) was examined by immunoblot
analysis. Protein band intensity is quantified and LC3B-II/Tubulin ratios are
normalized to the average of WT control condition (First lane). (n=2; Two-way
ANOVA is used for LC3B-II/Tubulin analysis.)

We also studied Control and *H-Ras* transformed *Trp53*^{-/-} MEF without

(WT) and with ablation of the *Mapk8* plus *Mapk9* genes (JNK[Δ1,2]) MEF under

hypoxia (1.5 % O_2) conditions (Figure 3.27.). Autophagic flux studies

demonstrated no significant effects of MAPK8/9 deficiency (Figure 3.28.). These

data indicate that MAPK8/9 are not required for autophagy in Control or *H-Ras*-

transformed *Trp53*^{-/-} MEF under hypoxia conditions.
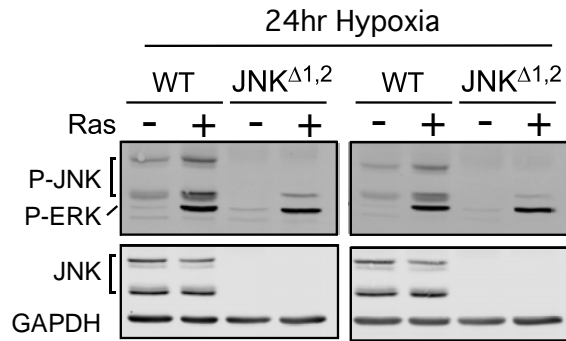
Figure 3.27. P-JNK, JNK, and GAPDH expression by WT-Puro, WT-HRAS, $Jnk^{\Delta1,2}$-Puro and $Jnk^{\Delta1,2}$-HRas immortalized (p53-/-) MEFs (P12) after 24 h incubation in 1.5% O_2.
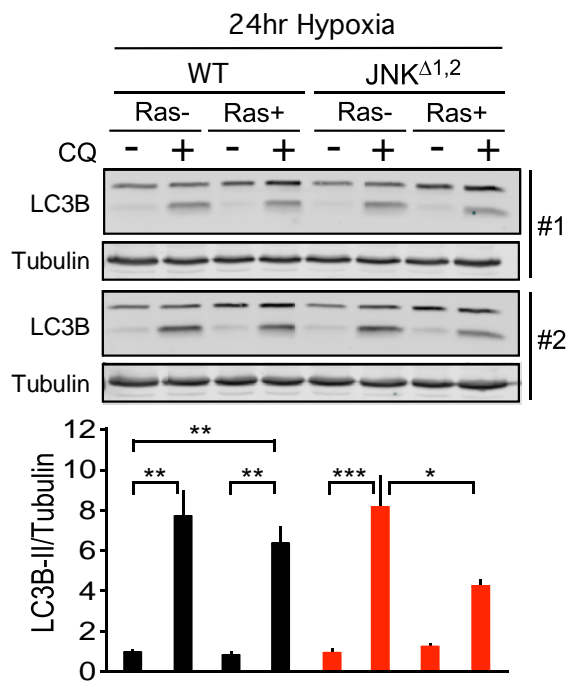
Figure 3.28. LC3B and GAPDH expression by MEFs after 24 h incubation in 1.5% O_2 in the presence or absence of 25 μM chloroquine (CQ) was examined by immunoblot analysis. Protein band intensity is quantified and LC3B-II/Tubulin ratios are normalized to the average of WT control condition (First lane).

3.2.8 MAPK8/9-regulated autophagy in primary hepatocytes

Autophagy plays a major role in systemic metabolic homeostasis [39] and hepatic lipid metabolism [40]. Moreover, hepatocytes have been reported to exhibit MAPK8/9-dependent autophagy [6]. We therefore examined the requirement of MAPK8/9 for autophagy using primary hepatocytes prepared from *Alb-cre*^{-/+} (Control) mice and *Alb-cre*^{-/+} *Mapk8*[LoxP/LoxP] *Mapk9*[LoxP/LoxP] (JNK[Δ1,2]) mice. We found that JNK[Δ1,2] hepatocytes exhibited increased accumulation of MAP1LC3B-II following lysosomal inhibition and the reduced accumulation of the autophagic substrate SQSTM1 in JNK[Δ1,2] hepatocytes compared with Control hepatocytes (Figure 3.29.). These observations suggest that MAPK8/9 may inhibit autophagy in hepatocytes.
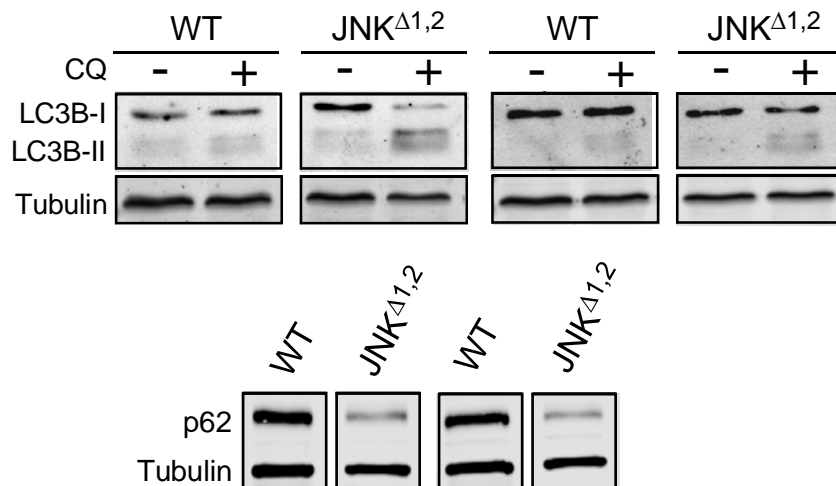
Figure 3.29. MAP1LC3B (LC3B) and ✓-Tubulin in WT and JNK[Δ1, 2] primary hepatocytes after incubation (6 h) with medium or EBSS/5 mM glucose in the presence or absence of 25µM chloroquine (CQ) was examined by immunoblot analysis (upper panel). The amount of SQSTM1 (p62) and α-Tubulin in WT and JNK[Δ1, 2] primary hepatocytes was examined by immunoblot analysis.

To confirm the conclusion that MAPK8/9 suppresses autophagic flux in primary hepatocytes, we examined wild-type (WT) hepatocytes treated with JNK-in-8, a potent and selective small molecule inhibitor of MAPK8/9 [41]. We found that treatment with JNK-in-8 caused increased accumulation of MAP1LC3B-II following lysosomal inhibition and reduced accumulation of the autophagic substrate SQSTM1 (Figure 3.30.). These data indicate that pharmacological inhibition of MAPK8/9 causes increased autophagic flux.
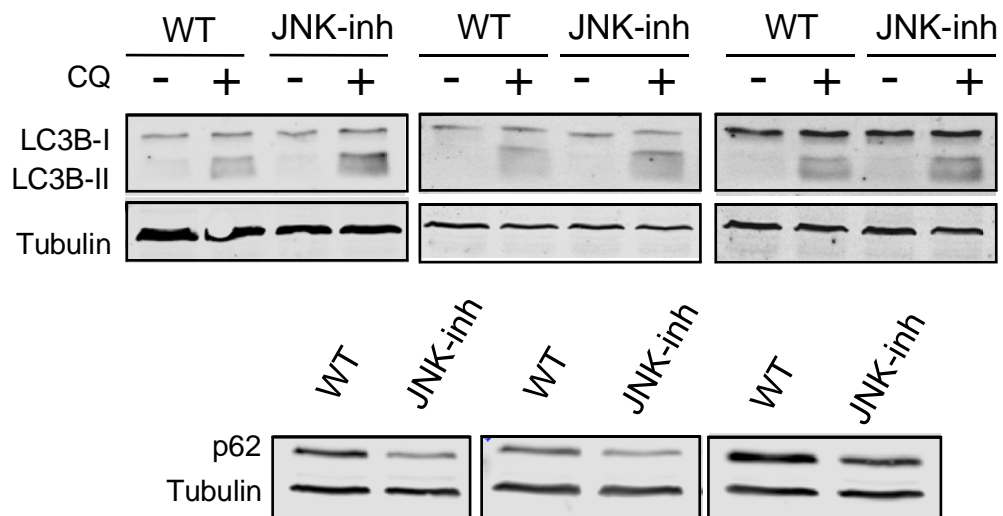
Figure 3.30. WT primary hepatocytes were incubated (6 h) without or with 2 µM JNK-in-8. MAP1LC3B (LC3B) and ✓-Tubulin in WT and JNK[Δ1, 2] primary hepatocytes in the presence or absence of 25 µM CQ was examined by immunoblot analysis (C). The amount of SQSTM1 (p62) and ✓-Tubulin was examined by immunoblot analysis (D).

The increased autophagy caused by MAPK8/9 loss-of-function in

hepatocytes compared with WT hepatocytes was unexpected. This increased

autophagy may reflect the established role of MAPK8/9 to strongly suppress the

transcriptional activity of the PPARᵥ nuclear receptor [42] that can promote

autophagy through increased expression of autophagic genes [43]. This role of

MAPK8/9 to suppress basal autophagy in hepatocytes is similar to the

established function of MAPK8/9/10 in neurons to suppress basal autophagy by

repression of autophagic gene expression [27].

3.3 DISCUSSION

Studies of the genetically tractable organism *Drosophila* demonstrate that the

basket gene (encodes a MAPK8/9 ortholog) can increase autophagy [44]. It is

established that Basket in *Drosophila* promotes autophagy by causing increased

expression of autophagy proteins [44]. This mechanism is also found in

mammals [45-51]. Thus, MAPK8/9 may promote autophagy by increasing the

expression of ATG4 [49], ATG5 [45], BECN1 [48], BNIP3 [47, 50], MAP1LC3B

[46, 51], and SQSTM1 [46]. MAPK8/9-regulated gene expression therefore

represents an evolutionarily conserved mechanism of autophagic regulation.

The specific physiological effects of MAPK8/9 on the expression of autophagic

proteins likely reflects the combinatorial actions of MAPK8/9-regulated

transcription factors together with other transcription factors that are activated by

different signal transduction pathways. MAPK8/9 may therefore play an essential

role in mammalian autophagy in some specific physiological or pathological contexts.

Recently, MAPK8 was proposed to promote starvation-induced autophagy in MEF by a non-transcriptional mechanism [5]. $Mapk8^{-/-}$ (JNK$^{\Delta1}$) MEF, but not $Mapk9^{-/-}$ (JNK$^{\Delta2}$) MEF, were reported to be resistant to starvation-induced autophagy [5]. The mechanism was proposed to be mediated by phosphorylation of BCL2 (on Thr-69, Ser-70, and Ser-87) by MAPK8, disruption of BCL2/BECN 1 complexes, and the initiation of BECN1-dependent autophagy [5]. This mechanism implies that MAPK8 is essential for BCL2 phosphorylation [5]. However, other studies indicate that MAPK8 may only serve a redundant role in BCL2 phosphorylation [20, 30-34]. The essential non-transcriptional role of MAPK8 in starvation-induced autophagy [5] is therefore likely to be mediated by BCL2 phosphorylation only in specific cellular contexts.

Possible roles of MAPK8 in starvation-induced autophagy include functional interactions with TORC1, a master regulator of starvation-induced autophagy [4]. Indeed, previous studies have demonstrated that MAPK8/9 can be activated in response to TORC1 signaling [35] and that TORC1 activation can require MAPK8/9 signaling [28]. However, we found no requirement for MAPK8/9 upstream (Figure 1) or downstream (Figure 2) of TORC1 during starvation-induced autophagy. The essential function of MAPK8/9 must therefore play a role in a pathway that is parallel to TORC1. These observations led us to test whether MAPK8/9 is required for starvation-induced autophagy. Our analysis

demonstrates that MAPK8/9 is not required for starvation-induced autophagy in mouse fibroblasts or epithelial cells (Figures 2 & S7).

Many reported studies support the conclusion that MAPK8/9 plays an essential role in the promotion of autophagy [5-23]. In contrast, our analysis does not indicate a major role for MAPK8/9 in starvation-induced autophagy. It is likely that small differences in cell culture conditions and starvation conditions may contribute to discrepancies between our analysis (Figure 2) and previously published reports of the role of MAPK8/9 in MEF [5]. The use of the small molecule SP600125, that inhibits MAPK8/9 and many other protein kinases [52], to draw conclusions concerning the specific role of MAPK8/9 may also contribute to conclusions [8, 10, 12-19, 22, 51] that contrast with those drawn from our analysis of MAPK8/9 knockout cells. Finally, some studies that have identified a role for MAPK8/9 do not focus on starvation-induced autophagy. One example is the requirement of MAPK8/9 for oncolytic adenovirus-mediated autophagy [20]. Clearly our conclusions concerning the lack of a major role for MAPK8/9 in autophagy are restricted to the starvation, transformation, and hypoxia paradigms that we studied and it is likely that MAPK8/9 may play a key role in autophagy caused by other agents.

In conclusion, our analysis demonstrates that there is no required role for MAPK8/9 in starvation-induced autophagy. However, this signaling pathway can regulate autophagy by a conserved mechanism that leads to regulated expression of autophagy proteins in *Drosophila* [44] and mammals [45-51].

MAPK8/9-regulated gene expression may lead to increased autophagy, but

different paradigms of MAPK8/9-regulated gene expression could lead to

reduced autophagy. For example, MAPK8/9-regulated gene expression

suppresses basal autophagy in neurons [27].   A similar mechanism may account

for MAPK8/9-mediated repression of autophagy in hepatocytes (Figure 5). It is

also possible that MAPK8/9 may promote autophagy by a non-transcriptional

mechanism mediated by BCL2 phosphorylation in some specific physiological or

pathological conditions. Collectively, our analysis shows that the role of

MAPK8/9 in autophagy may be context-dependent and substantially more

complex than previously considered.

3.4 METHODS

3.4.1 Cell culture

3.4.1.1 Primary MEFs

Primary MEF were prepared from embryonic day 13.5 WT, *Mapk8$^{-/-}$,

Mapk9$^{-/-}$, Rosa*-Cre^{ERT} and *Rosa*-Cre^{ERT} *Mapk8$^{LoxP/LoxP}$ Mapk9$^{-/-}$* mice and

cultured in DMEM supplemented with 10% FBS, 1% penicillin /streptomycin plus

1% L-glutamine (Invitrogen) [53]. Cre^{ERT} primary MEF were treated (24 h) with 1

µM 4-hydroxytamoxifen (Cat. No. H7904; Sigma) in culture media at passage #1.

Autophagy experiments were conducted on MEF between passages #2 and #3.

3.4.1.2 Immortalized MEFs

Immortalized WT and *Mapk8*$^{-/-}$ *Mapk9*$^{-/-}$ (JNK$^{\Delta 1,2}$) MEF have been described previously [54]. We have also described *Trp53*$^{-/-}$ MEF, *Trp53*$^{-/-}$ *Mapk8*$^{-/-}$ *Mapk9*$^{-/-}$ MEF, *H-Ras* transformed *Trp53*$^{-/-}$ MEF, and *H-Ras* transformed *Trp53*$^{-/-}$ *Mapk8*$^{-/-}$ *Mapk9*$^{-/-}$ MEF [55]. These cells were cultured in DMEM supplemented with 10% FBS, 1% penicillin /streptomycin plus 1% L-glutamine (Invitrogen).

3.4.1.3 Kidney Epithelial Cells

Primary kidney epithelial cells were isolated from *Rosa-Cre*^{ERT} mice or *Rosa-Cre*^{ERT} *Mapk8*$^{LoxP/LoxP}$ *Mapk9*$^{-/-}$ mice. Kidneys were digested (2 h) with 0.1% collagenase plus 0.1% trypsin in DMEM with 150 mM NaCl [56]. The cells were maintained in DMEM/F12 media containing 10% fetal bovine serum plus 150mM urea and 150mM sodium chloride. The cells were treated (24 h) with 1 µM 4-hydroxytamoxifen and employed for autophagy studies after 3 days.

3.4.1.4 Primary Hepatocytes

Primary hepatocytes were isolated from WT (*Alb-Cre*$^{+}$) and MAPK8/9-deficient (*Alb-Cre*$^{+}$ *Mapk8*$^{LoxP/LoxP}$ *Mapk9*$^{LoxP/LoxP}$) mice [42] using a modified 2-step perfusion method [57] with Liver Perfusion Media and Liver Digest Buffer (Invitrogen). Cells were seeded on plates (pre-coated (1 h) with collagen I (BD Biosciences) in DMEM supplemented with 10% FBS, 2 mM sodium pyruvate, 1 µM dexamethasone, 100 nM insulin plus 2% penicillin/streptomycin. After attachment (2 h), the medium was removed and the hepatocytes were incubated (22 h) in maintenance medium (DMEM (4.5g/L glucose)) supplemented with 10%

FBS, 0.2% BSA, 2 mM sodium pyruvate, 2% Pen/Strep, 0.1 µM dexamethasone, 1 nM insulin). Autophagy studies were performed within 48 h. Pharmacological studies of MAPK8/9 inhibition were performed by treating hepatocytes with 2 µM JNK-in-8 (Millipore Sigma Cat. No. 420150) or solvent (DMSO).

3.4.1.5 Autophagy studies

Autophagy promoted by amino acid starvation was examined using cells (70% confluent) washed three times with Earle's Balanced Salt Solution (EBSS) and then incubated with EBSS/5mM glucose. Autophagy was also examined in cells treated with a pharmacological inhibitor of mTOR (250nM Torin1; Tocris, cat. No. 4247) and TORC1 (200nM Rapamycin; Millipore Sigma, cat. No. R8781) or under hypoxia (1.5 % O_2) conditions. Autophagic flux was examined by measuring the MAP1LC3B-II / GAPDH ratio (or MAP1LC3B-II / ✔-Tubulin ratio) by immunoblot analysis, normalization of the data to the control condition (without autophagy induction or CQ), and calculation of the increased MAP1LC3B-II / GAPDH ratio caused by treatment of the cells with 25 µM chloroquine diphosphate (CQ) (Fluka Biochemika, Cat. No.25745) to inhibit lysosomal protein degradation [36].

3.4.1.6 Immunoblot analysis

Cell extracts were prepared using Triton lysis buffer (20 mM Tris at pH 7.4, 1% Triton X-100, 10% glycerol, 137 mM NaCl, 2 mM EDTA, 25 mM β-glycerophosphate, 1 mM sodium orthovanadate, 1 mM phenylmethylsulfonyl fluoride, 10 µg/mL aprotinin plus leupeptin). Extracts (20–40 µg of protein) were

examined by protein immunoblot analysis by probing with antibodies described in antibodies section. Immunocomplexes were detected using IRDye conjugated secondary antibodies (LI-COR) and quantitated by using the Odyssey infrared imaging system (LI-COR Biosciences).

3.4.1.7 Antibodies

ATK (Cat No. 9272), pThr308 AKT (Cat No. 5106), pSer-473 AKT (Cat No. 9271), pThr-183, pTyr-185 MAPK8/9 (Cat. No. 9255), MAP1LC3B (Cat. No. 2775), RPS6KB1 (Cat. No. 9202), pThr-389 RPS6KB1 (Cat. No. 9206) antibodies were from Cell Signaling. The SQSTM1 antibody (Cat. No. GP62-C) was from Progen, the MAPK8/9 antibody (Cat. No. AF1387) was from R&D Systems, the ✔Tubulin antibody (Cat. No. T5168) was from Millipore Sigma, and the GAPDH antibody (Cat. No. sc-25778) was from Santa Cruz.

3.4.1.8 MAP1LC3B puncta formation

Cells were transduced with a lentiviral vector that expresses eGFP-MAP1LC3B according to the manufacturer's instructions (LentiBrite eGFP-LC3 Lentiviral Biosensor; EMD Millipore, Cat. No. 17-10193). The cells were plated on a glass culture dish and incubated with culture media, EBSS/5mM glucose, or culture media supplemented with 250 nM Torin1. Live cell images were acquired at 0, 2, and 4 hours using Leica TCS SP2 confocal microscope and Leica Confocal Software.

3.4.1.9 Statistical Analysis

Data are presented as the mean and standard error. Statistical analysis was performed using two-tailed Student's t-test for pair-wise comparisons and, two-way ANOVA for multiple group comparisons as indicated at the figure legends

3.4 References for Chapter 3

1.   Levine B, Klionsky DJ: **Development by self-digestion: molecular mechanisms and biological functions of autophagy.** *Dev Cell* 2004, **6:**463-477.

2.   Cuervo AM: **Autophagy: in sickness and in health.** *Trends Cell Biol* 2004, **14:**70-77.

3.   Kim J, Klionsky DJ: **Autophagy, cytoplasm-to-vacuole targeting pathway, and pexophagy in yeast and mammalian cells.** *Annu Rev Biochem* 2000, **69:**303-342.

4.   Saxton RA, Sabatini DM: **mTOR Signaling in Growth, Metabolism, and Disease.** *Cell* 2017, **169:**361-371.

5.   Wei Y, Pattingre S, Sinha S, Bassik M, Levine B: **JNK1-mediated phosphorylation of Bcl-2 regulates starvation-induced autophagy.** *Mol Cell* 2008, **30:**678-688.

6.   Niso-Santano M, Malik SA, Pietrocola F, Bravo-San Pedro JM, Marino G, Cianfanelli V, Ben-Younes A, Troncoso R, Markaki M, Sica V, et al: **Unsaturated fatty acids induce non-canonical autophagy.** *EMBO J* 2015, **34:**1025-1041.

7.   Pattingre S, Bauvy C, Carpentier S, Levade T, Levine B, Codogno P: **Role of JNK1-dependent Bcl-2 phosphorylation in ceramide-induced macroautophagy.** *J Biol Chem* 2009, **284:**2719-2728.

8. Siddiqui MA, Malathi K: **RNase L induces autophagy via c-Jun N-terminal kinase and double-stranded RNA-dependent protein kinase signaling pathways.** *J Biol Chem* 2012, **287:**43651-43664.

9. Sun ZL, Dong JL, Wu J: **Juglanin induces apoptosis and autophagy in human breast cancer progression via ROS/JNK promotion.** *Biomed Pharmacother* 2016.

10. Vasilevskaya IA, Selvakumaran M, Roberts D, O'Dwyer PJ: **JNK1 Inhibition Attenuates Hypoxia-Induced Autophagy and Sensitizes to Chemotherapy.** *Mol Cancer Res* 2016, **14:**753-763.

11. Wei Y, Sinha S, Levine B: **Dual role of JNK1-mediated phosphorylation of Bcl-2 in autophagy and apoptosis regulation.** *Autophagy* 2008, **4:**949-951.

12. Yan H, Gao Y, Zhang Y: **Inhibition of JNK suppresses autophagy and attenuates insulin resistance in a rat model of nonalcoholic fatty liver disease.** *Mol Med Rep* 2017, **15:**180-186.

13. Zhu X, Zhou M, Liu G, Huang X, He W, Gou X, Jiang T: **Autophagy activated by the c-Jun N-terminal kinase-mediated pathway protects human prostate cancer PC3 cells from celecoxib-induced apoptosis.** *Exp Ther Med* 2017, **13:**2348-2354.

14. Chen YY, Sun LQ, Wang BA, Zou XM, Mu YM, Lu JM: **Palmitate induces autophagy in pancreatic beta-cells via endoplasmic reticulum stress and its downstream JNK pathway.** *Int J Mol Med* 2013, **32:**1401-1406.

15. Granato M, Santarelli R, Lotti LV, Di Renzo L, Gonnella R, Garufi A, Trivedi P, Frati L, D'Orazi G, Faggioni A, Cirone M: **JNK and macroautophagy activation by bortezomib has a pro-survival effect in primary effusion lymphoma cells.** *PLoS One* 2013, **8:**e75965.

16. He W, Wang Q, Srinivasan B, Xu J, Padilla MT, Li Z, Wang X, Liu Y, Gou X, Shen HM, et al: **A JNK-mediated autophagy pathway that triggers**

    c-IAP degradation and necroptosis for anticancer chemotherapy.
Oncogene 2014, **33:**3004-3013.

17.   Jin HO, Hong SE, Park JA, Chang YH, Hong YJ, Park IC, Lee JK:
**Inhibition of JNK-mediated autophagy enhances NSCLC cell
sensitivity to mTORC1/2 inhibitors.** *Sci Rep* 2016, **6:**28945.

18.   Liu E, Lopez Corcino Y, Portillo JA, Miao Y, Subauste CS: **Identification
of Signaling Pathways by Which CD40 Stimulates Autophagy and
Antimicrobial Activity against Toxoplasma gondii in Macrophages.**
Infect Immun 2016, **84:**2616-2626.

19.   Yang J, Yao S: **JNK-Bcl-2/Bcl-xL-Bax/Bak Pathway Mediates the
Crosstalk between Matrine-Induced Autophagy and Apoptosis via
Interplay with Beclin 1.** *Int J Mol Sci* 2015, **16:**25744-25758.

20.   Klein SR, Piya S, Lu Z, Xia Y, Alonso MM, White EJ, Wei J, Gomez-
Manzano C, Jiang H, Fueyo J: **C-Jun N-terminal kinases are required
for oncolytic adenovirus-mediated autophagy.** *Oncogene* 2015,
34:5295-5301.

21.   Zhang Q, Kuang H, Chen C, Yan J, Do-Umehara HC, Liu XY, Dada L,
Ridge KM, Chandel NS, Liu J: **The kinase Jnk2 promotes stress-
induced mitophagy by targeting the small mitochondrial form of the
tumor suppressor ARF for degradation.** *Nat Immunol* 2015, **16:**458-
466.

22.   Bock BC, Tagscherer KE, Fassl A, Kramer A, Oehme I, Zentgraf HW,
Keith M, Roth W: **The PEA-15 protein regulates autophagy via
activation of JNK.** *J Biol Chem* 2010, **285:**21644-21654.

23.   Lin Z, Liu T, Kamp DW, Wang Y, He H, Zhou X, Li D, Yang L, Zhao B, Liu
G: **AKT/mTOR and c-Jun N-terminal kinase signaling pathways are
required for chrysotile asbestos-induced autophagy.** *Free Radic Biol
Med* 2014, **72:**296-307.

24. He JD, Wang Z, Li SP, Xu YJ, Yu Y, Ding YJ, Yu WL, Zhang RX, Zhang HM, Du HY: **Vitexin suppresses autophagy to induce apoptosis in hepatocellular carcinoma via activation of the JNK signaling pathway.** *Oncotarget* 2016.

25. Long Z, Chen B, Liu Q, Zhao J, Yang Z, Dong X, Xia L, Huang S, Hu X, Song B, Li L: **The reverse-mode NCX1 activity inhibitor KB-R7943 promotes prostate cancer cell death by activating the JNK pathway and blocking autophagic flux.** *Oncotarget* 2016, **7:**42059-42070.

26. Palumbo C, De Luca A, Rosato N, Forgione M, Rotili D, Caccuri AM: **c-Jun N-terminal kinase activation by nitrobenzoxadiazoles leads to late-stage autophagy inhibition.** *J Transl Med* 2016, **14:**37.

27. Xu P, Das M, Reilly J, Davis RJ: **JNK regulates FoxO-dependent autophagy in neurons.** *Genes Dev* 2011, **25:**310-322.

28. Basu S, Rajakaruna S, Reyes B, Van Bockstaele E, Menko AS: **Suppression of MAPK/JNK-MTORC1 signaling leads to premature loss of organelles and nuclei by autophagy during terminal differentiation of lens fiber cells.** *Autophagy* 2014, **10:**1193-1211.

29. Shimizu S, Konishi A, Nishida Y, Mizuta T, Nishina H, Yamamoto A, Tsujimoto Y: **Involvement of JNK in the regulation of autophagic cell death.** *Oncogene* 2010, **29:**2070-2082.

30. Tournier C, Dong C, Turner TK, Jones SN, Flavell RA, Davis RJ: **MKK7 is an essential component of the JNK signal transduction pathway activated by proinflammatory cytokines.** *Genes Dev* 2001, **15:**1419-1426.

31. Du L, Lyle CS, Chambers TC: **Characterization of vinblastine-induced Bcl-xL and Bcl-2 phosphorylation: evidence for a novel protein kinase and a coordinated phosphorylation/dephosphorylation cycle associated with apoptosis induction.** *Oncogene* 2005, **24:**107-117.

32. Terrano DT, Upreti M, Chambers TC: **Cyclin-dependent kinase 1-mediated Bcl-xL/Bcl-2 phosphorylation acts as a functional link coupling mitotic arrest and apoptosis.** *Mol Cell Biol* 2010, **30:**640-656.

33. He C, Bassik MC, Moresi V, Sun K, Wei Y, Zou Z, An Z, Loh J, Fisher J, Sun Q, et al: **Exercise-induced BCL2-regulated autophagy is required for muscle glucose homeostasis.** *Nature* 2012, **481:**511-515.

34. Mellor HR, Rouschop KM, Wigfield SM, Wouters BG, Harris AL: **Synchronised phosphorylation of BNIP3, Bcl-2 and Bcl-xL in response to microtubule-active drugs is JNK-independent and requires a mitotic kinase.** *Biochem Pharmacol* 2010, **79:**1562-1572.

35. Lee JH, Budanov AV, Park EJ, Birse R, Kim TE, Perkins GA, Ocorr K, Ellisman MH, Bodmer R, Bier E, Karin M: **Sestrin as a feedback inhibitor of TOR that prevents age-related pathologies.** *Science* 2010, **327:**1223-1228.

36. Klionsky DJ, Abdelmohsen K, Abe A, Abedin MJ, Abeliovich H, Acevedo Arozena A, Adachi H, Adams CM, Adams PD, Adeli K, et al: **Guidelines for the use and interpretation of assays for monitoring autophagy (3rd edition).** *Autophagy* 2016, **12:**1-222.

37. Guertin DA, Sabatini DM: **The pharmacology of mTOR inhibition.** *Sci Signal* 2009, **2:**pe24.

38. Starobinets H, Debnath J: **Cancer: A suppression switch.** *Nature* 2013, **504:**225-226.

39. Lim YM, Lim H, Hur KY, Quan W, Lee HY, Cheon H, Ryu D, Koo SH, Kim HL, Kim J, et al: **Systemic autophagy insufficiency compromises adaptation to metabolic stress and facilitates progression from obesity to diabetes.** *Nat Commun* 2014, **5:**4934.

40. Singh R, Kaushik S, Wang Y, Xiang Y, Novak I, Komatsu M, Tanaka K, Cuervo AM, Czaja MJ: **Autophagy regulates lipid metabolism.** *Nature* 2009, **458:**1131-1135.

41. Zhang T, Inesta-Vaquera F, Niepel M, Zhang J, Ficarro SB, Machleidt T, Xie T, Marto JA, Kim N, Sim T, et al: **Discovery of potent and selective covalent inhibitors of JNK.** *Chem Biol* 2012, **19:**140-154.

42. Vernia S, Cavanagh-Kyros J, Garcia-Haro L, Sabio G, Barrett T, Jung DY, Kim JK, Xu J, Shulha HP, Garber M, et al: **The PPARalpha-FGF21 hormone axis contributes to metabolic regulation by the hepatic JNK signaling pathway.** *Cell Metab* 2014, **20:**512-525.

43. Lee JM, Wagner M, Xiao R, Kim KH, Feng D, Lazar MA, Moore DD: **Nutrient-sensing nuclear receptors coordinate autophagy.** *Nature* 2014, **516:**112-115.

44. Wu H, Wang MC, Bohmann D: **JNK protects Drosophila from oxidative stress by trancriptionally activating autophagy.** *Mech Dev* 2009, **126:**624-637.

45. Byun JY, Yoon CH, An S, Park IC, Kang CM, Kim MJ, Lee SJ: **The Rac1/MKK7/JNK pathway signals upregulation of Atg5 and subsequent autophagic cell death in response to oncogenic Ras.** *Carcinogenesis* 2009, **30:**1880-1888.

46. Artal-Martinez de Narvajas A, Gomez TS, Zhang JS, Mann AO, Taoda Y, Gorman JA, Herreros-Villanueva M, Gress TM, Ellenrieder V, Bujanda L, et al: **Epigenetic regulation of autophagy by the methyltransferase G9a.** *Mol Cell Biol* 2013, **33:**3983-3993.

47. Chaanine AH, Jeong D, Liang L, Chemaly ER, Fish K, Gordon RE, Hajjar RJ: **JNK modulates FOXO3a for the expression of the mitochondrial death and mitophagy marker BNIP3 in pathological hypertrophy and in heart failure.** *Cell Death Dis* 2012, **3:**265.

48. Li DD, Wang LL, Deng R, Tang J, Shen Y, Guo JF, Wang Y, Xia LP, Feng GK, Liu QQ, et al: **The pivotal role of c-Jun NH2-terminal kinase-mediated Beclin 1 expression during anticancer agents-induced autophagy in cancer cells.** *Oncogene* 2009, **28:**886-898.

49. Li Y, Luo Q, Yuan L, Miao C, Mu X, Xiao W, Li J, Sun T, Ma E: **JNK-dependent Atg4 upregulation mediates asperphenamate derivative BBP-induced autophagy in MCF-7 cells.** *Toxicol Appl Pharmacol* 2012, **263:**21-31.

50. Moriyama M, Moriyama H, Uda J, Kubo H, Nakajima Y, Goto A, Morita T, Hayakawa T: **BNIP3 upregulation via stimulation of ERK and JNK activity is required for the protection of keratinocytes from UVB-induced apoptosis.** *Cell Death Dis* 2017, **8:**e2576.

51. Sun T, Li D, Wang L, Xia L, Ma J, Guan Z, Feng G, Zhu X: **c-Jun NH2-terminal kinase activation is essential for up-regulation of LC3 during ceramide-induced autophagy in human nasopharyngeal carcinoma cells.** *J Transl Med* 2011, **9:**161.

52. Bain J, McLauchlan H, Elliott M, Cohen P: **The specificities of protein kinase inhibitors: an update.** *Biochem J* 2003, **371:**199-204.

53. Das M, Jiang F, Sluss HK, Zhang C, Shokat KM, Flavell RA, Davis RJ: **Suppression of p53-dependent senescence by the JNK signal transduction pathway.** *Proc Natl Acad Sci U S A* 2007, **104:**15759-15764.

54. Iordanov MS, Wong J, Newton DL, Rybak SM, Bright RK, Flavell RA, Davis RJ, Magun BE: **Differential requirement for the stress-activated protein kinase/c-Jun NH(2)-terminal kinase in RNAdamage-induced apoptosis in primary and in immortalized fibroblasts.** *Mol Cell Biol Res Commun* 2000, **4:**122-128.

55. Kennedy NJ, Sluss HK, Jones SN, Bar-Sagi D, Flavell RA, Davis RJ: **Suppression of Ras-stimulated transformation by the JNK signal transduction pathway.** *Genes Dev* 2003, **17:**629-637.

56. Follit JA, San Agustin JT, Xu F, Jonassen JA, Samtani R, Lo CW, Pazour GJ: **The Golgin GMAP210/TRIP11 anchors IFT20 to the Golgi complex.** *PLoS Genet* 2008, **4:**e1000315.

57.	Seglen PO: **Preparation of isolated rat liver cells.** *Methods Cell Biol* 1976, **13:**29-83.

CHAPTER 4: DISCUSSION AND OUTLOOK

4.1 Summary of the results

The data presented in Chapter-2, section 2 demonstrate that pancreatic β-cell specific *Mapk8ip1* (*Jip1*) gene ablation results in decreased insulin secretion in response to glucose. This conclusion is supported by both *in-vivo* (mice) and *ex-vivo* (isolated pancreatic islets) insulin release assays. JIP1 deficient mice do not show a decrease in the expression of *Insulin1* and *Insulin2* genes (determined by quantitative mRNA analysis of isolated islets). In addition, insulin content of the islets (determined by ELISA), and the average islet size (determined by insulin staining of pancreas sections) are similar in JIP1 deficient and control mice. These findings suggest that JIP1 may have a function in the regulation of insulin secretion, rather than its production.

JIP1 is implicated in the regulation of vesicle trafficking in neurons[1, 2] through interacting with kinesin[3, 4] and dynactin[5, 6] complexes. In this study, I showed that the islets isolated from JIP1^{Y705A} mutant mice that lack the JIP1-kinesin interaction, can recapitulate the insulin secretion defect observed in JIP1 deficient islets. This finding supports the concept that the JIP1-kinesin interaction may play a role in insulin vesicle trafficking in β-cells.

Fu et al. suggested that JNK activation can enhance kinesin-mediated anterograde trafficking of JIP1 in neurons[6]. I tested a possible role of JIP1-JNK interaction in glucose-stimulated insulin secretion from β-cells by studying the islets from JIP1$^{\Delta JBD}$ mutant mice that has disrupted JIP1-JNK interaction. Both JIP1$^{\Delta JBD}$ mutant islets, and wild type islets treated with a JNK-inhibitor showed a

decreased insulin secretion in response to glucose. These findings support the

concept that JNK positively regulates JIP1 mediated insulin secretion. On the

other hand, Morfini et al. suggested that the phosphorylation of kinesin by JNK

results in the dissociation of kinesin and its cargo from the microtubules[7, 8].

Thus, it is possible that JNK may have a dual role in insulin secretion. First, JNK

may mediate insulin vesicle trafficking via phosphorylating JIP1. Second, JNK

may induce insulin release at the secretion site via phosphorylating kinesin.

These and other possible mechanisms that may contribute to the JIP1 mediated

insulin secretion are discussed in more detail in the following sections.

JIP1 is implicated in the trafficking of autophagosomes in neurons[1].

Moreover, studies suggest a role for autophagy in both β-cell survival and insulin

secretion[9-12]. Thus, in addition to the possible roles of JIP1 and JNK in insulin

vesicle trafficking, JIP1-JNK signaling may also contribute to the autophagy

regulation. On the other hand, it is not clear if JNK plays a role in the promotion

or suppression of autophagy[13, 14].

The results discussed in Chapter-3 show that JNK is not essential for

starvation-induced autophagy induction in mouse embryonic fibroblasts (MEF).

Our results indicate a need for re-evaluation of the previously published reports

which show a requirement of the JNK signaling for starvation-induced autophagy.

Furthermore, we showed that JNK deficiency increases basal autophagy levels in

primary hepatocytes, suggesting that the role of JNK in autophagy can be

variable depending on the cellular context. On the other hand, these findings do

not eliminate a possible role for JIP1-JNK signaling in the regulation of autophagy in beta-cells, and a possible contribution of this role to insulin secretion.

Potential mechanisms related to our main findings and, approaches that can evaluate these mechanisms are discussed in more detail in the following section.

4.2 Discussion and outlook

4.2.1 JIP1-JNK signaling in insulin vesicle trafficking and secretion

Insulin is a polypeptide hormone, synthesized as pre-proinsulin in the rough ER. By the cleavage of its N-terminal hydrophobic signal sequence, it is converted into pro-insulin, which consists of A-chain (21 amino acids), B-chain (29 amino acids), and C-peptide[15]. Pro-insulin is packed into immature insulin vesicles in the trans-golgi system where the A-chain and the B-chain are linked by disulfide bonds. During maturation, acidification of vesicles mediates cleavage of the pro-insulin to insulin and C-peptide[16, 17]. Insulin is crystalized in the presence of zinc and calcium as the vesicle matures[18], which results in the typical morphology of the insulin vesicles detected by electron microscopy, a dense core (crystalized insulin) surrounded by a halo[19-21]. Upon stimulation, both insulin and the C-peptide is released into the circulation via the portal vein.

Insulin secretion requires trafficking of newly synthesized mature insulin vesicles to the secretion site (where endocrine cells are in contact with the endothelial cells of the capillary system) and, release of the insulin granules from the plasma membrane[22]. Upon stimulation, an increase in the intracellular Ca^{++} levels trigger the insulin release from beta-cells[22]. Many proteins are proposed to mediate pre-docking of the vesicles to the plasma membrane and Ca^{++} stimulated vesicle release, such as SNAREs (VAMP1[23], and Syntaxin4[24]), calcium-regulated proteins (Synaptotagmin I, II[25], III[26], VII[26],V, VII[27], VIII, IX[28, 29]), Munc18[24, 30], and granuphilin[31]

The studies presented in chapter-2, showing a role for the JIP1-kinesin interaction in insulin secretion indicate that JIP1 may contribute to insulin vesicle trafficking. However, it is unknown whether JIP1 can directly interact with insulin vesicle-associated proteins. JIP1 can interact with other vesicle membrane-associated proteins, such as LC3B[1] (Autophagosomes), Rab10[32], ApoER2[33], and LRP2[34]. Previous studies proposed a role for JIP1 in vesicle trafficking via the interaction of JIP1 with these vesicle-associated proteins[1, 2, 32]. In chapter 2, my findings suggested a parallel role for JIP1 in pancreas β-cells, where it may mediate insulin vesicle trafficking via interactions with kinesin. It is unlikely that JIP1 can directly bind to the insulin vesicle membrane, since, unlike JIP3[35] and JIP4[36], JIP1 doesn't have a predicted transmembrane domain[37]. However, JIP1 and JIP3 can form heterodimers[38, 39], thus,

evaluation of JIP3 and insulin vesicle interaction may be of importance for a possible JIP1-insulin vesicle interaction through JIP3.

A useful approach to understand whether JIP1 plays a role in insulin vesicle trafficking would be to evaluate the existence of direct or indirect interactions between JIP1 and insulin vesicle-associated proteins. BioID (The proximity-dependent biotin identification method) is a proteomics based method that enables the identification of the interaction partners of a protein by proximity-dependent biotinylation[40]. In this method, the protein of interest is fused with a biotin protein ligase at its C-terminus or N-terminus. In-vivo biotinylated proteins are then isolated via streptavidin pull-down and analyzed by mass spectrometry. Applying this method to JIP1 in the context of beta-cells can be useful to identify the candidate interaction partners of JIP1 in beta-cells.

In addition to the role of the JIP1-kinesin interaction in insulin secretion, my findings suggest that the JIP1-JNK interaction also contributes to the regulation of glucose-induced insulin secretion. The possible mechanisms for the role of JNK-JIP1-kinesin crosstalk in glucose-induced insulin secretion are discussed below.

Hypothesis-1: JIP1 phosphorylation by JNK enhances the kinesin-mediated insulin vesicle trafficking (Figure 4.1.)

Fu et al. proposed that, the interaction of phosphorylated JIP1 (on Ser^{421}) with the kinesin heavy chain can be sufficient to activate the kinesin transport on

the microtubules[6]. This study supports the concept that JIP1 phosphorylation by JNK can regulate JIP1-mediated cargo trafficking. My findings showed that both inhibition of the JIP1-JNK interaction by genetic mutation and the inhibition of JNK activity by a pharmacological inhibitor in isolated islets, resulted in decreased glucose-stimulated insulin secretion. Thus, upon glucose stimulation, JNK may be activated to stimulate kinesin mediated JIP1-insulin vesicle complex trafficking, which may be related to the reported role of kinesin in insulin secretion[41, 42].
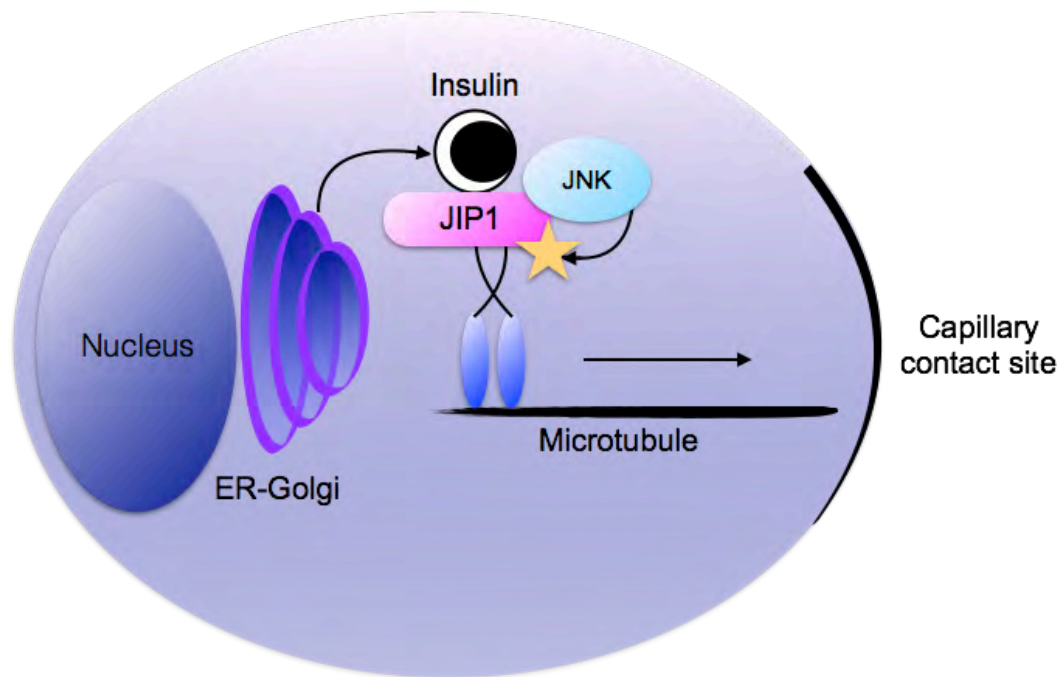
Figure 4.1: Cartoon presenting the hypothetical model, where JIP1 interacts with kinesin for tethering insulin vesicles to the microtubules; and upon glucose stimulation, activated JNK phosphorylates JIP1 to initiate anterograde trafficking.

Tanabe et al. reported that JNK activation is not induced in islets cultured in high glucose for long durations[43]. However, my results show that JIP1 deficient islets display moderately decreased JNK activation compared with control islets after a high glucose stimulation. Glucose-stimulated insulin secretion is a very prompt response, taking place within minutes after glucose stimulation. Future studies to measure time course of JNK activation in isolated primary islets would identify the dynamic regulation of JNK activation during early and late response of β-cell to glucose.

The data presented in Chapter-2 shows that treatment of isolated wild type islets with a pharmacological JNK-inhibitor (JNK-in-8) can suppress glucose-induced insulin secretion. In addition, disruption of JIP1-JNK interaction with a genetic mutation recapitulated this phenotype. These findings support the concept that JIP1-JNK crosstalk is important for the glucose-stimulated insulin secretion.

Further studies can be performed to confirm this conclusion. For instance, insulin release assays using isolated islets from mice with null mutations at JIP1 phosphorylation sites could be tested to assess if JIP1 phosphorylation is required for insulin secretion. Additionally, using mouse models with beta-cell specific JNK deletion to test islet function would confirm the role of JNK in glucose-stimulated insulin release.

<u>Hypothesis-2: Kinesin phosphorylation by JNK dissociates kinesin from</u>

<u>microtubules, and releases insulin vesicle at the secretion site (Figure 4.2.)</u>

Overexpression of JIP1 in *Drosophila* causes an accumulation of immobilized vesicles in the axons of neurons[2]. The presence of a scaffold protein in excess amounts compared to the other signaling components can inhibit signaling complex assembly by sequestration of signaling components on different scaffolds[37, 44]. Therefore, the inhibition of vesicle transport in JIP1-overexpressing *Drosophila* may be a consequence of an inhibition JNK signaling. Concordantly, co-overexpression of JNK, together with JIP1 resulted in an increased JNK activation, and decreased immobile vesicle accumulation in the axons. This finding was accompanied by a decreased JIP1-Kinesin association, suggesting that increased JNK signaling may result in the dissociation of JIP1 and its cargo from kinesin[2]. Similarly, Morfini et al. proposed that JNK-mediated kinesin phosphorylation results in dissociation of kinesin from microtubules, and inhibits kinesin-mediated cargo transport[7, 8].

Taken together, it is possible that, JIP1-JNK interaction in β-cells may contribute to insulin vesicle release from microtubules at the secretion site (Figure 4.2.). Evaluating vesicle recruitment to the membrane and glucose-stimulated vesicle release in JIP1 deficient and control β-cells can help to test this hypothesis. Decreased vesicle release in the presence of similar vesicle

recruitment to the membrane would support a possible role for JIP1-JNK signaling in insulin vesicle dissociation.
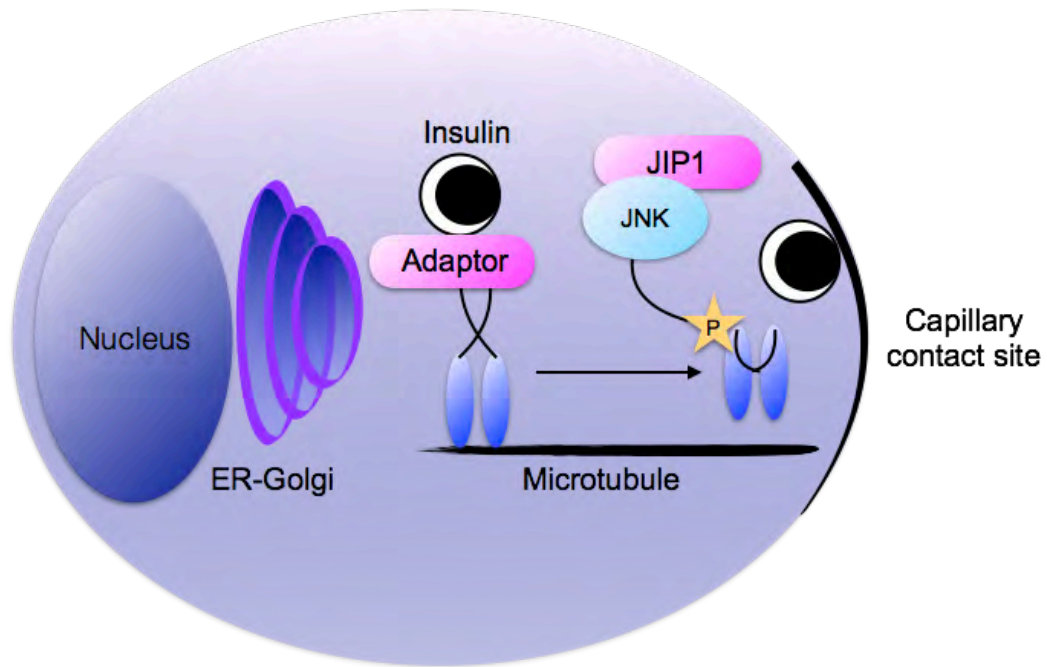
Figure 4.2: Cartoon presenting the hypothetical model, where JNK phosphorylates kinesin at the secretion site, which results in dissociation of kinesin and its cargo from microtubules, and consequently release of insulin.

To evaluate the recruitment of the insulin vesicles to the plasma membrane, total internal reflection fluorescence (TIRF) microscopy in live cells can be used[45]. Previously, a mouse model that expresses insulin-mCherry fusion protein in beta-cells was reported[46]. Crossing the insulin-mCherry mice with JIP1$^{\Delta ISL}$ mice to generate *Mapk8ip1*$^{LoxP/LoxP}$, MIP-*Cre*$^{+/-}$, *Insulin-mCherry*$^{+}$

mice would be useful to measure the *in-vivo* insulin-vesicles that are proximal to the plasma membrane in JIP1 deficient beta-cells.

Although TIRF microscopy is a powerful method to image vesicle dynamics at the plasma membrane, it does not give information regarding the vesicle release. The FluoZin-3 dye, which is cell-impermeable and becomes fluorescent upon Zn^{+2} binding, can be used to detect the release of Zn^{+2} rich insulin vesicles from beta-cells[47]. Another method that can be used to test if vesicle release is impaired in JIP1 deficient islets is carbon fiber amperometry method, which can quantitatively monitor the exocytosis of vesicles[48].

4.2.2 JIP1-RalA interaction in JNK activation and insulin secretion

JIP1 can interact with RalA, a member of the Ras small GTPase superfamily, and this interaction is proposed to be important for RalA-induced JIP1-mediated JNK activation in response to reactive oxygen species (ROS) in non-endocrine cells[49].

RalA is a regulator of endosomal membrane trafficking pathways[50], and previous studies reported that RalA can regulate hormone secretion from neuroendocrine cells[51, 52]. In addition, Lopez et al. showed that shRNA knockdown of RalA in islets isolated from wild type mice resulted in decreased glucose stimulated insulin secretion from perifused islets. Decreased cell membrane capacitance change in RalA deficient insulinoma cells suggests that that RalA may play a role in the insulin vesicle exocytosis[53]. Moreover, RalA

can interact with voltage-gated Ca^{++} channels and tether insulin vesicles to regulate bi-phasic insulin release[54]. Depletion of Sec5, a downstream effector of RalA, in β-cells results in decreased insulin release induced by membrane depolarization[55]. This phenotype is similar to my observation that JIP1 deficient islets display decreased insulin secretion after membrane depolarization induced by KCl treatment.

Hypothesis-3: Glucose-induced activation of RalA can induce JIP1-mediated JNK activation in β-cells to mediate insulin secretion in response to glucose

It is possible that activated RalA signaling play a role upstream of JIP1-JNK pathway in glucose-stimulated β-cells. RalA activation occurs as early as 5 minutes after secretagogue stimulation of insulinoma cells[56]. If JNK acts downstream of RalA signaling in glucose-stimulated insulin secretion, knockdown of RalA in wildtype islets would result in decreased JNK activity in high glucose condition, similar to the finding we observed in JIP1 deficient islets. In addition, if decreased JIP1-mediated JNK activity that I have observed is dependent on the JIP1-RalA interaction, depletion of RalA in JIP1 deficient islets should not result in further decrease in activated JNK levels.

Evaluating whether JIP1 and RalA co-immunoprecipitate from protein lysates of isolated islets incubated with low or high glucose can test not only the possible JIP1-RalA interaction in β-cells, but also if this interaction is regulated by

166

glucose stimulus. Furthermore, fluorescence imaging using low or high glucose

treated islets, can test whether a possible JIP1-RalA interaction is localized to the

plasma membrane or another relevant cellular compartment. Together, these

experiments can provide insight in the possible role of RalA upstream of JIP1-

JNK signaling in β-cells.

4.2.3 JIP1-JNK signaling in microtubule organization and insulin secretion

The role of JIP1 and JNK signaling in vesicle trafficking has been studied

mostly in neuronal cells[1, 2, 6-8, 57]. In neurons, microtubules are radially

oriented from the perinuclear region to the cell periphery and axons; and vesicles

are transported bi-directionally on the axonal microtubules for long distances[58].

On the other hand, insulin secreting beta-cells have a mesh-like, non-directional

microtubule distribution throughout the cytoplasm[42, 59]. Zhu et al. reported

that the dense, mesh-like distribution of microtubules in beta-cells can limit the

availability of insulin vesicles to the secretion site by mediating their withdrawal

from the membrane, and by trapping them in the cell interior[46]. In endocrine

cells, the Golgi is the main site of microtubule origination[60]. Zhu et al. showed

that glucose stimulation caused de-polymerization of existing microtubules in

beta-cells, and an increase in new microtubule polymerization originating from

the Golgi[46]. Moreover, de-polymerization of microtubules by nocodazole

treatment increased the glucose-stimulated insulin secretion, whereas increasing

the microtubule stability by taxol treatment inhibited glucose responsiveness of the β-cells[46].

Microtubule plasticity is modulated by microtubule associated proteins (MAPs)[61]. JNK can phosphorylate MAPs to regulate microtubule stability, and bundling in neurons[62]. For instance, JNK can phosphorylate SCG10/STMN2 (MAP)[63], MAP2, and MAP1B[64] which contributes to the regulation of microtubule assembly, stability and axonal length. It is reported that in β-cells phosphorylation of microtubule associated protein MAP2 can mediate Ca-triggered insulin secretion[65].

JIP1 can also interact with Tau (MAP-II) and is implicated in its phosphorylation and subcellular localization. Moreover, overexpression of MLK3, which can bind JIP1 and activate JNK[44], resulted in increased microtubule stability, while siRNA depletion of MLK3 increased the sensitivity of cells to taxol, a microtubule stabilizing agent[66]. Taken together, it is possible that decreased glucose-stimulated insulin secretion in JIP1 deficient β-cells is a result of altered microtubule plasticity.

Hypothesis-4: JIP1-mediated JNK activation and microtubule-associated protein phosphorylation by JNK may modulate microtubule plasticity and glucose responsiveness in β-cells (Figure 4.3.)
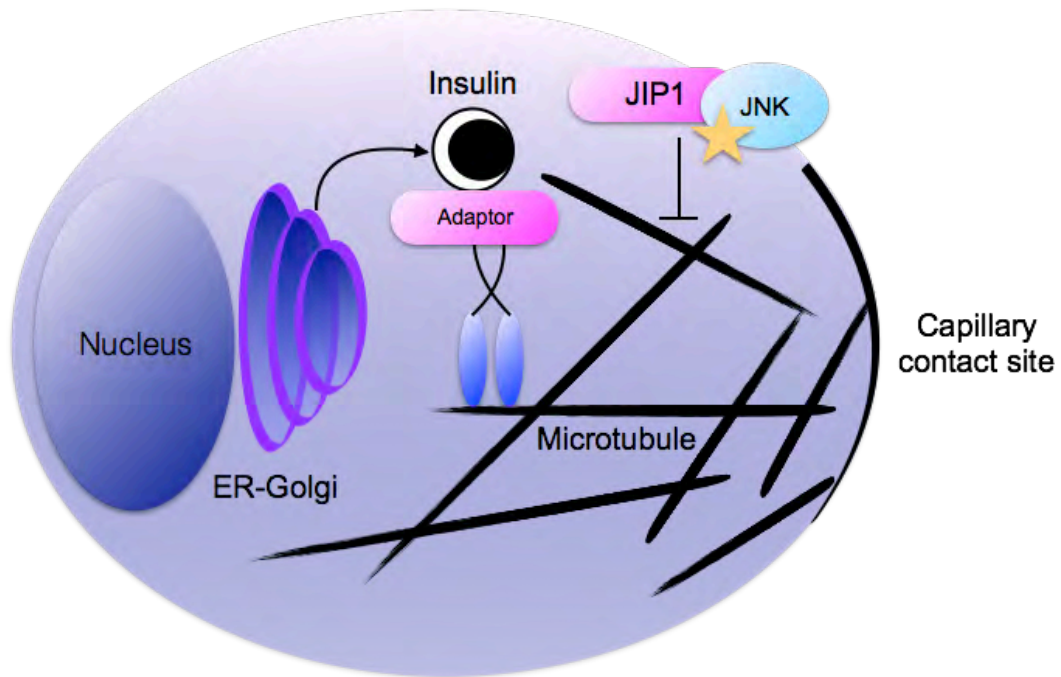
Figure 4.3. Cartoon presenting the hypothetical model, where JNK phosphorylates microtubule associated proteins in response to glucose, which results in the alteration of the dense microtubule network and enhanced mobilization of the insulin vesicles to the secretion site.

Imaging microtubule density in control and JIP1 deficient islets under low glucose and high glucose conditions would be useful to evaluate whether microtubule plasticity is altered in JIP1 deficient β-cells in response to glucose stimulation. First, JIP1 deficient β-cells may display an increased microtubule density compared with controls. This result would support the idea that increased microtubule density in JIP1 deficient β-cells can withhold the insulin vesicles away from secretion site and decrease glucose-stimulated insulin release. In this case, treatment of JIP1 deficient islets with nocodazole

(microtubule destabilizing agent) during a high glucose perifusion of the islets would rescue the glucose-stimulated insulin secretion defect observed in the mutant islets. Second, microtubule density in JIP1 mutant islets may be similar or decreased when compared with the controls, but there may be a decrease in the microtubule plasticity in response to glucose[46]. This finding would support the hypothesis that JIP1-mediated JNK signaling may regulate the microtubule associated protein phosphorylation and microtubule plasticity in response to glucose.

In addition to the study in β-cells discussed above, Bargi-Souza et al. showed a similar finding regarding the microtubule dynamics during thyroid stimulating hormone (TSH) secretion from the pituitary gland[67]. In this study, rats with thyroidectomy (removal of thyroid gland) showed increased TSH secretion caused by the absence of thyroid hormones, and consequently the absence of negative feedback inhibition. Increased TSH secretion was accompanied by a decrease in tubulin and actin staining in the pituitary gland. Moreover, recovery of negative feedback inhibition by hormone replacement therapy in these rats increased tubulin and actin density in the pituitary gland[67]. Altogether, these studies suggest that a possible inhibitory effect of dense microtubule network on hormone secretion can be a regulatory mechanism in both β-cells and pituitary gland.

To test if TSH granules in pituitary gland are surrounded by a dense microtubule network as seen in β-cells, I have stained WT pituitary gland

sections with antibodies to β-TSH and α-tubulin. Confocal images of stained

pituitary gland sections in Figure 4.4. suggest that TSH granules in pituitary gland

are surrounded by a dense tubulin network, similar to the insulin vesicles in

pancreas β-cells[46].

TSH secretion from the anterior pituitary gland is stimulated by Thyrotropin

Releasing Hormone (TRH). Microtubule imaging by super resolution microscopy

in JIP1 deficient and control pituitary glands before and after TRH induction can

be useful to evaluate the microtubule plasticity in response to TRH induction. In

addition, nocodazole and TRH combined treatment of JIP1 deficient and control

pituitary glands would show whether microtubule depolarization can rescue TRH-

induced TSH secretion defect in JIP1 deficient pituitary glands.
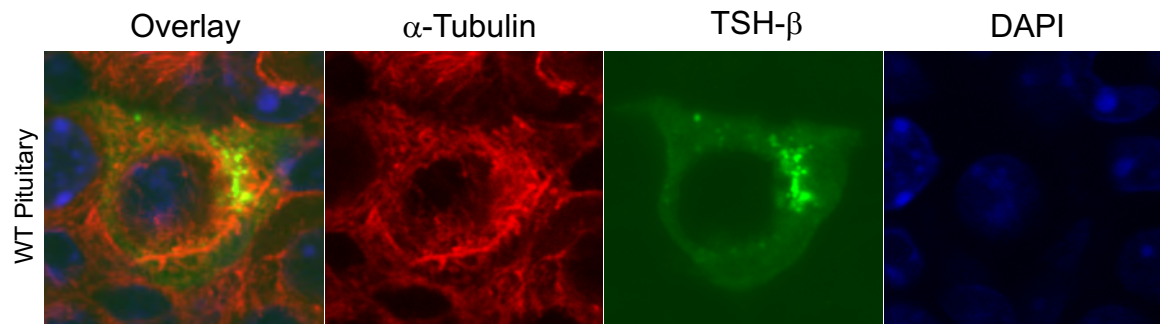
Figure 4.4. Pituitary glands were dissected and fixed in formalin overnight. After
processing with ethanol gradients, tissues were embedded in paraffin. 7µm thick
sections were cut and rehydrated before staining with antibodies to α-tubulin and
β-TSH. Images were obtained using Leica confocal microscope.

4.2.4 JIP1, primary cilium, and insulin secretion

Most of the terminally differentiated cells, including β-cells, have a primary cilium[68, 69]. The primary cilium is an antenna-like cell protrusion that is formed by centrioles near the plasma membrane and can function as the sensor of the cells[70-72]. The primary cilium is linked to the planar cell polarity pathway, and functions in regulating the cellular signaling such as Wnt[73], Notch[74], and Hedgehog[75].

The primary cilium is implicated in β-cell function and regulation of insulin secretion[76]. For instance, islets from mouse with Bardet-Biedl-Syndrome 4 (Bbs4) mutation exhibited decreased glucose-stimulated insulin secretion[77]. Bbs4 mutation impairs cilia function, while the cilia are structurally intact[78]. This result suggests that, cellular signaling mediated by primary cilium may be important for the regulation of insulin secretion.

By immunofluorescence imaging of pancreas sections, I have detected puncta staining of JIP1 in the islets (Figure 4.5.), which indicates a possible specific and functional sub-cellular compartmentalization of JIP1 in β-cells.

Additionally, in dispersed islets, JIP1 staining was observed throughout the cytoplasm and nucleus, with a denser spot near the plasma membrane. This dense local staining co-localized with γ-tubulin staining a marker used for basal body detection (Figure 4.6.). Also, immunofluorescence staining of intact isolated islets recapitulated the JIP1 co-localized with γ-tubulin (Figure 4.7.).

Paraffin embedded pancreas sections
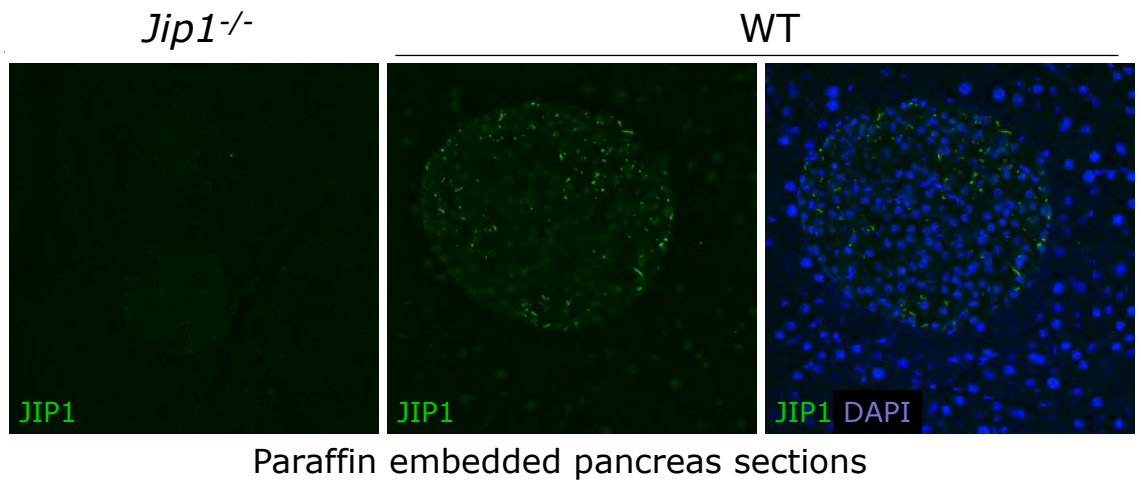
Figure 4.5. Paraffin embedded pancreas sections from JIP1 deficient (*Mapk8ip1*$^{-/-}$ / *Jip1*$^{-/-}$) and wild type mice were stained with an antibody to JIP1 (Santa, Cruz m-300) (green) and DAPI (for DNA staining) (blue). Images were taken using Leica confocal microscope.
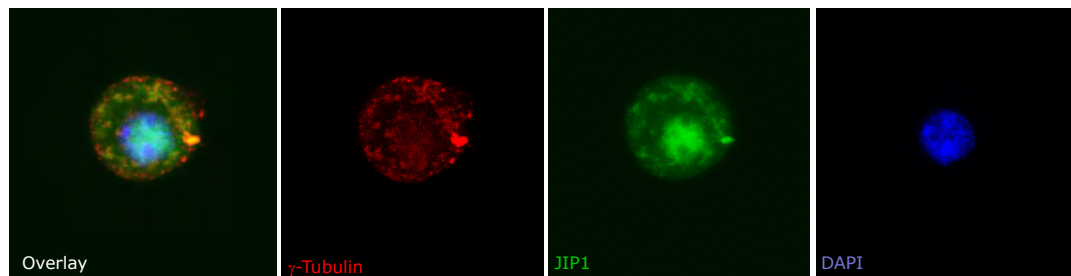
Figure 4.6. Wild type primary β-cells were obtained by dispersion of the isolated islets, and cultured in RPMI medium with 5mM glucose. Cells were fixed with methanol at -20 ^{o}C and stained with an antibody to γ-tubulin (red), JIP1 (Santa Cruz, m-300) (green) and DAPI (for DNA staining) (blue). Images were taken using Leica confocal microscope. Observed nuclear staining may be a non-specific background, since it is not observed in stained pancreas sections in figure 4.5.
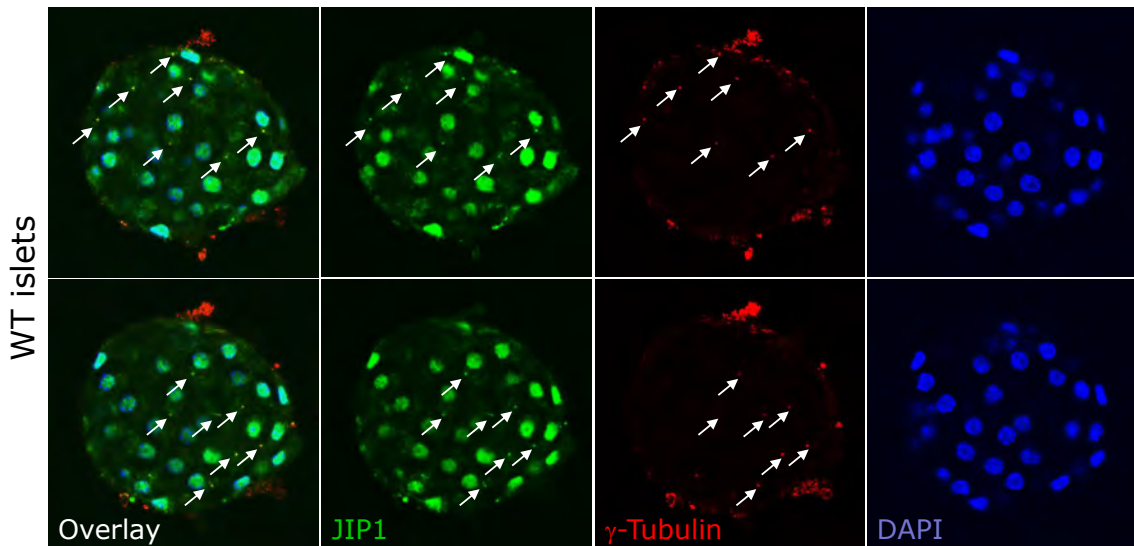
Figure 4.7. Isolated islets were cultured on glass coverslips for 24-48 hours in RPMI medium with 5mM glucose. After fixation with methanol at -20 ^{o}C islets were stained with antibodies to JIP1 (Santa Cruz m-300)(green), γ-tubulin (red) and DAPI (for DNA staining) (blue). Images were taken using confocal microscope. Arrows indicate the co-localization of JIP1 with γ-tubulin. Observed nuclear staining may be a non-specific background, since it is not observed in stained pancreas sections in figure 4.5.

Electron microscopic analysis of β-cells demonstrated an increased occurrence of double cilia in JIP1 deficient islets (Figure 4.8.). The existence of more than one primary cilium (double cilia) in a cell is an unusual finding. Mahjoub et al. reported that centrosome amplification induced by ectopic Plk4 Kinase expression[79] resulted in cells with multiple primary cilia (Super-ciliated cells)[80]. Moreover, existence of multiple primary cilia in cells led to the dysregulation of ciliary signaling[81]. My preliminary data showing the possible

174

localization of JIP1 to the basal body (Figure 4.6 & 4.7), and the double primary

cilia occurrence (Figure 4.8) in JIP1 deficient islets, suggest that JIP1 may play a

role in the primary cilium function in β-cells.

WT   JIP1$^{ex\Delta}$

	total cell # (4mice)	cell# with prim cill.	# double cillia
WT	101	14	1
JIP1ex2Δ	89	19	5
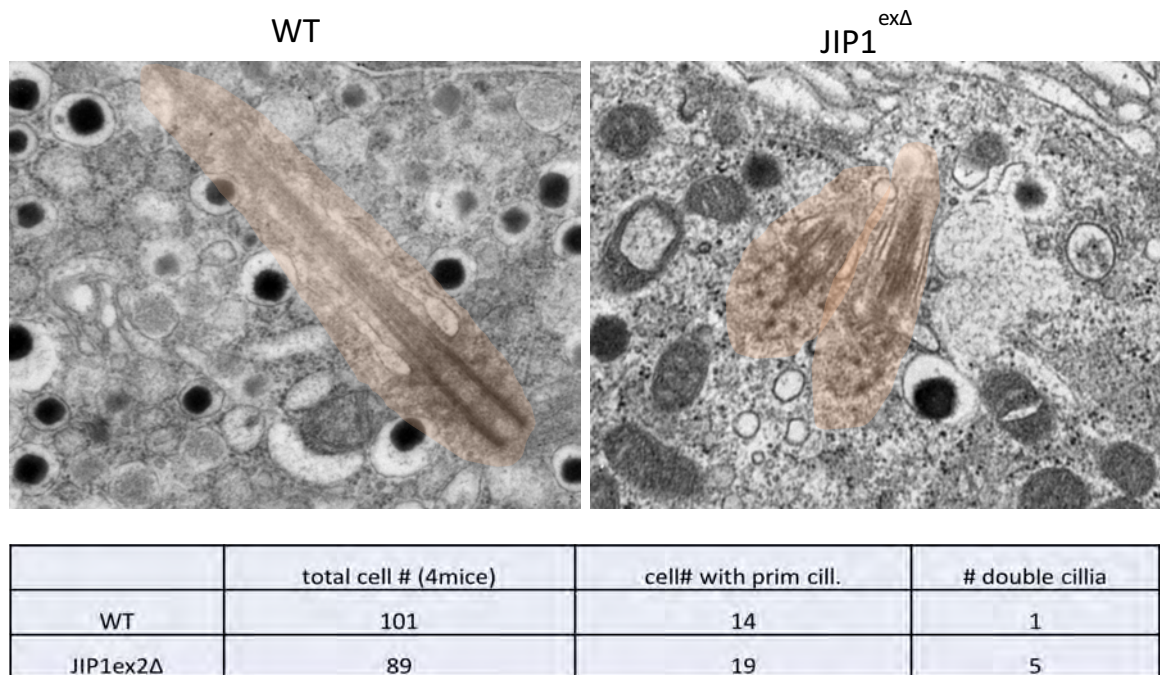
Figure 4.8. Pancreas section were imaged by electron microscopy as described
in Chapter 2.3. Representative images showing primary cilium (highlighted by
false color) in wild type and double primary cilia in JIP1 deficient samples.

The localization of JIP1 to the basal body, and increased frequency of

double cilia in JIP1 deficient islets require further experimental confirmation. As

discussed in section 4.2.1. evaluating JIP1 interaction partners with BioID

method can detect possible JIP1 interaction with proteins related to the

centrosome or primary cilium. In addition, immunofluorescence staining of

dispersed primary β-cells with primary cilium marker, such as acetylated tubulin, or IFT88 would confirm the increased frequency of multiple primary cilia occurrence in JIP1 deficient β-cells. These cells can also be evaluated under different glucose concentrations.

4.2.5 JIP1, cell polarity, and insulin secretion

In most cases, primary cilium dysfunction and cell polarity defects co-exist, implying that these two pathways are closely linked to each other[82]. Cell polarization is essential for many terminally-differentiated cell function including β-cells in pancreas islets. β-cells are polarized, and organized around the capillaries (rosette structure) so that the insulin can be released to the capillary contact sites[83, 84] (Figure 4.9). Moreover, disruption of this organization can alter insulin secretion from beta-cells[84].
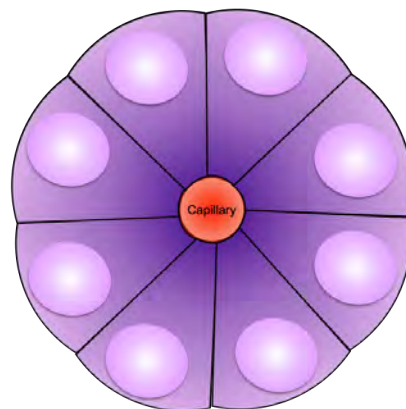
Figure 4.9. Cartoon showing the rosette structure of polarized β-cell. β-cells align around the capillaries and nuclei (light purple) are positioned at the opposite site of the capillary contact site.

JNK plays a role in the Planar Cell Polarity (PCP) and Wnt signaling pathway[85, 86]. In addition, JIP1/JNK-mediated cargo transport in neurons was implicated in neuronal polarity[32]. Additionally, in consideration with the role of JNK in microtubule associated protein phosphorylation, and the close relationship between cell polarity and microtubule dynamics, it is possible that JNK may be involved in the regulation of β-cell polarity.

To test if there is a decreased phosphorylation of microtubule associated protein STMN2 in JIP1 deficient β-cells, I stained pancreas sections from control and JIP1 deficient mice with an antibody against phosphorylated STMN2-Ser^{73} (Figure 4.10.). Preliminary results suggested that the amount of P-STMN2-Ser^{73} is similar in control and JIP1 deficient islets. However, a polarized localization of P-STMN2-Ser^{73} was noticeable in β-cells, where P-STMN2 was present on only a single side of the nucleus and mostly towards the capillary contact site in a rosette structure, especially in pancreas sections from glucose stimulated wildtype mice (Figure 4.10. upper right panel). This finding raises the question whether JIP1-mediated JNK activation can play a role in the polarized localization of microtubule associated protein phosphorylation and local microtubule stability regulation in response to glucose.
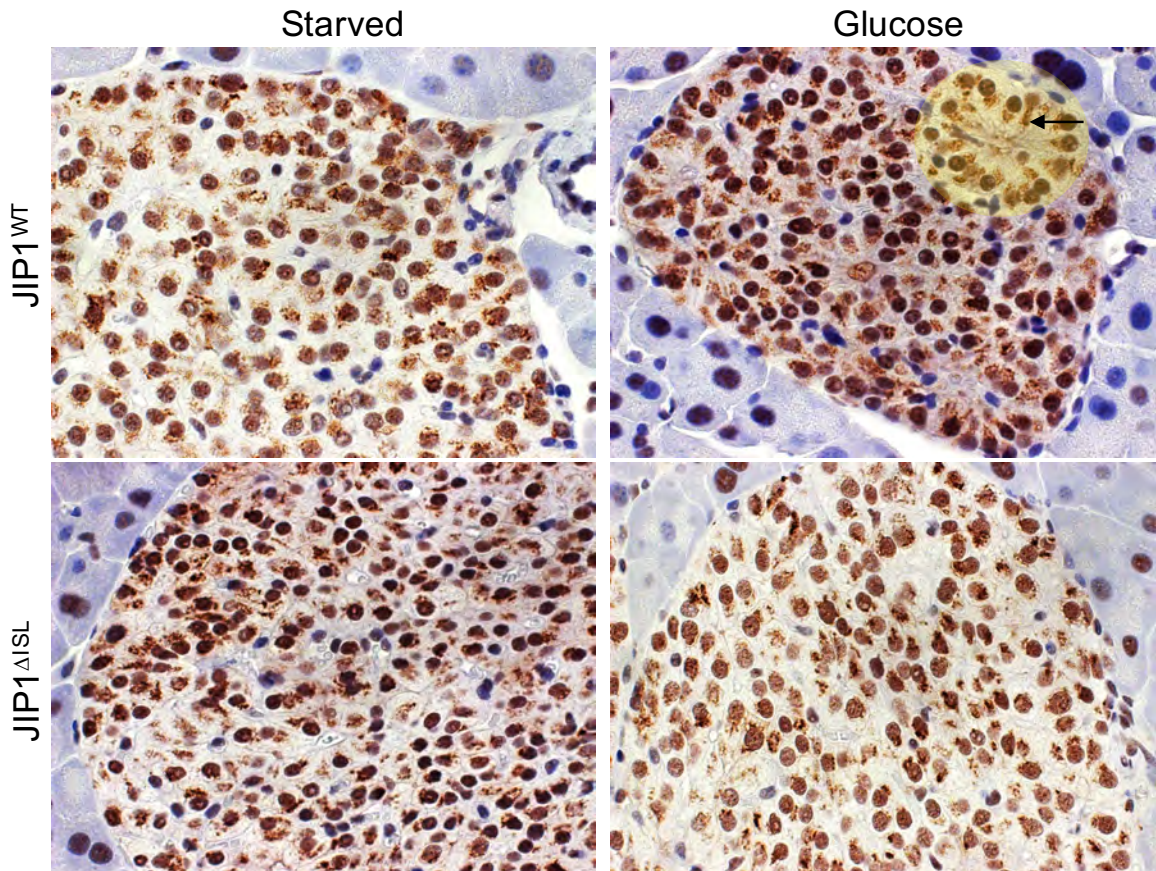
Figure 4.10. Paraffin embedded pancreas sections from wild type and JIP1 deficient mice (after PBS or glucose injection) were stained with an antibody against P-STMN2-Ser^{73} (DAB). Rosette structure is highlighted by false color in upper right panel. P-STMN2-Ser^{73} staining localized asymmetrically at one side of the nucleus (an example is indicated by the arrow in upper left panel). This localization became more structured in glucose stimulated islets, positioning inner side of the nucleus in rosette structures.

To test if the rosette structure of β-cell organization is disrupted in JIP1 deficient islets, it is crucial to perform quantitative imaging analysis of β-cell

borders and nuclei, in addition to capillary cells in the islets. Granot and Swisa et al. reported quantitative analysis of nuclear positioning in rosette structures of β-cells by staining pancreas sections with a DNA marker, and antibodies to E-cadherin (for β-cell borders), and Laminin (for capillary staining)[84]. A similar approach could quantitatively evaluate the subcellular localization of P-MAP in control and JIP1 deficient islets after PBS or glucose injection. In addition, 3D visualization of islets by staining multiple serial sections would give more insight on the cellular-vascular organization.

4.2.6 Possible functional differences of JIP1 splice/translation variants

In Chapter 2, I have shown that the JIP1 protein is detected as two thick smear-like bands on immunoblots, corresponding to ~90 KD and ~110 KD sizes. So far, it is not known which amino acid sequences correspond to these differentially sized JIP1 proteins. Previous studies showed that upon stimulation of cells with cytokines, the low molecular weight (LMW) JIP1 was more sensitive to proteosomal degradation when compared to the high molecular weight (HMW) JIP1, suggesting that HMW and LMW JIP1 proteins may have distinct functions and stability.

Deleting exon-2 results in the loss of high molecular weight (HMW) JIP1 protein, while low molecular weight (LMW) JIP1 is preserved. JIP1 exon-2 is 106 base pair in length, and its deletion with the subsequent exon1-exon3 junction results in frameshift and early stop codon in coding sequences starting from

distal exon1 and proximal exon-1. Thus, the existence of the LMW JIP1 protein

after JIP1 exon2 deletion suggests that either there is an alternative translation

start site downstream of exon-2 that can by-pass the deletion and translate the

LMW protein, or an alternative splice junction in the absence of exon-2 results in

an in-frame codon reading.
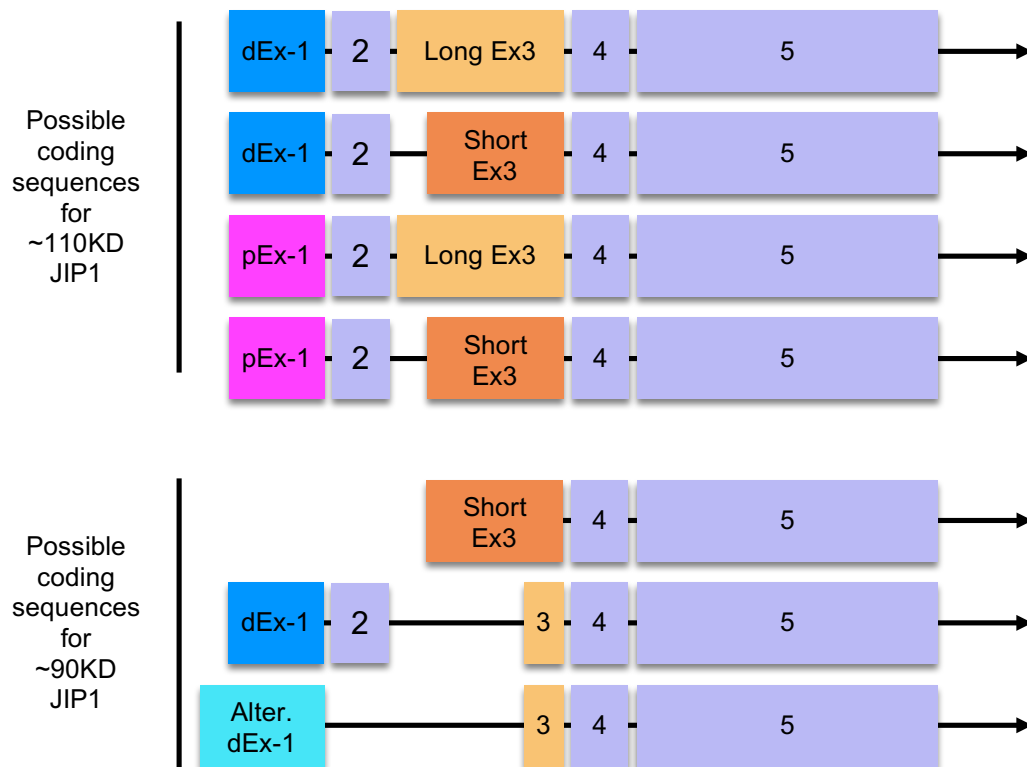
Figure 4.11. Cartoon representing predicted coding sequences for high molecular
weight and low molecular weight JIP1 proteins. Splice junction are detected by
mRNA sequencing from brain samples. (Alter: Alternative)

My results and previously published data[87] suggest that the HMW JIP1 protein band can possibly consist of at least 4 proteins (Figure 4.11.). The slight difference in the size and different phosphorylation status of these JIP1 isoforms may cause the thick smear-like observation of JIP1 protein bands from the brain samples.

The presence of a LMW JIP1 protein after Exon2 deletion supports the idea that the in-frame ATG at the beginning of short Exon3 junction may serve as an alternative translation start site coding the LMW JIP1 protein. In addition, *Jip1*^{-/-} mice that lack exon2 and exon3 display loss of both LMW and HMW JIP1 proteins, showing that exon3 is required for the presence of LMW JIP1 protein.

Sequencing of the cDNA from wildtype and JIP1 exon2 deleted samples identified a new splice junction between exon1 and the end of exon3. This junction skips JNK binding domain on exon3. An alternative start site on distal exon1, detected by published ribosome profiling data, can translate an alternative exon1 that has an in-frame junction with exon3.

The high variation of JIP1 N-terminus coding sequence suggests that the regulation of this region at the mRNA and translational levels may regulate the functional specificity of JIP1 in a cell and context-dependent manner. For instance, in the brain, both LMW and HMW JIP1 are observed in high abundancy, while in β-cells, HMW JIP1 is more prominent (Figure 2.)[88]. Our results show that, LMW JIP1 does not contain exon2, while its existence is

dependent on exon3 (exon2 and exon3 deletion results in the loss of LMW

protein).

Immunoprecipitation of endogenous JIP1 proteins from various tissues

followed by mass spectrum analysis is crucial to identify amino acid sequence of

JIP1 proteins. Also, by using CRISPR technology, mutating the in-frame ATG on

exon3 to test if the presence of LMW JIP1 protein is dependent on the alternative

translation start from exon3 could provide informative understanding.

4.2.7 Role of JIP1-JNK interaction in TSH secretion

In addition to insulin secretion, my analysis shows that JIP1 mediates

TRH-induced TSH secretion from the anterior pituitary gland. Abe et al.

proposed that JIP1 can play a role in the regulation of *Tsh-β* expression[89].

However, my results suggest that JIP1 is not required for *Tsh-β* expression, since

control and JIP1 deficient pituitary glands show similar *Tsh-β* mRNA levels. On

the other hand, my results do not exclude a possible role for JIP1 in TRH-

induced TSH expression, or in di-urinal TSH secretion regulation.

Our lab previously reported that deletion of JNK1 and JNK2 in the anterior

pituitary gland results in increased TSH secretion[90]. This was accompanied by

decreased *Dio2* expression, an enzyme that converts T4 to active form T3 in the

pituitary gland, and mediate negative feedback inhibition. Thus, decreased

negative feedback inhibition resulted in increased *Tsh-β* gene expression in

JNK1,2 deficient anterior pituitary gland. The results of this study suggest that

the regulation of *Tsh-β* expression by JNK is independent of JIP1, since there

was no alteration in the gene expression in JIP1 deficient anterior pituitary

glands. Also, increased TSH secretion from JNK1,2 pituitary glands reported by

Vernia et al. suggests that JNK activity may not be essential for TSH

secretion[90].

All JNK isoforms (JNK1, JNK2, and JNK3) are expressed in the pituitary

gland[91]. It is therefore possible that the presence of JNK3 may compensate for

a potential role of JNK1 and JNK2 in the hormone secretion. Ablation of JIP1 in

the JNK1,2 deficient anterior pituitary gland will be important to test whether JIP1

deficiency would result in decreased TSH secretion in the absence of JNK1,2. In

addition, evaluating JNK3 activity in these mice would identify a possible JIP1-

JNK3 crosstalk in TSH secretion.

4.2.8 JIP1-JNK pathway, autophagy, and endocrine function

Fu et al. showed that JIP1 can mediate autophagosome trafficking and

autolysosome formation in neurons[1]. Autophagy is implicated in the function of

β-cells and regulation of insulin secretion[92]. It is proposed that autophagy can

regulate islet expansion in obesity[11, 93, 94], and β-cell insulin content[10].

Pancreas-specific ATG7 deficiency in mice results in decreased β-cell

mass, and decreased insulin secretion[11], On the other hand, my data shows

that JIP1 deficient mice have similar islet size and islet insulin content compared

with controls. This finding suggests that a severe autophagy defect in JIP1

deficient islets is unlikely. However, it is possible that JIP1 may mediate autophagosome trafficking in β-cells, and the deficiency of JIP1 may affect only a subset of cellular autophagy. Muller et al. recently showed that old insulin vesicle can be targeted to the autophagosomes, while young insulin vesicles are preferentially secreted[12]. Evaluating co-localization of JIP1, insulin vesicles, and LC3B, an autophagosomal marker, in β-cells would give insight on a possible role for JIP1 in autophagosomal degradation of old insulin vesicles.

JNK is also implicated in the regulation of autophagy. However, whether JNK activity is required for autophagy is unclear. Wei et al. proposed that JNK is activated mouse embryonic fibroblasts (MEF) after starvation, and JNK-mediated BCL2 phosphorylation is required for Beclin1 activation autophagy induction[13]. On the other hand, Xu et al. showed that JNK deficient primary neurons exhibit increased autophagy[14].

The results in Chapter3 show that JNK is not activated by starvation in primary and immortalized MEF. Moreover, JNK deficient MEF showed similar levels of autophagy induction compared with the control MEF under starvation condition. This result suggests that JNK is not essential for autophagy induction. On the other hand, JNK deficient primary hepatocytes displayed increased basal autophagy flux, suggesting that JNK may play a role in autophagy in a cell and context specific manner.

Further studies to evaluate the basal and induced autophagy in JIP1/JNK deficient endocrine tissues such as islets or pituitary gland would provide more

insight on the role of JIP1/JNK pathway in autophagy dynamics in the context of hormone secretion and endocrine cell function.

4.3 Concluding Remarks

Proper functioning of endocrine cells is crucial for organismal homeostasis. Regulated hormone secretion is a complex mechanism, and the signaling pathways that fine-tune the amount and the timing of the hormone secretion are still unclear.

The data presented in this study suggests that JIP1, a scaffold protein in cellular stress signaling pathway, mediates regulated-insulin secretion from pancreas β-cells in response to glucose. Our study showing the role of JIP1-kinesin interaction and JIP1-JNK interaction in glucose-stimulated insulin secretion, implies a mechanism that link cellular trafficking and stress signaling pathways in the regulated hormone secretion.

In addition to the known role of JIP1 in metabolism and insulin resistance, this finding is also relevant to many endocrine pathologies where excess hormone secretion may need inhibitory control, such as adenomas. Identification of the cell-specific functions of scaffold proteins can provide a platform to manipulate context-specific signaling complexes, without deteriorating other cellular functions.

4.4 References of Chapter 4

1. Fu MM, Nirschl JJ, Holzbaur ELF: **LC3 binding to the scaffolding protein JIP1 regulates processive dynein-driven transport of autophagosomes.** *Dev Cell* 2014, **29:**577-590.

2. Horiuchi D, Barkus RV, Pilling AD, Gassman A, Saxton WM: **APLIP1, a kinesin binding JIP-1/JNK scaffold protein, influences the axonal transport of both vesicles and mitochondria in Drosophila.** *Curr Biol* 2005, **15:**2137-2141.

3. Verhey KJ, Meyer D, Deehan R, Blenis J, Schnapp BJ, Rapoport TA, Margolis B: **Cargo of kinesin identified as JIP scaffolding proteins and associated signaling molecules.** *J Cell Biol* 2001, **152:**959-970.

4. Whitmarsh AJ, Kuan CY, Kennedy NJ, Kelkar N, Haydar TF, Mordes JP, Appel M, Rossini AA, Jones SN, Flavell RA, et al: **Requirement of the JIP1 scaffold protein for stress-induced JNK activation.** *Genes Dev* 2001, **15:**2421-2432.

5. Standen CL, Kennedy NJ, Flavell RA, Davis RJ: **Signal transduction cross talk mediated by Jun N-terminal kinase-interacting protein and insulin receptor substrate scaffold protein complexes.** *Mol Cell Biol* 2009, **29:**4831-4840.

6. Fu MM, Holzbaur EL: **JIP1 regulates the directionality of APP axonal transport by coordinating kinesin and dynein motors.** *J Cell Biol* 2013, **202:**495-508.

7. Morfini GA, You YM, Pollema SL, Kaminska A, Liu K, Yoshioka K, Bjorkblom B, Coffey ET, Bagnato C, Han D, et al: **Pathogenic huntingtin inhibits fast axonal transport by activating JNK3 and phosphorylating kinesin.** *Nat Neurosci* 2009, **12:**864-871.

8. Morfini G, Pigino G, Szebenyi G, You Y, Pollema S, Brady ST: **JNK mediates pathogenic effects of polyglutamine-expanded androgen receptor on fast axonal transport.** *Nat Neurosci* 2006, **9:**907-916.

9. Sheng Q, Xiao X, Prasadan K, Chen C, Ming Y, Fusco J, Gangopadhyay NN, Ricks D, Gittes GK: **Autophagy protects pancreatic beta cell mass and function in the setting of a high-fat and high-glucose diet.** *Sci Rep* 2017, **7:**16348.

10. Marsh BJ, Soden C, Alarcon C, Wicksteed BL, Yaekura K, Costin AJ, Morgan GP, Rhodes CJ: **Regulated autophagy controls hormone content in secretory-deficient pancreatic endocrine beta-cells.** *Mol Endocrinol* 2007, **21:**2255-2269.

11. Jung HS, Chung KW, Won Kim J, Kim J, Komatsu M, Tanaka K, Nguyen YH, Kang TM, Yoon KH, Kim JW, et al: **Loss of autophagy diminishes pancreatic beta cell mass and function with resultant hyperglycemia.** *Cell Metab* 2008, **8:**318-324.

12. Muller A, Neukam M, Ivanova A, Sonmez A, Munster C, Kretschmar S, Kalaidzidis Y, Kurth T, Verbavatz JM, Solimena M: **A Global Approach for Quantitative Super Resolution and Electron Microscopy on Cryo and Epoxy Sections Using Self-labeling Protein Tags.** *Sci Rep* 2017, **7:**23.

13. Wei Y, Pattingre S, Sinha S, Bassik M, Levine B: **JNK1-mediated phosphorylation of Bcl-2 regulates starvation-induced autophagy.** *Mol Cell* 2008, **30:**678-688.

14. Xu P, Das M, Reilly J, Davis RJ: **JNK regulates FoxO-dependent autophagy in neurons.** *Genes Dev* 2011, **25:**310-322.

15. Dodson G, Steiner D: **The role of assembly in insulin's biosynthesis.** *Curr Opin Struct Biol* 1998, **8:**189-194.

16. Rhodes CJ, Lucas CA, Mutkoski RL, Orci L, Halban PA: **Stimulation by ATP of proinsulin to insulin conversion in isolated rat pancreatic**

islet secretory granules. Association with the ATP-dependent proton pump.** *J Biol Chem* 1987, **262:**10712-10717.

17. Orci L, Ravazzola M, Amherdt M, Madsen O, Perrelet A, Vassalli JD, Anderson RG: **Conversion of proinsulin to insulin occurs coordinately with acidification of maturing secretory vesicles.** *J Cell Biol* 1986, **103:**2273-2281.

18. Howell SL, Tyhurst M, Duvefelt H, Andersson A, Hellerstrom C: **Role of zinc and calcium in the formation and storage of insulin in the pancreatic beta-cell.** *Cell Tissue Res* 1978, **188:**107-118.

19. Greider MH, Howell SL, Lacy PE: **Isolation and properties of secretory granules from rat islets of Langerhans. II. Ultrastructure of the beta granule.** *J Cell Biol* 1969, **41:**162-166.

20. Lange RH: **Crystalline islet B-granules in the grass snake (Natrix natrix (L.)): tilting experiments in the electron microscope.** *J Ultrastruct Res* 1974, **46:**301-307.

21. Dunn MF: **Zinc-ligand interactions modulate assembly and stability of the insulin hexamer -- a review.** *Biometals* 2005, **18:**295-303.

22. Hou JC, Min L, Pessin JE: **Insulin granule biogenesis, trafficking and exocytosis.** *Vitam Horm* 2009, **80:**473-506.

23. Wheeler MB, Sheu L, Ghai M, Bouquillon A, Grondin G, Weller U, Beaudoin AR, Bennett MK, Trimble WS, Gaisano HY: **Characterization of SNARE protein expression in beta cell lines and pancreatic islets.** *Endocrinology* 1996, **137:**1340-1348.

24. Jewell JL, Oh E, Thurmond DC: **Exocytosis mechanisms underlying insulin release and glucose uptake: conserved roles for Munc18c and syntaxin 4.** *Am J Physiol Regul Integr Comp Physiol* 2010, **298:**R517-531.

25. Lang J, Fukuda M, Zhang H, Mikoshiba K, Wollheim CB: **The first C2 domain of synaptotagmin is required for exocytosis of insulin from**

pancreatic beta-cells: action of synaptotagmin at low micromolar calcium. *EMBO J* 1997, **16:**5837-5846.

26. Gao Z, Reavey-Cantwell J, Young RA, Jegier P, Wolf BA: **Synaptotagmin III/VII isoforms mediate Ca2+-induced insulin secretion in pancreatic islet beta -cells.** *J Biol Chem* 2000, **275:**36079-36085.

27. Dolai S, Xie L, Zhu D, Liang T, Qin T, Xie H, Kang Y, Chapman ER, Gaisano HY: **Synaptotagmin-7 Functions to Replenish Insulin Granules for Exocytosis in Human Islet beta-Cells.** *Diabetes* 2016, **65:**1962-1976.

28. Gut A, Kiraly CE, Fukuda M, Mikoshiba K, Wollheim CB, Lang J: **Expression and localisation of synaptotagmin isoforms in endocrine beta-cells: their function in insulin exocytosis.** *J Cell Sci* 2001, **114:**1709-1716.

29. Iezzi M, Kouri G, Fukuda M, Wollheim CB: **Synaptotagmin V and IX isoforms control Ca2+ -dependent insulin exocytosis.** *J Cell Sci* 2004, **117:**3119-3127.

30. Oh E, Kalwat MA, Kim MJ, Verhage M, Thurmond DC: **Munc18-1 regulates first-phase insulin release by promoting granule docking to multiple syntaxin isoforms.** *J Biol Chem* 2012, **287:**25821-25833.

31. Gomi H, Mizutani S, Kasai K, Itohara S, Izumi T: **Granuphilin molecularly docks insulin granules to the fusion machinery.** *J Cell Biol* 2005, **171:**99-109.

32. Deng CY, Lei WL, Xu XH, Ju XC, Liu Y, Luo ZG: **JIP1 mediates anterograde transport of Rab10 cargos during neuronal polarization.** *J Neurosci* 2014, **34:**1710-1723.

33. Stockinger W, Brandes C, Fasching D, Hermann M, Gotthardt M, Herz J, Schneider WJ, Nimpf J: **The reelin receptor ApoER2 recruits JNK-interacting proteins-1 and -2.** *J Biol Chem* 2000, **275:**25625-25632.

34. Gotthardt M, Trommsdorff M, Nevitt MF, Shelton J, Richardson JA, Stockinger W, Nimpf J, Herz J: **Interactions of the low density lipoprotein receptor gene family with cytosolic adaptor and scaffold proteins suggest diverse biological functions in cellular communication and signal transduction.** *J Biol Chem* 2000, **275:**25616-25624.

35. Bowman AB, Kamal A, Ritchings BW, Philp AV, McGrail M, Gindhart JG, Goldstein LS: **Kinesin-dependent axonal transport is mediated by the sunday driver (SYD) protein.** *Cell* 2000, **103:**583-594.

36. Kelkar N, Standen CL, Davis RJ: **Role of the JIP4 scaffold protein in the regulation of mitogen-activated protein kinase signaling pathways.** *Mol Cell Biol* 2005, **25:**2733-2743.

37. Dickens M, Rogers JS, Cavanagh J, Raitano A, Xia Z, Halpern JR, Greenberg ME, Sawyers CL, Davis RJ: **A cytoplasmic inhibitor of the JNK signal transduction pathway.** *Science* 1997, **277:**693-696.

38. Kelkar N, Gupta S, Dickens M, Davis RJ: **Interaction of a mitogen-activated protein kinase signaling module with the neuronal protein JIP3.** *Mol Cell Biol* 2000, **20:**1030-1043.

39. Hammond JW, Griffin K, Jih GT, Stuckey J, Verhey KJ: **Co-operative versus independent transport of different cargoes by Kinesin-1.** *Traffic* 2008, **9:**725-741.

40. Roux KJ, Kim DI, Raida M, Burke B: **A promiscuous biotin ligase fusion protein identifies proximal and interacting proteins in mammalian cells.** *J Cell Biol* 2012, **196:**801-810.

41. Varadi A, Tsuboi T, Johnson-Cadwell LI, Allan VJ, Rutter GA: **Kinesin I and cytoplasmic dynein orchestrate glucose-stimulated insulin-containing vesicle movements in clonal MIN6 beta-cells.** *Biochem Biophys Res Commun* 2003, **311:**272-282.

42. Varadi A, Ainscow EK, Allan VJ, Rutter GA: **Involvement of conventional kinesin in glucose-stimulated secretory granule movements and exocytosis in clonal pancreatic beta-cells.** *J Cell Sci* 2002, **115:**4177-4189.

43. Tanabe K, Liu Y, Hasan SD, Martinez SC, Cras-Meneur C, Welling CM, Bernal-Mizrachi E, Tanizawa Y, Rhodes CJ, Zmuda E, et al: **Glucose and fatty acids synergize to promote B-cell apoptosis through activation of glycogen synthase kinase 3beta independent of JNK activation.** *PLoS One* 2011, **6:**e18146.

44. Whitmarsh AJ, Cavanagh J, Tournier C, Yasuda J, Davis RJ: **A mammalian scaffold complex that selectively mediates MAP kinase activation.** *Science* 1998, **281:**1671-1674.

45. Loder MK, Tsuboi T, Rutter GA: **Live-cell imaging of vesicle trafficking and divalent metal ions by total internal reflection fluorescence (TIRF) microscopy.** *Methods Mol Biol* 2013, **950:**13-26.

46. Zhu X, Hu R, Brissova M, Stein RW, Powers AC, Gu G, Kaverina I: **Microtubules Negatively Regulate Insulin Secretion in Pancreatic beta Cells.** *Dev Cell* 2015, **34:**656-668.

47. Gee KR, Zhou ZL, Qian WJ, Kennedy R: **Detection and imaging of zinc secretion from pancreatic beta-cells using a new fluorescent zinc indicator.** *J Am Chem Soc* 2002, **124:**776-778.

48. Huang L, Shen H, Atkinson MA, Kennedy RT: **Detection of exocytosis at individual pancreatic beta cells by amperometry at a chemically modified microelectrode.** *Proc Natl Acad Sci U S A* 1995, **92:**9608-9612.

49. van den Berg MC, van Gogh IJ, Smits AM, van Triest M, Dansen TB, Visscher M, Polderman PE, Vliem MJ, Rehmann H, Burgering BM: **The small GTPase RALA controls c-Jun N-terminal kinase-mediated FOXO activation by regulation of a JIP1 scaffold complex.** *J Biol Chem* 2013, **288:**21729-21741.

50.	van Dam EM, Robinson PJ: **Ral: mediator of membrane trafficking.** *Int J Biochem Cell Biol* 2006, **38:**1841-1847.

51.	Moskalenko S, Henry DO, Rosse C, Mirey G, Camonis JH, White MA: **The exocyst is a Ral effector complex.** *Nat Cell Biol* 2002, **4:**66-72.

52.	Wang L, Li G, Sugita S: **RalA-exocyst interaction mediates GTP-dependent exocytosis.** *J Biol Chem* 2004, **279:**19875-19881.

53.	Lopez JA, Kwan EP, Xie L, He Y, James DE, Gaisano HY: **The RalA GTPase is a central regulator of insulin exocytosis from pancreatic islet beta cells.** *J Biol Chem* 2008, **283:**17939-17945.

54.	Xie L, Kang Y, Liang T, Dolai S, Xie H, Parsaud L, Lopez JA, He Y, Chidambaram S, Lam PP, et al: **RalA GTPase tethers insulin granules to L- and R-type calcium channels through binding alpha2 delta-1 subunit.** *Traffic* 2013, **14:**428-439.

55.	Xie L, Zhu D, Kang Y, Liang T, He Y, Gaisano HY: **Exocyst sec5 regulates exocytosis of newcomer insulin granules underlying biphasic insulin secretion.** *PLoS One* 2013, **8:**e67561.

56.	Ljubicic S, Bezzi P, Vitale N, Regazzi R: **The GTPase RalA regulates different steps of the secretory process in pancreatic beta-cells.** *PLoS One* 2009, **4:**e7770.

57.	Chiba K, Araseki M, Nozawa K, Furukori K, Araki Y, Matsushima T, Nakaya T, Hata S, Saito Y, Uchida S, et al: **Quantitative analysis of APP axonal transport in neurons: role of JIP1 in enhanced APP anterograde transport.** *Mol Biol Cell* 2014, **25:**3569-3580.

58.	Kevenaar JT, Hoogenraad CC: **The axonal cytoskeleton: from organization to function.** *Front Mol Neurosci* 2015, **8:**44.

59.	Heaslip AT, Nelson SR, Lombardo AT, Beck Previs S, Armstrong J, Warshaw DM: **Cytoskeletal dependence of insulin granule movement dynamics in INS-1 beta-cells in response to glucose.** *PLoS One* 2014, **9:**e109082.

60. Efimov A, Kharitonov A, Efimova N, Loncarek J, Miller PM, Andreyeva N, Gleeson P, Galjart N, Maia AR, McLeod IX, et al: **Asymmetric CLASP-dependent nucleation of noncentrosomal microtubules at the trans-Golgi network.** *Dev Cell* 2007, **12:**917-930.

61. Maccioni RB, Cambiazo V: **Role of microtubule-associated proteins in the control of microtubule assembly.** *Physiol Rev* 1995, **75:**835-864.

62. Coffey ET: **Nuclear and cytosolic JNK signalling in neurons.** *Nat Rev Neurosci* 2014, **15:**285-299.

63. Tararuk T, Ostman N, Li W, Bjorkblom B, Padzik A, Zdrojewska J, Hongisto V, Herdegen T, Konopka W, Courtney MJ, Coffey ET: **JNK1 phosphorylation of SCG10 determines microtubule dynamics and axodendritic length.** *J Cell Biol* 2006, **173:**265-277.

64. Chang L, Jones Y, Ellisman MH, Goldstein LS, Karin M: **JNK1 is required for maintenance of neuronal microtubules and controls phosphorylation of microtubule-associated proteins.** *Dev Cell* 2003, **4:**521-533.

65. Krueger KA, Bhatt H, Landt M, Easom RA: **Calcium-stimulated phosphorylation of MAP-2 in pancreatic betaTC3-cells is mediated by Ca2+/calmodulin-dependent kinase II.** *J Biol Chem* 1997, **272:**27464-27469.

66. Swenson KI, Winkler KE, Means AR: **A new identity for MLK3 as an NIMA-related, cell cycle-regulated kinase that is localized near centrosomes and influences microtubule organization.** *Mol Biol Cell* 2003, **14:**156-172.

67. Bargi-Souza P, Romano RM, Salgado Rde M, Goulart-Silva F, Brunetto EL, Zorn TM, Nunes MT: **Triiodothyronine rapidly alters the TSH content and the secretory granules distribution in male rat thyrotrophs by a cytoskeleton rearrangement-independent mechanism.** *Endocrinology* 2013, **154:**4908-4918.

68.   Satir P, Pedersen LB, Christensen ST: **The primary cilium at a glance.** *J Cell Sci* 2010, **123:**499-503.

69.   Munger BL: **A light and electron microscopic study of cellular differentiation in the pancreatic islets of the mouse.** *Am J Anat* 1958, **103:**275-311.

70.   Sorokin SP: **Reconstructions of centriole formation and ciliogenesis in mammalian lungs.** *J Cell Sci* 1968, **3:**207-230.

71.   Garcia-Gonzalo FR, Reiter JF: **Scoring a backstage pass: mechanisms of ciliogenesis and ciliary access.** *J Cell Biol* 2012, **197:**697-709.

72.   Pazour GJ, Witman GB: **The vertebrate primary cilium is a sensory organelle.** *Curr Opin Cell Biol* 2003, **15:**105-110.

73.   Lancaster MA, Schroth J, Gleeson JG: **Subcellular spatial regulation of canonical Wnt signalling at the primary cilium.** *Nat Cell Biol* 2011, **13:**700-707.

74.   Ezratty EJ, Stokes N, Chai S, Shah AS, Williams SE, Fuchs E: **A role for the primary cilium in Notch signaling and epidermal differentiation during skin development.** *Cell* 2011, **145:**1129-1141.

75.   Keady BT, Samtani R, Tobita K, Tsuchya M, San Agustin JT, Follit JA, Jonassen JA, Subramanian R, Lo CW, Pazour GJ: **IFT25 links the signal-dependent movement of Hedgehog components to intraflagellar transport.** *Dev Cell* 2012, **22:**940-951.

76.   diIorio P, Rittenhouse AR, Bortell R, Jurczyk A: **Role of cilia in normal pancreas function and in diseased states.** *Birth Defects Res C Embryo Today* 2014, **102:**126-138.

77.   Gerdes JM, Christou-Savina S, Xiong Y, Moede T, Moruzzi N, Karlsson-Edlund P, Leibiger B, Leibiger IB, Ostenson CG, Beales PL, Berggren PO: **Ciliary dysfunction impairs beta-cell insulin secretion and promotes development of type 2 diabetes in rodents.** *Nat Commun* 2014, **5:**5308.

78. Mokrzan EM, Lewis JS, Mykytyn K: **Differences in renal tubule primary cilia length in a mouse model of Bardet-Biedl syndrome.** *Nephron Exp Nephrol* 2007, **106:**e88-96.

79. Habedanck R, Stierhof YD, Wilkinson CJ, Nigg EA: **The Polo kinase Plk4 functions in centriole duplication.** *Nat Cell Biol* 2005, **7:**1140-1146.

80. Mahjoub MR, Stearns T: **Supernumerary centrosomes nucleate extra cilia and compromise primary cilium signaling.** *Curr Biol* 2012, **22:**1628-1634.

81. Mahjoub MR: **The importance of a single primary cilium.** *Organogenesis* 2013, **9:**61-69.

82. Goetz SC, Anderson KV: **The primary cilium: a signalling centre during vertebrate development.** *Nat Rev Genet* 2010, **11:**331-344.

83. Bonner-Weir S: **Morphological evidence for pancreatic polarity of beta-cell within islets of Langerhans.** *Diabetes* 1988, **37:**616-621.

84. Granot Z, Swisa A, Magenheim J, Stolovich-Rain M, Fujimoto W, Manduchi E, Miki T, Lennerz JK, Stoeckert CJ, Jr., Meyuhas O, et al: **LKB1 regulates pancreatic beta cell size, polarity, and function.** *Cell Metab* 2009, **10:**296-308.

85. Geetha-Loganathan P, Nimmagadda S, Fu K, Richman JM: **Avian facial morphogenesis is regulated by c-Jun N-terminal kinase/planar cell polarity (JNK/PCP) wingless-related (WNT) signaling.** *J Biol Chem* 2014, **289:**24153-24167.

86. Yamanaka H, Moriguchi T, Masuyama N, Kusakabe M, Hanafusa H, Takada R, Takada S, Nishida E: **JNK functions in the non-canonical Wnt pathway to regulate convergent extension movements in vertebrates.** *EMBO Rep* 2002, **3:**69-75.

87. Kim IJ, Lee KW, Park BY, Lee JK, Park J, Choi IY, Eom SJ, Chang TS, Kim MJ, Yeom YI, et al: **Molecular cloning of multiple splicing variants**

of JIP-1 preferentially expressed in brain.** *J Neurochem* 1999, **72:**1335-1343.

88.   Bonny C, Nicod P, Waeber G: **IB1, a JIP-1-related nuclear protein present in insulin-secreting cells.** *J Biol Chem* 1998, **273:**1843-1846.

89.   Abe H, Murao K, Imachi H, Cao WM, Yu X, Yoshida K, Wong NC, Shupnik MA, Haefliger JA, Waeber G, Ishida T: **Thyrotropin-releasing hormone-stimulated thyrotropin expression involves islet-brain-1/c-Jun N-terminal kinase interacting protein-1.** *Endocrinology* 2004, **145:**5623-5628.

90.   Vernia S, Cavanagh-Kyros J, Barrett T, Jung DY, Kim JK, Davis RJ: **Diet-induced obesity mediated by the JNK/DIO2 signal transduction pathway.** *Genes Dev* 2013, **27:**2345-2355.

91.   Consortium GT: **Human genomics. The Genotype-Tissue Expression (GTEx) pilot analysis: multitissue gene regulation in humans.** *Science* 2015, **348:**648-660.

92.   Chen ZF, Li YB, Han JY, Wang J, Yin JJ, Li JB, Tian H: **The double-edged effect of autophagy in pancreatic beta cells and diabetes.** *Autophagy* 2011, **7:**12-16.

93.   Fujitani Y, Kawamori R, Watada H: **The role of autophagy in pancreatic beta-cell and diabetes.** *Autophagy* 2009, **5:**280-282.

94.   Ebato C, Uchida T, Arakawa M, Komatsu M, Ueno T, Komiya K, Azuma K, Hirose T, Tanaka K, Kominami E, et al: **Autophagy is important in islet homeostasis and compensatory increase of beta cell mass in response to high-fat diet.** *Cell Metab* 2008, **8:**325-332.